Graduate Student Theses, Dissertations, & Professional Papers

Graduate School

2000

Identification and characterization of a bacteriophage of Borrelia burgdorferi

Christian H. Eggers

The University of Montana

INFORMATION TO USERS

This manuscript has been reproduced from the microfilm master. UMI films the text directly from the original or copy submitted. Thus, some thesis and dissertation copies are in typewriter face, while others may be from any type of computer printer.

The quality of this reproduction is dependent upon the quality of the copy submitted. Broken or indistinct print, colored or poor quality illustrations and photographs, print bleedthrough, substandard margins, and improper alignment can adversely affect reproduction.

In the unlikely event that the author did not send UMI a complete manuscript and there are missing pages, these will be noted. Also, if unauthorized copyright material had to be removed, a note will indicate the deletion.

Oversize materials (e.g., maps, drawings, charts) are reproduced by sectioning the original, beginning at the upper left-hand corner and continuing from left to right in equal sections with small overlaps.

Photographs included in the original manuscript have been reproduced xerographically in this copy. Higher quality 6" x 9" black and white photographic prints are available for any photographs or illustrations appearing in this copy for an additional charge. Contact UMI directly to order.

UMI
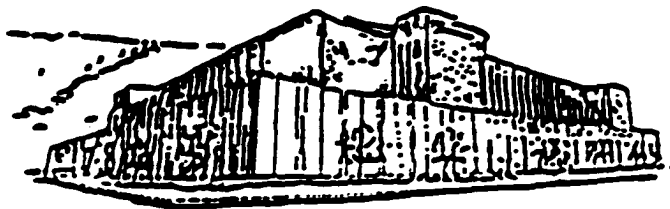
Maureen and Mike
MANSFIELD LIBRARY

The University of **MONTANA**

Permission is granted by the author to reproduce this material in its entirety, provided that this material is used for scholarly purposes and is properly cited in published works and reports.

** *Please check "Yes" or "No" and provide signature* **

Yes, I grant permission   ✓

No, I do not grant permission   _____

Author's Signature _Christian H Seger_

Date _5/30/00_

Any copying for commercial purposes or financial gain may be undertaken only with the author's explicit consent.

Identification and Characterization of a Bacteriophage of *Borrelia burgdorferi*

Christian H. Eggers

B. S. Colorado State University, Fort Collins, Colorado 1995
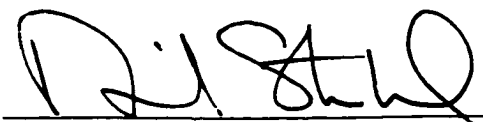
Presented in partial fulfillment of the requirements for the degree of

Doctor of Philosophy

The University of Montana

2000

_____
Chairman, Board of Examiners

_____
Dean, Graduate School

_____
Date

UMI Number: 9967330

UMI®

Eggers, Christian H., Ph.D., May 2000

Biochemistry/Microbiology
Molecular Biology Emphasis

Identification and Characterization of a Bacteriophage of *Borrelia burgdorferi*

Director: Dr. D. Scott Samuels

We have identified a bacteriophage of the Lyme disease spirochete, *Borrelia burgdorferi*. This bacteriophage has a polyhedral head with a diameter of 46 nm and a contractile tail 92 nm in length. Previously, several bacteriophage-like particles have been visualized in association with *B. burgdorferi*, though none have been characterized at the molecular level. We have designated the bacteriophage described here ϕBB-1.

ϕBB-1 packages 32 kilobase pairs (kb) of linear double-stranded DNA with non-covalently closed ends. The lysogenic prophage has been mapped to the 32-kb circular plasmid (cp32) family of *B. burgdorferi*. The cp32s are a group of closely-related plasmids and more than one of these cp32s can be maintained in a single cell. Restriction maps of the phage genome indicate that more than one cp32 is packaged, and the phage genome is circularly permuted and possibly terminally redundant.

The ϕBB-1 prophage is inducible from *B. burgdorferi* strains CA.11-2A and B31, as well as *Borrelia bissettii* strain DN127, with 10 μg ml^{-1} 1-methyl-3-nitro-nitroso-guanidine (MNNG). Coinciding with phage release, and a moderate decrease in cell density, is an increase in the synthesis of the BlyA and BlyB proteins, a possible holin-like system implicated in host cell lysis.

We have inserted a kanamycin-resistance cassette into one of the cp32s of *B. burgdorferi* CA-11.2A. ϕBB-1 packages the cp32 containing the kanamycin-resistance cassette and is capable of transducing the antibiotic resistance marker into *B. burgdorferi* strains CA-11.2A, B31, and a high passage clone of strain SH2-82, 1A7. This is the first direct evidence of lateral gene transfer in *B. burgdorferi*.

ii

Acknowledgments

I would like to thank my advisor, Scott Samuels. His patience and technical expertise were never so sorely tested as in the first year or two (or four or five) that I was in his lab. He will continue to be the leading example of the kind of scientist and, more importantly, the kind of person that I hope to be. I would also like to thank the other members of my graduate committee: George Card, Mike Minnick, Walt Hill, Keith Parker, and Kit Tilly. Their support and effort on my behalf have been appreciated.

Thank you to the members of the Samuels laboratory, past and present. They have made the lab a fun place to work and a great place to learn. A special thank you to Betsy Kimmel, who, with her unceasing support, has put almost as much work into this dissertation as I have (although she will be the first to tell you that all the mistakes are certainly mine).

Others who have contributed to this work by providing strains, reagents, or valuable advice are: Sherwood Casjens, Patti Rosa, Brian Stevenson, Jay Carroll, Rich Marconi, Tom Schwan, Chris Damman, Don Oliver, Jim Bono, Thad Stanton, Kent Barbian, Melissa Caimano, and Justin Radolf. Those who assisted in the instruction of my use (and sometimes misuse) of the electron microscope deserve special recognition: Jim Driver, Mike Gilbert, Bill Granath, Claude Garon and Fred Hayes.

I owe a large debt of gratitude to my entire family. Thank you to my sister, Felicia, and her family, Bill and Sebastian, for their steadfast interest and moral support. Finally, I would like to thank my parents, Howard and Noël, without whom, none of this would have been possible. Their love, understanding, patience and support have been invaluable to me while undertaking this endeavor.

No man is an island, entire of itself;
Every man is a piece of the continent, a part of the main;
If a clod be washed away by the sea, Europe is the less,
As if a promontory were, as well as if a manor of thy friends or of thine own were;
Any man's death diminishes me, because I am involved in mankind;
And therefore never send to know for whom the bell tolls;
It tolls for thee

John Donne
(1572-1631)

Table of Contents

iv

List of Tables

List of Figures

vii

viii

Chapter 1

Introduction

1.1 *Borrelia burgdorferi* and Lyme disease.

With more than 10,000 new cases reported each year between 1993 and 1997, Lyme disease is the most common arthropod-borne disease in the United States (17, 45, 53, 118). According to the Centers for Disease Control and Prevention, the annual reported incidence of Lyme disease in the United States has increased 25-fold since national surveillance began in 1982 (44, 45). An etiological agent of Lyme disease, *Borrelia burgdorferi*, is a member of the spirochetes, a group of phylogenetically distinct bacteria that also includes the human pathogens that cause relapsing fever, leptospirosis and syphilis (12, 30, 161).

In the United States, *B. burgdorferi* is transmitted by hard-bodied ticks, the deer tick (*Ixodes scapularis*) in the northeastern and north-central regions and the western black-legged tick (*Ixodes pacificus*) on the Pacific coast (30, 31, 46). Humans serve only as accidental hosts, interrupting the normal cycle of transmission of the bacterium between the tick and a wild vertebrate, usually a rodent (66, 146).

The earliest manifestation of Lyme disease is a characteristic 'bull's eye' skin rash, or erythema migrans, at the site of infection, accompanied by a self-limited flu-like illness (21). At this stage, the disease can be controlled and treated with proper therapy, including the use of the antibiotics amoxicillin or doxycycline (54). In as many as 70% of untreated patients, late manifestations of this bacterial invasion can result in the dysfunction of the central nervous system and chronic arthritis (158).

1

There are three recognized closely-related species of *Borrelia* that have been implicated in causing human disease, although more than ten genospecies (closely-related species that are distinguishable only by genomic analysis) comprise *Borrelia burgdorferi* sensu lato (13, 104, 182). In North America, *B. burgdorferi* sensu stricto is the predominant agent of Lyme disease, but in Europe all three disease-causing species are found, with *Borrelia garinii* and the *Borrelia afzelii* being more prevalent (157). Observed regional differences in the manifestations of Lyme disease are probably related to different genospecies of *B. burgdorferi* sensu lato (4, 158, 159, 162, 183).

1.2 The complex genome of *B. burgdorferi*.

B. burgdorferi has a complex genome consisting of a linear chromosome and both linear and circular plasmids (Figure 1) (15, 18, 20, 40, 42, 43, 51, 67, 68, 152, 188). The ends of the linear DNA molecules of *B. burgdorferi* are covalently closed hairpin loops, similar to the ends of the vaccinia virus (18, 41, 68, 83, 84). The prophage of the coliphage N15 is the only other prokaryotic linear replicon identified to date containing analogous telomeric hairpin loops (85, 173, 174).

Some isolates of *B. burgdorferi* can contain up to 21 different plasmids often sharing regions of DNA homology and, where examined, having a copy number per cell equal to that of the chromosome (16, 40, 42, 43, 68, 82, 107, 121, 153, 169, 196). With an approximate size of 1.5 million base pairs, more than 40% of the genomic DNA of *B. burgdorferi* can be contained in extrachromosomal elements (42, 68). Long-term cultivation of *B. burgdorferi* can result in the loss of some of the plasmids, with an accompanying decrease in infectivity or pathogenesis, suggesting an important role for some plasmid-encoded proteins (15, 119, 147, 152, 188). Included in the number of

chromosome (910 kbp)

lp56

lp54

lp38

lp36

lp28 (x4)

lp25

lp17

cp32 (x7)

cp26

cp9
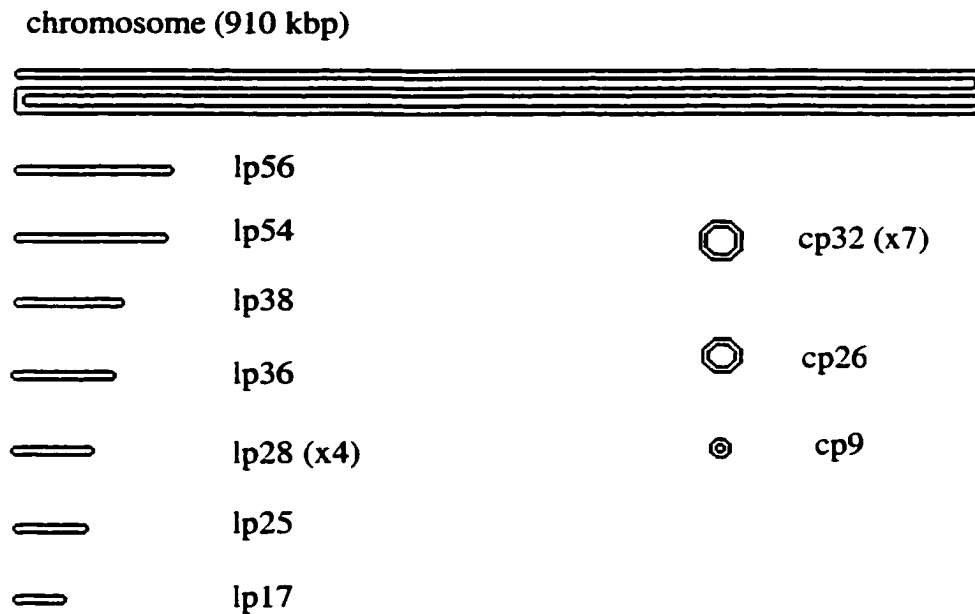
Figure 1. The complex genome of *Borrelia burgdorferi*. The genomic complement of the sequenced isolate, *B. burgdorferi* strain B31, is represented in this figure. This isolate is believed to be missing both a 5-kb and a 21-kb linear plasmid and at least two cp32s found in the original B31 isolate (42, 68). There are also plasmids found in other *B. burgdorferi* sensu lato strains that are not found in B31, including two slightly different 18-kb circular plasmids, both derived from cp32 (32, 168). The plasmids are named for the topology of the molecule [linear plasmid (lp), circular plasmid (cp)] and the approximate size in kb. This schematic is an adaptation from Fraser, *et al.*, *Nature* 1997 (68).

plasmid-encoded genes with assigned products are several genes for major outer surface proteins [for review see (42, 68)] and two genes important in purine nucleotide biosynthesis, *guaA* and *guaB* (108).

1.3 The 32-kb circular plasmids.

One of the *B. burgdorferi* plasmids, the 32-kb circular plasmid (cp32), has several

related but distinct isoforms (42, 43, 121, 169, 196). In *B. burgdorferi* strain B31 there

appear to be seven or more members of the cp32 family and many of these can be

maintained in a single isolate (43). A complete cp32 is also inserted into the large linear

56-kb plasmid (68) and lp54 may contain an ancient integration of a cp32 (42).

Additionally, the unstable small circular plasmids (<10 kb) and cp18 are basically

truncated cp32 molecules (32, 48, 59, 68, 168).

The members of the cp32 family share large regions of homologous DNA that

include almost the entire plasmid. There are three regions of significant variability that

correspond to: (1) the putative partitioning region, (2) a region encoding three families of

lipoproteins, including the OspE-related proteins, the OspF-related proteins, and a group

of proteins that contain OspE/F-like leader sequences (Elp), but do not otherwise

resemble the other two groups (although all three families are also categorized under the

designation Erp for OspE/F-related proteins), and (3) the region encoding the multicopy

lipoprotein genes (*mlp*) (5, 32, 42, 43, 97, 121, 167-169, 190, 196). Many of the

lipoprotein genes encoded on the cp32s are selectively expressed within the mammalian

host (111, 166, 190). The variability of the lipoproteins encoded on the different cp32s

has been proposed as a possible mechanism of immune evasion and establishment of

chronic infection, suggesting an evolutionary rationale for the physiological cost that

maintaining several homologous replicons might have on a cell (32, 167, 172, 190).

Casjens *et al.* have proposed that the cp32 molecules may be the genomes of

lysogenic prophages (40, 43). The authors cite several lines of evidence for this

hypothesis, including the conserved size of the ubiquitous cp32 molecules among *B. burgdorferi* sensu lato strains and the apparent gene orders and transcription patterns of the cp32 molecules, consistent with other known bacteriophages (43).

1.4 Bacteriophages of spirochetes.

Bacteriophages. Bacteriophages, viruses that infect bacteria, have long been recognized as a cornerstone of molecular biology (3, 91). A bacteriophage and its host are intimately associated and the two often share an evolutionary history (2, 49). Some phages, particularly those that can package and transduce antibiotic-resistance markers or those that encode virulence factors that contribute to the spread or maintenance of the bacterial host, can have profound effects on bacterial physiology or epidemiology (3, 47).

Because of their small genomes and inherent dependence upon at least some of the bacterial hosts' cellular machinery, the use of bacteriophages as tools for dissecting DNA replication has been essential for understanding this process in many bacterial systems (95). Additionally, bacteriophages constitute naturally-occurring vectors for lateral gene transfer and may be used to shuttle genes between bacterial cells (25, 95).

Temperate phages, those that can either lysogenize or abrogate the host machinery for a lytic infection, have been used to study recombination, stress response and replication (95). In a lysogen, the phage genome, termed the prophage, is maintained quiescently and is propagated along with the host DNA. During lysogeny, a prophage can be integrated into the host chromosome (like λ phage), maintained as an autonomously replicating plasmid (like phage P1) or maintained in either of those two states (like P22) (25).

Bacteriophages of spirochetes other than *Borrelia*. Bacteriophage-like

particles in association with a spirochete were first observed in 1969 (126). In fact,

phage particles spontaneously released from a number of animal-associated spirochetes

have been visualized by electron microscopy (23, 52, 125, 127, 133). Bacteriophage-like

particles have also been seen in association with human spirochetes that were either

treated with mitomycin C, a DNA-strand crosslinker (33, 110) or, rarely, left untreated

(34).

Three lytic phages of *Leptospira biflexa*, a saprophytic species, were isolated

from sewage water on the outskirts of Paris. These phages were identified by electron

microscopy and the nucleic acid from the virions was characterized as double-stranded

DNA ranging from 50 to 60 kb. These bacteriophages represented the first molecular

characterization of a phage associated with a spirochete and a potentially useful tool for

studying the molecular genetics of *Leptospira* species (134).

VSH-1, a generalized transducing phage released from *Brachyspira* (formerly

Serpulina) *hyodysenteriae* cells treated with mitomycin C, was used to demonstrate the

first instance of lateral gene transfer in a spirochete (88). This phage packages ~7.5-kb of

host genomic DNA and has been used to transduce chromosomal antibiotic-resistant

markers between strains of *B. hyodysenteriae* (87, 88).

Bacteriophage of *Borrelia*. Bacteriophage-like particles with elongated heads

and straight tails were described in association with *B. burgdorferi* soon after the

spirochete was identified as a causative agent of Lyme disease (77). Structurally-

identical phage particles were also reported in a relapsing fever agent, *Borrelia hermsii*

(19). More recently, two different bacteriophages, both with isometric heads, but one

with a contractile tail and one with a non-contractile tail, were released from clinical *B. burgdorferi* isolates treated with ciprofloxacin, a topoisomerase-inhibitor (117, 144). We also know of a single event when a phage-like particle packaging host DNA, like PBSX (8) and VSH-1 (87, 88), was recovered from a spontaneously-lysed culture of *B. burgdorferi* (137). This was an isolated incident and we have not observed the release of this particle in our studies.

Until this work, no report had characterized a bacteriophage of *B. burgdorferi* beyond structural observations by electron microscopy. Here we identify and present the initial molecular characterization of a bacteriophage of *B. burgdorferi*, which we have named ϕBB-1. This bacteriophage is spontaneously released from growing cultures of a California isolate of *B. burgdorferi* and the prophage is inducible from at least two other strains with 1-methyl-3-nitro-nitrosoguanidine (MNNG). ϕBB-1 packages the 32-kb circular plasmids, molecules that may play an important role in the infection and virulence of *B. burgdorferi*. We have recently demonstrated the ability of this bacteriophage to transduce an antibiotic-resistance marker between cells, the first direct evidence of lateral gene transfer in *B. burgdorferi*.

With this work as a foundation, ϕBB-1 may become a tool for studying DNA metabolism and other molecular processes of the *B. burgdorferi* plasmids. In addition to being the first *B. burgdorferi* phage characterized at a molecular level, ϕBB-1 has several features that make this phage intrinsically interesting and worth further study. These include the constitutive autonomous replication of the prophage as a circular plasmid, the ubiquity of the prophage throughout the Lyme disease complex, a population of phage

heads containing more than one isoform of the phage genome, a possible role in host-immune invasion and in the molecular evolution of different cp32 molecules, and a requirement, shared with the bacterium, for maintenance and selective expression within two very different hosts (invertebrate and mammalian).

The physical identification of ϕBB-1, the initial characterization of the packaged nucleic acid and a method of inducing the prophage are presented in chapter 3. More extensive analyses of the nucleic acid content of the phage, including preliminary mapping studies, are described in chapter 4. The search for possible phage proteins is discussed in chapter 5 and transduction by ϕBB-1 is analyzed in chapter 6.

Chapter 2

Materials and Methods

2.1 General methods.

Bacterial strains. *B. burgdorferi* sensu stricto strain CA-11.2A (109), a clone of the California *B. burgdorferi* strain CA-11, was provided by P. Rosa (Rocky Mountain Laboratories, Hamilton, MT). Low passage CA-11 (149), low-passage B31-1M1T, and the high passage SH2-82 clone, 1A7, were provided by T. Schwan (Rocky Mountain Laboratories). *B. burgdorferi* 297 (160) was obtained from M. Caimano and J. Radolf (University of Connecticut Health Center, Farmington, CT) and the low passage *B. burgdorferi* strain B31-CDC was provided by S. Wikel (University of Connecticut Health Center, Farmington, CT). B31-UM and HB19 (161) were part of our collection. All other isolates of *B. burgdorferi* and other *Borrelia* species were kindly provided by R. Marconi (Medical College of Virginia at Virginia Commonwealth University, Richmond, VA). Unless otherwise specified, the *B. burgdorferi* strain B31 used in this study was B31-UM, designated by us to indicate the high passage strain from our laboratory.

Culture conditions. Bacterial isolates were routinely cultivated in Barbour-Stoenner-Kelly (BSK) complete medium (14) (Sigma; St. Louis, MO) at 34°C with a 5% CO_2 atmosphere. Culture densities were determined using a modification of a previously described protocol (138). One ml of culture was centrifuged at room temperature at 14,000 × g for 5 min. The pellet was washed with 1 ml of dPBS (138 mM NaCl, 2.7 mM KCl, 8.1 mM Na_2HPO_4, 1.5 mM KH_2PO_4), centrifuged as above, and the pellet resuspended in 1 ml dPBS. The absorbance of the sample was measured at 600 nm using

9

a Spectronics® Genesys 2 spectrophotometer (Rochester, NY). The A_{600} was multiplied by the factor 1.4×10^9 to calculate the number of cells per ml of culture.

Bacteriophage recovery. CA-11.2A cells were cultured as described above until the cells reached log phase ($>10^7$ cells ml^{-1}), approximately 3 days after a 1:100 inoculation. All subsequent steps in the recovery of the phage were performed at 4°C. The culture was centrifuged at $6,000 \times g$ for 10 min and the supernatant was collected. The culture supernatant was precipitated with polyethylene glycol (PEG) by modifying a previously described protocol for concentrating phage (135). Precipitations were done in aliquots ≤100 ml for the best results as determined by the amount of phage yielded per ml of original culture supernatant. NaCl was added to a 1M final concentration (F. C.) and the supernatant was rotated for 1 h on a shaker, followed by centrifugation at $5,000 \times g$ for 10 min. The supernatant was retained and 10% (w/v) PEG 8000 (we have found that using Sigma PEG 8000 results in better yields) was slowly added. The culture was rotated for 1 h, and the precipitate was recovered by centrifugation at $6,000 \times g$ for 10 min. The supernatant was decanted and the precipitate was resuspended in suspension medium (SM) (100 mM NaCl, 10 mM MgSO$_4$, 50 mM Tris-HCl [pH 7.5]; no gelatin). The resuspension volume was 400 μl of SM per 10 ml of original culture supernatant. The resuspended material was extracted once with an equal volume of chloroform, and the aqueous layer recovered. The sample was extracted a second time with 10% chloroform and the aqueous layer, which contained the phage, was recovered. The chloroform treatments were critical for PEG removal, as polyethylene glycol will inhibit

many downstream enzymatic reactions, including restriction digests. Samples were stored at 4°C.

DNA extraction. For the extraction of extracellular phage DNA from cell-free supernatants, precipitated samples were prepared as described above. Prior to DNA extraction, $MgCl_2$ (1 M stock) was added to bring the sample to 16 mM (F.C.) and the samples were treated at 37°C for 0.5 h with 1 unit of RQ1-DNase (Promega; Madison, WI) per 250 µl of sample. After DNase treatment, EDTA (0.5 M stock) was added to bring the sample to 100 mM (F.C.) and the sample was treated with a final concentration of 0.3% sodium dodecyl sulfate (SDS) (10% stock) and 100 µg ml^{-1} of proteinase K (PK) (20 mg ml^{-1} stock) at 65°C for 10 min (171). The sample was extracted twice, once with an equal volume of phenol-chloroform-isoamyl alcohol (25:24:1) and a second time with an equal volume of chloroform-isoamyl alcohol (24:1). The aqueous layer was recovered and the DNA was precipitated with 200 mM NaCl (F.C.) and two volumes of absolute ethanol (EtOH) as described previously (138). The sample was incubated at –20°C for ≥30 min, then centrifuged at 14,000 × g for 20 min at 4°C. The pellet was washed with 70% EtOH and centrifuged at 14,000 × g for 5 min at 4°C. The DNA pellet was resuspended in 20 µl of TE (10 mM Tris-HCl [pH 8.0], 1 mM EDTA) per 100 µl of original PEG-precipitate.

Total chromosomal DNA was extracted from *B. burgdorferi* cells based on a protocol described previously (138). *B. burgdorferi* cells were collected by centrifugation at 6,000 × g for 10 min at 4°C, washed in 1 ml dPBS for every 10 ml of original culture, pelleted again as above, and resuspended in a final volume of 0.2 ml

TES (50 mM Tris-HCl [pH 8.0], 50 mM EDTA, 15% sucrose; autoclave and store at

4°C) for every 10 ml of original culture. The cells were lysed by the addition of 1% SDS

(F.C.) and incubated for 30 min at 37°C after 4 mg ml^{-1} PK (F.C.) was added. The DNA

sample was extracted twice with organic solvents, and precipitated with NaCl and EtOH

as described above. The precipitated DNA was resuspended in 30 µl TE per 10 ml of

original supernatant.

Agarose gel electrophoresis. DNA samples were heated for 3 to 5 min at 65°C

in 1% N-laurylsarcosine, 10 mM EDTA, 3% Ficoll 400, 0.05 mg ml^{-1} bromophenol blue

(BPB) and 0.05 mg ml^{-1} xylene cyanole and cooled briefly prior to loading. For

conventional gel electrophoresis, the DNA was resolved on agarose gels (SeaKem LE;

Bio*Whittaker Molecular Applications; Rockland, ME) of percentages as indicated,

usually 0.5%, in TAE (40 mM Tris-acetate, 1 mM EDTA) at 30 V (2.4 V cm^{-1}) for 5 h or

as indicated. Gels were stained with 0.5 µg ml^{-1} ethidium bromide (EtBr) for 0.5 to 1 h

and destained in water for 1 to 2 h. Alternatively, 0.5 µg ml^{-1} EtBr was sometimes added

directly to the gel prior to casting. The DNA was visualized on a UV transilluminator

and images were captured on a Gel Doc 1000 system (Bio-Rad; Hercules, CA).

For field-inversion gel electrophoresis (FIGE), DNA samples were prepared as

above. Samples were resolved on 0.8% agarose gels (SeaKem GTG; Bio*Whittaker

Molecular Applications) in TBE (45 mM Tris-borate, 2 mM EDTA) at 80 V (4.3 V cm^{-1}).

Field-inversion was performed using a PPI-200 programmable power inverter (MJ

Research; Waltham, MA) with the programs determined using the GelTimes software

supplied by the manufacturer. The running buffer was supplemented with 100 mM

glycine (as suggested by the manufacturer; we recommend this addition to slow the oxidation of the platinum wire caused by field-inversion) and the buffer was recirculated during electrophoresis. After electrophoresis, gels were stained with EtBr and visualized as described above.

Two-dimensional gel electrophoresis was performed essentially as described previously (138). A 20 µl sample of total *B. burgdorferi* DNA was fractionated on a 0.35% agarose gel in TAE at 20 V (1.1 V cm^{-1}) for 16 h. After 16 h, the gel was rotated 90° and equilibrated with 15 µM chloroquine for 8 h. Electrophoresis was continued in the second dimension in the presence of 15 µM chloroquine at 20 V for another 16 h. The gel was soaked in three changes of water over 5 h to remove the chloroquine before staining with EtBr and visualizing as described above.

Southern hybridization. Gels were vacuum-blotted to either Hybond N$^+$ nylon membrane (Amersham Pharmacia Biotech; Piscataway, NJ) or Immobilon-Ny$^+$ (Millipore; Bedford, MA) and cross-linked as described previously (105). Vacuum-blotting was carried out at ≤50 mbars pressure with 0.25 M HCl for 4 min, denaturation solution (0.5 M NaOH, 1.5 M NaCl) for 5 min, neutralization solution (0.5 M Tris-HCl [pH 7.2], 1.5 M NaCl, 1.0 mM EDTA) for 5 min and 20X SSC (3 M NaCl, 0.3 M sodium citrate) for 1 h. Solutions were aspirated off at the end of each step. The wells and markers were marked with a membrane-marking pen, and the blot cross-linked in a UV stratalinker 1800 (Stratagene; La Jolla, CA) as instructed by the manufacturer.

Probes for Southern hybridization were generated from source DNA as indicated in each experiment. One hundred nanograms of DNA to be used as a probe were labeled

with [α-^{32}P]dATP with a random primer kit (Prime-it II; Stratagene) as instructed by

the manufacturer. Radiolabeled probes were purified from unincorporated label by

passage through G-50 spin columns (Boehringer Mannheim; Indianapolis, IN) as

instructed by the manufacturer. The blots were prehybridized in 15 to 20 ml of either

Quikhyb (Stratagene) or hybridization solution [6X SSC, 0.5% SDS, 5X Denhardt's (50X

Denhardt's: 5 g Ficoll 400, 5 g polyvinylpyrrolidone, 5 g fraction V BSA in 500 ml; filter

and store at -20°C)] supplemented with 1 mg of salmon sperm DNA (boiled for 5 min

and cooled briefly on ice prior to addition) for 15 to 20 min at 68°C with rotation in a

hybridization oven (Hybaid; Franklin, MA). After prehybridization, the radiolabeled

probe was added to the hybridization buffer and hybridization was conducted for ≥1 h

(Quikhyb) or ≥6 h (hybridization solution) at 68°C. The blots were washed twice in 2X

SSC-0.1%SDS at 25°C (15 min each) and once at 50°C in 0.1X SSC-0.1% SDS (30 min),

wrapped in cellophane and exposed to either Hyperfilm ECL (Amersham Pharmacia) or

Fujifilm RX film for 16 to 24 h at -80°C with intensifying screens.

Membranes to be reprobed were stripped in a hybridization bottle with 15 to 20

ml of mild stripping solution (5 mM Tris-HCl [pH 8.0], 2 mM EDTA, 0.1X Denhardt's

solution). Stripping was carried out in a hybridization oven at 65°C for ≥2 h. If stripping

was not complete after this relatively mild treatment, then the membranes were washed in

0.4 M NaOH for 30 min at 45°C, followed by two washes at room temperature in

moderate stripping solution (200 mM Tris-HCl [pH 7.0], 2 mM EDTA, 0.1X Denhardt's

solution) for 30 min each. If membrane counts were still above background, several

hundred ml of 0.1% SDS were brought to a boil and poured onto the membrane, then

allowed to cool to room temperature. This last protocol is very harsh on the membrane and was used only as a final option (10, 62). Stripped membranes were laid on Fujifilm RX film 12 to 16 h to ensure the previous probe was removed.

Induction of the φBB-1 prophage with 1-methyl-3-nitro-nitrosoguanidine (MNNG). Isolates were cultured in BSK complete medium as described above until a density of ~5 × 10^7 cells ml^{-1} was reached. Cells were pelleted at 6,000 × g and the supernatant was collected for PEG-precipitation as described above. The cell pellet was resuspended in a volume of BSK complete medium equal to that of the original culture. The sample was treated with 10 μg ml^{-1} MNNG (Sigma) and incubated at 34°C for 2 h. The cultures were centrifuged at 6,000 × g and the supernatant was discarded as waste. The cells were resuspended in an equal volume of BSK complete medium and allowed to recover for 60 h at 34°C. After 60 h, the cells were pelleted at 6,000 × g and the supernatants were collected. Phage was precipitated and the DNA was extracted and resolved on a 0.5% agarose gel by conventional gel electrophoresis as described above. The gel was stained with EtBr as described above.

SDS-polyacrylamide agarose gel electrophoresis (PAGE). Unless otherwise described, proteins were resolved on 12.5% SDS-PAGE gels (0.375 M Tris-HCl [pH 8.8], 0.1% SDS, 12.5% polyacrylamide [30% stock solution; 37.5:1 acrylamide to bis-acrylamide; Boehringer Mannheim], 0.24% N,N,N',N'-tetramethylethylenediamine [TEMED; Bio-rad], 0.025% ammonium persulfate, volume up to 10 ml with water; makes enough for two mini-gels). The electrophoresis was performed in a Mini-Protean II apparatus (Bio-Rad) as described by the manufacturer. Samples were diluted with

either 2X or 4X SDS-PAGE loading dye (1X SDS-PAGE loading dye: 62.5 mM Tris-HCl [pH 8.0], 2% SDS, 10% glycerol, 5% 2-mercaptoethanol, 1.25×10^{-3}% BPB). The gels were electrophoresed at 100 V through a 3.8% stacking gel (0.125 M Tris-HCl [pH 6.6], 0.1% SDS, 3.8% polyacrylamide (same solution as above), 0.24% TEMED, 0.025% ammonium persulfate, volume up to 4 ml with water, makes enough for two mini-gels) and then resolved at 200 V through the 12.5% running gel until the tracking dye reached the bottom of the gel. Gels were either stained with Coomassie brilliant blue (CBB; 0.25% CBB-R in 40% methanol, 12% acetic acid; stir overnight and filter before use) and destained in 30% methanol, 10% acetic acid or stained with the Silver Stain Plus kit (Bio-Rad) as instructed by the manufacturer.

Western blotting. Proteins were resolved by SDS-PAGE as described for each experiment. Five μl of pre-stained broad range markers were used as standards (Bio-Rad). For 12.5% gels, the electrophoresis was continued until the dye front reached the bottom of the gel. For 17.5% gels, the gels were electrophoresed as described above until the aprotinin marker (6.5 kDa) was ~1 cm from the bottom of the gel, approximately 30-45 min after the blue dye front migrated off of the gel.

The gels to be blotted were soaked in two changes of 1X blotting buffer (20 mM K_2HPO_4), 15 min each. The gels were then blotted to PVDF membranes (Immobilon-P; Millipore; prepared by wetting in methanol, rinsing with water and then soaking in 1X blotting buffer). Western blotting was performed at 30 V for 90 min in a Mini Trans-Blot® Electrophoretic Transfer Cell (Bio-Rad) in 1X blotting buffer as described by the manufacturer. After blotting, the membranes were soaked in dPBS/Tween (500 μl

Tween-20 in 1 L dPBS) for 20 min and then incubated overnight at 4°C in the primary

antibody solution (diluted to the appropriate concentration in 20% fetal bovine serum in

dPBS/Tween; stored at 4°C in 0.02% NaN$_3$).

After the primary antibody was removed, the membranes were washed in five

changes of dPBS/Tween (5 min each). Ten μl of the secondary antibody [hydrogen

peroxidase-conjugated goat-α-rabbit (Bio-Rad); diluted in 25 ml dPBS/Tween] were

added to the membranes for 90 min. After the secondary antibody was removed, the

blots were washed three times in dPBS/Tween for 5 min each. Blots were then rinsed in

several changes of water over 30 min. Before development, the membranes were washed

one time in 1X dPBS for 5 min. For developing each Western, a 4-chloro-1-napthol

tablet (Sigma) was dissolved in 10 ml of MeOH, then 40 ml of dPBS were added,

followed by the addition of 20 μl of 30% hydrogen peroxide. The solution was added to

the membrane. When development was complete, the blots were air-dried for 5 to 10

min and the images were captured by a scanner.

2.2 Chapter 3 methods.

Analysis of the extracellular phage nucleic acid. Nucleic acid was extracted

from cell-free supernatants as described above. To demonstrate the susceptibility of the

DNA to DNase after protein removal, the DNA extracted from 100 μl of PEG-

precipitated sample was resuspended in 20 μl of water instead of TE, and MgCl$_2$ and

RQ1-DNase were added as described above. A sample that was treated with DNase prior

to protein removal and the sample that was treated with DNase post-protein removal were

resolved on 0.5% agarose gels by conventional electrophoresis as described above.

Additionally, similarly prepared samples were resolved on 15-cm agarose gels by FIGE using Program 2 on the PPI-200 programmable power inverter. Electrophoresis was performed for 16 h, after which the gel was stained with EtBr.

To denature DNA samples for the covalently closed ends assay, 10 μl of either recovered extracellular DNA or lp17 DNA were treated with an equal volume of 0.2 N NaOH and incubated at 25°C for 10 min. Four μl of 1 M Tris-HCl (pH 8.0) were added and the sample was incubated at 25°C for 5 min. Samples were prepared and resolved by electrophoresis on 0.5% agarose gels as described above.

To purify the small linear plasmid of *B. burgdorferi* for the covalently closed ends assay, plasmid DNA was extracted from a log-phase *B. burgdorferi* B31 culture with the Wizard Midipreps *Plus* DNA purification system (Promega) as instructed by the manufacturer. Plasmids were resolved by electrophoresis (see above) and sized with the λ monocuts marker (New England Biolabs; Beverly, MA). The linear 17-kb plasmid was excised from the gel and extracted with the QIAEX II gel extraction kit (Qiagen; Valencia, CA) as instructed by the manufacturer.

Visualization of bacteriophage particles. A culture of *B. burgdorferi* CA-11.2A was induced with MNNG and the phage particles precipitated as above. The resuspended particles were ultracentrifuged at 100,000 × g for 0.5 h at 4°C in a TL100 (Beckman; Palo Alto, CA) in a polycarbonate tube (TLA100.2 rotor). The pellet was resuspended in 1 ml SM and ultracentrifuged again at 40,000 × g for 1 h at 4°C in a TL100 (TLA100.2 rotor; polycarbonate tube). The pellet was finally resuspended in 100 μl SM. A drop of precipitated phage suspension was applied to a grid (copper 300-mesh, carbon-coated)

(Ted Pella; Redding, CA). The sample was stained with 1% phosphotungstic acid (PTA) and examined on a Hitachi 7100 transmission electron microscope (TEM). More than twenty-five phage heads and tails were measured and the values averaged to determine approximate size of the phage heads and tails (61). The standard error of the mean was determined (SEM = $\sigma/\sqrt{n}$) for both structures.

Identifying the prophage DNA. Twenty μl of total cellular *B. burgdorferi* CA-11.2A DNA was fractionated on a 0.35% agarose gel by two-dimensional gel electrophoresis as described above. The chloroquine was removed from the gel; the gel was stained with EtBr and destained in water as described above. The gel was vacuum-blotted to Hybond-N$^+$ for Southern hybridization also as described above.

The probes used for hybridization were either total phage DNA, prepared as described above and digested with *Hind*III (New England Biolabs) as instructed by the manufacturer, or a small *B. burgdorferi* probe, *ospC*1-300 (cp26-specific). The probe was generated from a 1:100 dilution of total *B. burgdorferi* DNA by polymerase chain reaction (PCR) using a cocktail as described by the manufacturer of the *Taq* polymerase (Sigma) (cycling parameters: 25 cycles of 92°C for 30 s, 50°C for 30 s, and 72°C for 1 min; diluted 1:100 and amplified a second time) (Table 1).

The probes were labeled by random primer labeling using the Prime-it II kit. Southern hybridization was first performed with total phage DNA as described above using 15 to 20 ml of QuikHyb. The membrane was stripped using the mild stripping protocol described above before being probed a second time with the *ospC*1-300 probe.

Cloning fragments of phage DNA. Phage DNA was subjected to *Hind*III-

digestion as described by the manufacturer (New England Biolabs). The fragments of phage DNA were ligated into the *Hind*III-site of the pBluescript II SK+ cloning vector (Stratagene) using T4 DNA ligase (New England Biolabs) as instructed by the manufacturer. The pBluescript plasmid was previously digested with *Hind*III and the phosphates removed from the ends with calf-intestinal phosphatase (CIP) as instructed by the manufacturer (New England Biolabs). Colonies were screened on plates containing 50 μg ml^{-1} carbenicillin (Sigma) and spread with 15 μl 200 mg ml^{-1} IPTG and 20 μl 5 mg ml^{-1} X-Gal for blue/white screening. White colonies were screened by PCR as described above using the SK/KS primer pair (Stratagene; 25 cycles of 92°C for 30 s, 50°C for 30 s, 72°C for 3 min). About 20 positive colonies were sequenced using the SK primer. The sequences were submitted to a BLAST search (114) to determine homology and identity to known sequences.

Determining bacteriophage titer. Bacteriophage particles were precipitated and resuspended in SM at a 25-fold concentration as described above (10 ml concentrated into 400 μl). The phage DNA was extracted and electrophoresed as described above for initial evaluation of phage content and concentration. Two μl of extracted phage DNA were diluted into 98 μl of water and the optical density was measured at 260 nm. The A$_{260}$ was multiplied by 50 (dilution factor) and the constant of 50 ng μl^{-1} DNA. The resulting number, which gives the concentration of phage DNA in ng μl^{-1}, was divided by the approximate number of ng of DNA per cp32 molecule (one cp32 molecule equal one full φBB-1 genome; the assumption was made that one phage head contains one 32-kb genome). The equation for the number of ng of DNA per cp32 molecule is:

$$32,000 \text{ bp} \times (1 \text{ mol bp} \times [6.0 \times 10^{23} \text{ bp}]^{-1}) \times (640 \text{ g} \times [1 \text{ mol bp}]^{-1}) \times (1 \text{ ng} \times [10^{-9} \text{ g}]^{-1})$$

$$1 \text{ phage genome} = 1 \text{ cp32} = 32,000 \text{ bp} = 3.4 \times 10^{-8} \text{ ng of DNA per phage head}$$

Using this constant and the concentration of the DNA, the number of phage head equivalents in 1 µl of extracted sample can be approximated. Dividing this number by the concentration factor (a combination of both the concentration step from the original supernatant to the PEG-precipitated sample and the concentration step from the PEG-precipitated sample to the resuspended DNA) results in the titer of full-headed phage in 1 µl of original culture supernatant (multiply by 1000 for the more traditional phage ml^{-1} titer value).

Development of an induction protocol. To determine the effective concentration of MNNG for prophage induction, a batch culture was grown to mid- to late-log phase ($\geq 5 \times 10^7$ cells ml^{-1}). The culture was centrifuged at $6,000 \times g$ for 10 min, and the supernatant collected for PEG-precipitation as described above. The cell pellet was resuspended in a volume of BSK complete equivalent to the original culture and then separated into 10 ml aliquots prior to treatment with MNNG (stock concentration is 50 mg ml^{-1} in dimethyl sulfoxide, stored at -20°C) from a range of 0 to 50 µg ml^{-1}. After 2 h of exposure, the cultures were centrifuged at $6,000 \times g$ for 10 min, the supernatant discarded as waste and the cells resuspended in 10 ml of BSK complete and incubated at 34°C for 1 to 2 days. The supernantants were collected and assayed for phage DNA on a 0.5% agarose gel as described above.

To evaluate the kinetics of MNNG-exposure on phage release, a batch culture was grown, centrifuged and the cells were resuspended as described above. The culture was divided into two equal samples. One sample culture was treated with 10 μg ml^{-1} MNNG, split into 10 ml aliquots and incubated at 34°C for 0 to 6 h with a matched untreated control. After recovery, phage DNA was extracted from cell-free supernatants as described above. The DNA was resolved on a 0.5% agarose gel and stained with EtBr.

For the recovery time course, a ~250 ml culture was grown to the appropriate density, centrifuged, the cell pellet resuspended as described above and then split into two aliquots, one treated with 10 μg ml^{-1} MNNG for 2 h and one untreated. After 2 h, both cultures were centrifuged and the cell pellets resuspended in fresh BSK complete. During recovery at 34°C, 10 ml samples were taken from both the treated and untreated cultures every 12 h (up to 108 h) and assayed. The supernatant was assayed for phage DNA as described above. The density of the cell pellet was determined by the A$_{600}$ as described above. The cell density at each time point was compared to the density at the 0 time to determine relative growth and plotted on a logarithmic scale against time.

To assay various isolates for phage production in both untreated and MNNG-treated cultures, isolates were cultured in BSK complete medium as described above. Cells were pelleted at 6,000 × g and the supernatant was collected for PEG-precipitation as described above. The cell pellet was resuspended in a volume of BSK complete medium equal to that of the original culture and the culture was split into two equal aliquots. One aliquot was treated with 10 μg ml^{-1} MNNG as described above, while the other aliquot was handled in the same manner without MNNG treatment and served as an

untreated control. After the 60 h recovery time, supernatants were collected from both

the treated and untreated cultures. Phage was precipitated and the DNA extracted and

resolved on a 0.5% agarose gel by conventional gel electrophoresis as described above.

The gel was stained with EtBr, followed by the more sensitive GelStar nucleic acid stain

(Bio*Whittaker Molecular Applications) as instructed by the manufacturer. After

visualization, the gel was rinsed in water for >1 h to remove excess GelStar stain and

then blotted and hybridized with a cp32-specific probe as described above. The cp32-

specific probe was probe 4 (43), generated by PCR from total phage DNA (25 cycles of

92°C for 30 s, 50°C for 30 s, and 72°C for 1 min; diluted 1:100 and amplified a second

time) (Table 1).

2.3 Chapter 4 methods.

Variable region PCR. A variable region conserved among the cp32 molecules

available in the database (42, 114, 176) was identified by a Clustal analysis (MacVector

6.5.1, Oxford Molecular; Madison, WI) of the *B. burgdorferi* B31 cp32 sequences.

Oligonucleotides, designated VR1, were generated to highly conserved sequences

flanking this region using MacVector (Table 1). The cp32-VR1 reverse primer (27

nucleotides) is conserved on all known cp32s and the cp32 integrated into lp56. The

cp32-VR1 (26 nucleotides) forward primer has one mismatch on cp32-9 and 2

mismatches on lp56, but is conserved on all other known cp32s.

Amplification of VR1 from the different cp32s was performed by PCR. The PCR

mix was 5 units of *Taq* polymerase (Sigma), 1X buffer (supplied by the manufacturer), 4

mM $MgCl_2$, 0.2 mM each dNTP, and 50 pmol of both the VR1F and VR1R primer per

100 μl (remaining volume was water). The amplification was 25 cycles of 92°C for 1

min, 45°C for 1 min, and 72°C for 3 min. The templates used were 1 µl of total DNA, extracted as above, or 1 µl of phage DNA, extracted as described above.

The PCR products were resolved on 0.8% agarose gels subjected to FIGE, as described above. The PPI-200 power inverter was programmed using the GelTimes software (MJ Research) based on a 25-cm agarose gel electrophoresed at 80V (2.6 V/cm) with a maximum resolution in the range of 2 to 6 kb. The time of the electrophoresis was approximately 30 h. The gel was stained with EtBr as above. Variable region sizes were determined using Multi-analyst Software 1.0 (Bio-Rad).

Semi-quantitative PCR. DNA was extracted from uninduced CA-11.2A cells, CA-11.2A cells that were treated with MNNG according to the induction protocol as described above, and phage released from the MNNG-treated CA-11.2A cells. The template DNA was diluted 1:100 in water for amplification.

PCR using the VR1 primers was performed under the conditions described above with some modification. A sample was mixed as described above for each template, then divided into eight 20 µl aliquots. During PCR, an aliquot was removed from the Robocycler Gradient 96 thermocycler (Stratagene) after the extension incubation of every third cycle beginning after the sixth cycle. Samples were collected after cycle 6, 9, 12, 15, 18, 21, 24 and 27 (eight samples for each of the three DNA templates). The samples were electrophoresed and the gel was stained with EtBr as described for the VR1 PCR products above.

Restriction mapping of phage DNA. Phage DNA was extracted from the cell-free supernatants of MNNG-treated *B. burgdorferi* CA-11.2A as described above. The

DNA was subjected to digestion with different restriction enzymes (New England Biolabs) as instructed by the manufacturer. Double digests with enzymes that required different buffers were performed in the optimal buffer suggested by the manufacturer.

Agarose gel electrophoresis was performed by FIGE as described above, with several modifications. The samples were resolved on a 0.8% agarose gel in 0.5X TBE running buffer supplemented with 100 mM glycine at 80 V (4.2 V cm^{-1}) for 16 h. The program for the PPI-200 inverter was determined by the GelTimes software, based on 4.2 V cm^{-1}, a 15 cm gel, and a resolution of 2 to 40 kb. Gels were stained with EtBr as described above. After visualization, the gels were destained in water and then vacuum-blotted to Immobilon-Ny$^+$ (we have found this to be a superior membrane for multiple probing/stripping cycles) as described above.

Southern hybridization was performed as described above with the following modifications. The probes used were the cp32-specific probes, probe 4 and probe 2 (43), a probe to the *blyB* operon (B) of cp32 kindly provided by Don Oliver (Wesleyan University, Middletown, CT) (50, 75), and two probes that were generated for this work, the VR1 probe (V) and a probe that flanks an *Nde*I-site (N) at the ~20,000 bp region (see Figures 12 and 25). Probes 4, 2 and the *blyB* probe were generated by PCR as described for probe 4 above. Probe N was generated with the cp32SK*Nde*I primers (Table 1) essentially as described for probe 4, except an annealing temperature of 44°C was used. The V probe was generated using the cp32VR1 primers (Table 1) as described above.

Hybridization was carried out in hybridization solution for ≥ 6 h at 68°C. The blots were washed as described above, wrapped in cellophane and exposed to Fujifilm

RX film for 16 to 24 h at -80°C with intensifying screens, as described above.

Approximate sizes of the dominant fragments were determined manually by comparison

to markers of known sizes and assembled into partial restriction maps. Blots to be

reprobed were stripped in successively harsher solutions as described above until the

previous probe was completely removed so that the next probe could be applied.

Size comparison of phage DNA and linearized CA-11.2A cp32s. CA-11.2A

plasmids were extracted using Wizard Midipreps *Plus* as described above and digested

with *Apa*I, *Bsu*36I, *Msc*I, and *Nru*I, enzymes that are known to cut B31 cp32s once or not

at all (42, 114, 176). Based on Southern hybridization with probe 4 as above, *Bsu*36I was

selected as an enzyme that linearizes at least one of the CA-11.2A plasmids. Undigested

phage DNA extracted as described above and *Bsu*36I-digested CA-11.2A plasmid DNA

were resolved on 0.8% agarose gels by FIGE for 30 h as described above. The

electrophoresis parameters were based on resolving fragments between 30 and 35 kb on a

15-cm gel. The gel was stained with EtBr. To confirm which digested fragment was the

linearized cp32, the gel was blotted and hybridized with probe 4 as described above.

Characterizing the permutation of φBB-1 DNA. Phage DNA was extracted

from the cell-free supernatants of MNNG-treated CA-11.2A cells as described above. A

small aliquot of DNA was tested to assay susceptibility to restriction digestion (we

suggest this as a routine step, because there is batch-to-batch variation between

preparations, based on the effectiveness of PEG removal). Ten µl of susceptible phage

DNA was digested with *Hind*III as instructed by manufacturer. The DNA was then

subjected to FIGE using program 2 as described above, but a 25-cm gel was used and the

electrophoresis time was extended to 26 h. The gel was stained with EtBr and visualized as described above. After visualization, the gel was vacuum-blotted to Hybond-N$^+$ as described above.

An additional 10 µl of phage DNA from the same preparation was treated with calf-intestinal alkaline phosphatase (CIP) (New England Biolabs) as instructed by the manufacturer. The CIP was inactivated at 75°C for 10 min in the presence of 5 mM EDTA, then extracted with phenol:chloroform and precipitated with EtOH. The DNA pellet was resuspended in 10 µl water and then end-labeled with [γ^{32}P]-dATP using T4 polynucleotide kinase (New England Biolabs) as instructed by the manufacturer. The probe was purified by passage through a G-50 spin column. The end-labeled phage DNA was then subjected to digestion with HindIII for 4 h at 37°C.

Southern hybridization of the blot of the HindIII-digested DNA was performed as described above using the end-labeled, digested phage DNA probe. After the final stringency wash, the film was wrapped in cellophane and exposed to Fujifilm RX film for 7 to 10 days at -80°C with intensifying screens.

2.4 Chapter 5 methods

Cesium chloride purification of phage. Phage particles were precipitated from cell-free supernatants as described above. Cesium chloride (CsCl)-gradients were prepared in 2.2 ml polyallomer tubes (Beckman). Three hundred µl of 1.7 g ml^{-1} CsCl, 400 µl of 1.5 g ml^{-1} CsCl, and 200 µl of 1.3 g ml^{-1} CsCl were carefully layered successively into the centrifuge tubes and the remaining volume (~1.3 ml) was filled with precipitated sample. The gradients were centrifuged at 104,000 x g in a TL100

ultracentrifuge for 4 h at 4°C using a swinging bucket rotor (TLS55). Fractions from

the gradient were collected successively from the top of the centrifuge tubes in 400 µl

aliquots. Fraction five, containing intact φBB-1 particles, was saved and pooled from

multiple gradients. The fractions were dialyzed against 0.5 to 1 L SM using a

microdialyzer (Gibco-BRL; Rockville, MD) and dialysis membrane with a molecular

weight cut-off of 12-14 kDa (Gibco-BRL). Two hundred µl of the dialyzed sample was

saved and the rest of the sample was applied to another CsCl-gradient. This was repeated

a third time. Five µl of each dialyzed sample and an undialyzed sample of the original

PEG-precipitated material was resolved by SDS-PAGE on 12.5% polyacrylamide gels as

described above.

Phage DNA was extracted from 50 µl of each sample and resolved on 0.5%

agarose gels at 50 V (4 V cm^{-1}) for 3 h by conventional gel electrophoresis and stained

with EtBr as described above. A drop of the phage-containing fraction from the third

gradient was stained with 1% PTA and analyzed by TEM as described above.

In preparation for N-terminal sequencing, proteins were resolved by SDS-PAGE

as described above. After electrophoresis, the gels were transferred to Immobilon-P as

described above in the Western blotting protocol. After the transfer, the membrane was

stained in CBB (prepared for this purpose; 0.25% CBB-R in 50% methanol), destained in

50% methanol and air-dried. The band of interest was excised and stored at -20°C until

submission for sequencing.

Preparation and analysis of a low protein medium. For the low protein

medium, a basal solution was made containing 8% (v/v) 10X CMRL-1066 (without L-

glutamine and sodium bicarbonate; Gibco-BRL), 4 g L^{-1} Neopeptone (Difco), 1.6 g L^{-1}

Yeastolate (TC; Difco), 6 g L^{-1} N-2-hydroxyethylpiperazine-N''-2-ethanesulfonic acid

(HEPES), 4 g L^{-1} glucose, 0.56 g L^{-1} sodium citrate, 0.64 g L^{-1} sodium pyruvate, 0.32 g

L^{-1} N-acetylglucosamine, 1.76 g L^{-1} sodium bicarbonate and 5 ml L^{-1} glycerol (adjust to

pH 7.6 with 1 N NaOH, adjust volume with water and sterilize by filtration through a

0.22-μm filter) (14, 36, 136). For the serum requirement experiment, 40 g L^{-1} bovine

serum albumin (BSA; fraction V, Pentax; Miles) was added prior to sterilization. Rabbit

serum (trace hemolyzed; Pel-Freez Biologicals) was added to smaller aliquots of the

basal medium in the required percentage (0 to 8% over nine 10 ml aliquots) and the

medium was filtered again through a 0.22-μm filter. To determine the BSA requirement,

the basal medium was made with 3% rabbit serum, filtered, and split into smaller

samples. BSA was added in the appropriate amount (ranging from 0 to 40 g L^{-1} over

eight 10 ml aliquots) and the solution was filtered again. To assess the ability of CA-

11.2A cultures to produce φBB-1, cultures were treated with MNNG as described above.

After treatment, cells were pelleted and resuspended in the samples of low-protein

medium formulated as described. After recovery, the supernatants were collected, the

phage was precipitated, and the DNA extracted as described above.

The final low protein medium (BSK-che1) used for the analysis of possible phage

proteins is the basal medium described above with no exogenous BSA added and 3%

rabbit serum. CA-11.2A cultures were treated with MNNG as described above, the cells

washed once in BSK-che1 and resuspended finally in a volume of BSK-che1 equal to that

of the original culture. After the recovery period, samples of φBB-1 were precipitated

from BSK-che1 as described above. After PEG-precipitation, 6 μl of 4X SDS- PAGE

loading dye was added to 18 μl of either the precipitated phage sample or the BSK-che1

control. Proteins were resolved on 12.5% polycrylamide gels by SDS-PAGE as

described above. Proteins were prepared for N-terminal sequencing as described above.

Protein extracts for BlyA and BlyB analysis. 200 ml cultures of *B. burgdorferi*

B31, CA-11 and CA-11.2A were grown to log phase, then split into two equal aliquots.

One of the aliquots was treated with 10 μg ml^{-1} MNNG as described above, with the

untreated control treated in the same manner without chemical induction. After the

appropriate recovery time (~60 h), 10 ml aliquots were collected from each sample for

protein extracts. The cells were pelleted at 8,000 × g for 10 min at 4°C, washed in 1 ml

dPBS^{++} (dPBS containing 0.1 g L^{-1} CaCl$_2$, 0.213 g L^{-1} MgCl$_2$•6 H$_2$O), pelleted again at

14,000 × g for 5 min at 4°C in a microfuge, and finally resuspended in 1 ml of dPBS^{++}.

The density of the cells by A$_{600}$ was determined and the cells were centrifuged at 14,000

× g as above, and resuspended in an amount of water in μl equal to the determined A$_{600}$

multiplied by 200. An equal volume of 2X SDS-PAGE loading dye was then added and

the sample was boiled for 5 min. As a control, MM294 cells (*E. coli*) containing a

plasmid (pTG3) that expresses *blyA* and *blyB* (75) were grown in 50 μg ml^{-1} carbenicillin

overnight. Whole cell lysates were extracted from these cells as described for the *B.*

burgdorferi cells.

Lysates were resolved on 17.5% polyacrylamide by SDS-PAGE (prepared as for a

12.5% gel, except with 17.5% polyacrylamide) as described above. Five μl of each

protein extract (B31 –MNNG/ +MNNG, CA-11 -/+, CA-11.2A -/+ and MM294 control)

were loaded onto each of four gels, so that the gels were identical to each other. The electrophoresis time was extended until approximately 30 to 45 minutes after the dye front had migrated off the bottom of the gel. After electrophoresis, one gel was stained with CBB and destained as described above. The other gels were blotted to Immobilon-P as described above. The membranes were probed with the following primary antibodies, each diluted 1:5000 from stock: BlyA, BlyB (stock IgG antibodies generated from rabbits and provided by Damman and Oliver) or OspC [stock IgG antibody generated from a rabbit and provided by Tom Schwan (149)].

BlyA and BlyB localization. A 100-ml culture of log phase CA-11.2A cells was treated with MNNG as described above. After recovery, the cells were pelleted at 6,000 × g at 4°C for 10 min. The cell pellet was resuspended in 2 ml of ice-cold TBSP (20 mM Tris-HCl [pH 7.4], 150 mM NaCl, 5 mM EDTA, 1 mM PMSF) and pelleted again at 14,000 × g for 10 min at 4°C. The pellet was resuspended in 2 ml of TBSP and then sonicated (8 cycles of 30 s at 3.5, 1 min recovery on ice). Cell lysis was evaluated by dark-field microscopy at 100X magnification. Unlysed cells were removed by centrifugation at 6,000 × g for 10 min at 4°C. The cell extracts were centrifuged at 100,000 × g for 3 h at 4°C in a TL100 (TLA100.2 rotor; polycarbonate tubes). This centrifugation gave rise to a supernatant fraction (S100) and a pellet fraction (P100). The P100 was resuspended in a volume of TBSP equivalent to the S100 fraction. For SDS-PAGE analysis, 2× SDS-PAGE loading dye was added to each fraction and the sample was boiled for 5 min. The protein samples were resolved on 17.5% polyacrylamide gels

as described above. Matched gels were blotted to Immobilon-P for Western blotting

with the BlyA and BlyB antibodies as described above.

RNA extraction. 100 ml cultures of B31 and CA-11.2A were prepared as

described for protein extraction above. The cultures were centrifuged at 6,000 × g for 10

min and the supernatants collected for PEG-precipitation as described above. All

subsequent steps were performed with sterile-filter tips, autoclaved glassware and

solutions used only for RNA experiments and prepared with diethyl pyrocarbonate

(DEPC)-treated water (100 μl DEPC in 1 L of water, let stand overnight, then autoclave).

RNA extraction was done using the Trizol reagent (Sigma) as described by the

manufacturer. The cell pellets were resuspended completely in 10 ml Trizol and

incubated at room temperature for 5 min. After 5 min, 2 ml of $CHCl_3$ was added, the

sample mixed vigorously and incubated at room temperature for 3 min. The sample was

then centrifuged at 12,000 × g for 15 min at 4°C. The aqueous phase was recovered and

5 ml of isopropanol was added to the sample, mixed and then incubated at room

temperature for 10 min. The RNA was pelleted at 12,000 × g for 10 min at 4°C. The

RNA pellet was resuspended in 10 ml of 75% EtOH and centrifuged again at 7,500 × g

for 5 min at 4°C. The RNA pellet was air dried for 10 to 15 min and then resuspended in

50 to 100 μl of DEPC-treated water. The sample was incubated at 55 to 60°C for 10 min.

The optical density at A_{260} was determined and multiplied by a factor of 40 μg ml^{-1} and

the dilution factor to determine concentration. The RNA was stored at -80°C.

Northern Analysis of *blyAB* RNA. For resolution of RNA to be probed, a 150

ml 1.2% gel was poured. 1.8 g GTG agarose was dissolved in 130.5 ml of DEPC-treated

water, cooled to 65°C, and 15 ml of 10X MOPS running buffer (0.4 M 3-[N-Morpholino]propane-sulfonic acid [MOPS], 0.1 M sodium acetate, 0.01 M EDTA, in DEPC-water; autoclave to sterilize) and 4.5 ml formaldehyde was added prior to casting the gel in a 15 × 15 cm tray. Ten to 15 μg of RNA were resolved for each sample (B31 -/+, CA-11 -/+, CA-11.2A -/+). The RNA was mixed in 50% formamide, 1X MOPS, 16% formaldehyde, and DEPC-water (total volume ~30 μl). After mixing, the sample was heated for 10 min at 55°C and 1X formaldehyde loading buffer (6X formaldehyde loading buffer: 1 mM EDTA, pH 8.0, 0.25% [w/v] BPB, 0.25% [w/v] xylene cyanol, 50% [v/v] glycerol) and 0.02 μg μl^{-1} EtBr was added. Samples were loaded onto the gel so that each half of the gel was identical to the other.

The RNA was resolved at 70 V (3.7 V cm^{-1}) for 3 to 4 h (until the dye front had migrated three-fourths the length of the gel). After electrophoresis, the gel was washed in two changes of DEPC-water for 10 min. Vacuum blotting of the gel was performed under 50 mbar of pressure. The gel was blotted to Immobilon-Ny$^+$ using DEPC-water for 10 min, denaturing solution (50 mM NaOH, 1.5 M NaCl) for 10 min, neutralization solution (0.5 M Tris-HCl [pH 7.4], 1.5 M NaCl) for 10 min followed by 20X SSC for 3 h (all solutions made in DEPC-water). The membrane was cross-linked using a UV Stratalinker 1800 (Stratagene) as described above and air-dried on clean 3MM filter paper.

For Northern hybridization, the membrane was cut in half and both halves were rehydrated in 6X SSC (in DEPC-water). Before addition of either the *blyA* or *blyB* probe, the membranes were prehybridized for 15 to 20 min at 42°C in 20 ml of 5X SSC, 1%

SDS, 5X Denhardt's, 50% formamide with 1 mg of sheared salmon sperm DNA (DNA

is denatured and cooled prior to addition). The probes for Northern hybridization were

generated as for Southern hybridization (see above) using the Prime-it II labeling kit

(Stratagene) as per the manufacturer's instructions. The probes labeled were fragments

of DNA generated by PCR (as described for probe 4 above) with either the *blyA* or *blyB*

primers (Table 1). The probes were boiled, chilled, and added to the prehybridized

membrane and hybridization was performed overnight at 42°C.

After hybridization, the membranes were washed twice with 2X SSC-0.1% SDS

at room temperature for 10 min each. This was followed by a high stringency wash of

0.2X SSC-0.1%SDS at 42°C for 1 h. The membranes were then wrapped in cellophane

and exposed to Fujifilm RX film in a cassette with an intensifying screen as described for

Southern hybridization above.

2.5 Chapter 6 methods

Construction of pCE210. We constructed a plasmid for the insertion of the

kanamycin-resistance cassette into prophage DNA. *Hind*III-digested φBB-1 DNA was

ligated into the pBluescript II SK$^+$ vector as described in the methods for chapter 3. This

generated plasmids that contained phage DNA fragments of various sizes less than 4 kb.

Three of the largest clones, SK6, SK12, and SK19 were found to be virtually identical

when ~400 base pairs of one end of each fragment was sequenced. All had inserts that

were ~3.5 kb. For continued analysis, the plasmid containing SK12 was selected and

renamed pCE100.

The SK12 phage DNA insert was amplified from pCE100 using the SK/KS

primer pair as described in the chapter 3 methods. With the amplified insert as a

template, a survey of several different restriction enzymes revealed that *Nde*I cut the

phage insert once, leaving two bands of ~1.1 kb and ~2.4 kb, sizes suitable for

homologous recombination into a locus of prophage DNA in *B. burgdorferi* cells.

pTAKanG, the plasmid containing the kanamycin-resistance-cassette (kan^R), was

obtained from Jim Bono (Rocky Mountain Labs, Hamilton, MT). This plasmid encodes a

fusion of the *B. burgdorferi flgB* promotor and the kan^R from pOK12, which was

performed by ligation of *Nde*I overhangs (28). To insert the kanamycin-cassette into the

*Nde*I site of the phage insert, pCE100 was linearized by digestion with *Nde*I according to

the manufacturer's instructions. The plasmid containing the *flgB* promoter/kan^R fusion

was digested with *Eco*RI. *Eco*RI sites flank the insertion site in the multiple-cloning site

of the pCR®2.1 vector that is the backbone of pTAKanG. The digested kanamycin-

resistance cassette was resolved on a 0.8% agarose gel as described above and the ~1.3

kb band was gel purified using the QIAEX gel extraction kit (Qiagen) as instructed by the

manufacturer. Both the linearized pCE100 and the purified kan^R were treated with Mung

Bean nuclease (MBN; New England Biolabs) to blunt the ends of the DNA as instructed

by the manufacturer.

After MBN treatment, the enzyme was inactivated by adding SDS to a final

concentration of 0.01%, followed by an EtOH-precipitation as recommended by the

manufacturer. The vector and insert were ligated together using T4 DNA ligase. After an

overnight ligation at 25°C, the product was transformed into chemically competent cells.

One hundred μl aliquots were plated on LB plates containing 50 μg ml^{-1} kanamycin

(LB agar:10 g Tryptone B, 5 g yeast extract, 10 g sodium chloride and 15 g Bactoagar

[Difco] per liter; the solution was autoclaved, cooled to 65°C, 1 ml of a 50 mg ml^{-1}

kanamycin stock solution was added and ~30 ml of the agar was poured into each 100

mm petri dish). The competent cells were prepared using a $CaCl_2$-solution essentially as

described elsewhere (10, 76). The plates were incubated at 37°C for 12-14 h. Colonies

were screened using the SK/KS primer pair (~5-kb fragment), followed by PCR with a

combination of one of the SK/KS primers and one of the cp32SK12NdeI primer pair

(junctional PCR) to check the orientation of the insertion. The product of PCR from

pCE100 with the SK/KS primers was used as a negative control. One of the clones that

contained the kan^R cassette was selected and designated pCE210.

Generating kan^R-transformants of *B. burgdorferi* CA-11.2A. pCE210 was

digested with BssHII, cutting the insert out of the plasmid that contains ampicillen-

resistance. The DNA was resolved on a 0.5% agarose gel and the insert containing the

φBB-1 DNA/kan^R-cassette hybrid was extracted with the QIAEX gel extraction kit. Ten

μl of the purified insert DNA (~2 μg) was electroporated into competent *B. burgdorferi*

CA-11.2A cells. The preparation of *B. burgdorferi* competent cells, the transformation

protocol, and the plating in solid medium were performed as described previously (136).

Transformants were selected in 500 μg ml^{-1} kanamycin. The plates were incubated at

34°C for 7 to 10 days until colonies were visible.

Colonies were screened by PCR (92°C 30 s, 44°C 30 s, 72°C 1 min) using the

cp32SKNdeI primers that flank the insertion site. PCR products were resolved on 1%

agarose gels and stained with GelStar nucleic acid stain. Clones containing the ~1.2-kb kan^R-insertion were picked using a Pasteur pipette and inoculated into 10 ml of BSK-complete supplemented with 500 μg ml^{-1} kanamycin.

Analysis of transformants. CA-11.2A/kan^R transformants were cultured until log phase. Aliquots were removed from each sample and stored in 20% glycerol at -80°C. The remaining cultures were centrifuged at 8,000 × g for 10 min at 4°C to pellet the cells. The supernatant was removed and phage particles PEG-precipitated as described above. The cell pellets were washed once in dPBS, pelleted in a microfuge at 14,000 × g for 5 min and finally resuspended in 100 μl TES. SDS and PK were added and the DNA was extracted as described above.

Chromosomal DNA was resolved by two-dimensional electrophoresis as described above. The gel was stained, destained and vacuum blotted to Immobilon-Ny$^+$ as described above. Southern hybridization was performed using either the cp32-specific probe 4 prepared by PCR, or pOK12 that was extracted from *E. coli* cultures using Wizard Midipreps *Plus*. Probes were labeled using the Prime-it II kit. Phage DNA extracted from the transformants' supernatants was also resolved by FIGE, blotted and probed with probe 4 and pOK12 as described above.

Transduction of an antibiotic-resistance marker. To assess the transduction of the kan^R-marker by φBB-1 released from the *B. burgdorferi* CA-11.2A/kan^R transformant, we purified phage particles from a 100-ml culture of late log phase MNNG-treated cells. The titer of the final sample was approximately 10^{11} phage ml^{-1} of the final resuspension in SM, as assayed by DNA concentration and calculated as described above.

For transduction, ϕBB-1/kan^R(CA-11.2A) samples were taken from the stock and treated with 10% CHCl$_3$ to eliminate possible contamination, incubated at room temperature for 15 min, then centrifuged at 14,000 × g and the aqueous phase recovered. Sterile 1 M MgCl$_2$ was added to the sample to bring the final Mg^{2+} concentration to 16 mM and 1 µl RQ1 DNase was added per 250 µl of volume. After 0.5 h at 37°C, 100 µl ($\sim10^{10}$ phage) of the prepared phage sample was mixed with 10^7 cells (1000:1) and BSK complete was added for a final volume of 1 ml. As controls, a sample of phage preparation was incubated in 1 ml without cells, and a sample of 10^7 cells was incubated in 1 ml without phage. A sample of the ϕBB-1/kan^R (CA-11.2A) was also incubated with PK prior to addition to the cells, as another negative control.

The samples were incubated at 34°C overnight. After ~16 h of incubation, the phage/cell mixtures were plated in solid medium and selected with 500 µg ml^{-1} kanamycin as described elsewhere (136). Colonies were picked and screened by PCR with the cp32SKNdeIF and Kan^{R}1207F primers using the parameters as for the cp32SKNdeI primer pair. Positive clones were picked into 10 ml of BSK-complete with 500 µg ml^{-1} kanamycin.

When the putative transductants reached late log phase, aliquots were removed and frozen in 20% glycerol at −80°C. DNA was extracted from the remainder of the culture and the clones were screened again by PCR for the kan^R-cassette using the above primers as well as the flanking cp32SKNdeIF and cp32SKNdeIR primers (PCR was performed as above; 25 cycles of 92°C 30 s, 44°C 30 s, 72°C 1 min). Transduction assays for other strains were done essentially as described above.

To evaluate the ability of DNA to transfer between dead kan^R-transformed cells

and live cells, mimicking the phenotype produced by transduction, 10^8 CA-11.2A/kan^R

cells were treated with 50% chloroform, followed by two treatments with 10%

chloroform to duplicate the organic conditions under which ϕBB-1/kan^R (CA-11.2A) was

purified. The aqueous phases from these treatments were recovered, treated with DNase,

and incubated with 10^6 live CA-11.2A cells. As a control, a sample of the dead CA-

11.2A/kan^R cells prepared as described was also treated with PK prior to mixing with the

live cells. A sample of dead CA-11.2A/kan^R cells prepared as above were also plated in

the absence of selection to assess viability.

Analyzing the transductant variable regions. Amplification of the variable

regions of the parental and transduced strains was done as described in the chapter 4

methods. DNA was resolved on a 0.8% agarose gel was done by FIGE as described for

VR1 above, except a time of 30 h was used. The gel was stained with EtBr and the

image captured on the Gel Doc 1000 system. Sizes of the variable regions were

determined using the Multi-Analyst software.

For cloning, amplified variable regions from DNA of both the parental and

transductant cells were resolved by FIGE on a 0.8% agarose gel as described above,

except the gel was electrophoresed for 36 h. After visualization by EtBr-staining, the

bands of interest were extracted from the 0.5X TBE gel using the QIAEX gel extraction

kit.

After gel extraction, 13.4 μl of the DNA were mixed with 1 μl of *Taq* polymerase

(5 U), 2 μl 10X *Taq* PCR buffer, 3.2 μl 25 mM MgCl$_2$, and 0.4 μl 10 mM dATP. The

DNA was polyadenylated at 72°C for 0.5 h. The tailed DNA was cloned into the

pCR®2.1-TOPO vector in TOP10F' cells using the TOPO TA Cloning® kit (Invitrogen;

Carlsbad, CA) as instructed by the manufacturer. The colonies were screened for the loss

of β-galactosidase activity as described above and possible positive (white) colonies were

selected. These colonies were screened using the cp32VR1 primers.

Analysis of recombinants. Plasmid DNA was extracted from log phase cultures

of CA-11.2A, CA-11.2A/kan^R, CA-11.2A TR3, B31, B31 TR1, 1A7 and 1A7 TR5 using

the Wizard *Plus* Midi preps. CA-11.2A TR3, B31 TR1, and 1A7 TR5 are the

kanamycin-resistant strains generated by transducing the kan^R-cassette into the parental

strains CA-11.2A, B31 and 1A7 with φBB-1/kan^R (CA-11.2A). The concentration of

DNA was determined by measuring the absorbance at 260 nm. 500 ng of DNA was

digested with either *Eco*RV or *Xba*I. The DNA was resolved on a 0.8% agarose gel by

FIGE as described for the mapping gels in chapter 4. The gels were electrophoresed for

14 h.

The gels were stained with EtBr as described, then destained, documented, and

vacuum-blotted as described above. The blots were probed with the cp32SK*Nde*I PCR

product (amplified from total CA-11.2A DNA as described above and amplified a second

time using 1 μl of the first PCR as the template) as described above. After exposure to

film, the blots were stripped and then probed with pOK12, the source of the kan^R-gene.

Table 1. Oligonucleotides used in this study.

Name[1]	Template	Sequence (5'-3')
CP-4 (probe 4)	cp32 DNA	AATACGTTGATCATGCGAAATGAC
CP-5 (probe 4)	cp32 DNA	TTACTTTCTACCATATGGGCTTGCC
cp32SK12*Nde*IF (N)	cp32 DNA	ACTTTGTTGTAGTGATTATTTGTTC
cp32SK12*Nde*IR (N)	cp32 DNA	GGGGAAAGAATTGTTGAAG
cp32-VR1F (V)	cp32 DNA	AAATAAAACTTAGGAGTTGGTTTTGAA
cp32-VR1R (V)	cp32 DNA	TAACTTTCCTAGCGTTAACTTCTGAT
ERP-177 (probe 2)	cp32 DNA	GAAAAGCCCATTAAAGATAGGTTG
ERP-178 (probe 2)	cp32 DNA	AAGTAACAACCCCATTTTTGTATCTCC
Kan[R]1207F	*kan*[R]-cassette	ATTACGCTGACTTGACGGG
ospC 1F	cp26	AGACTAATAAAATAATAAGAATA
ospC 300R	cp26	GTATTTTGACTCAAAACTTTA
rev7 (*blyA* probe)	cp32 DNA	CAGAACTTCTTATCAAT
rev08 (*blyA* probe)	cp32 DNA	GCCATTACCATTGCC
rev8 (*blyB* probe: B)	cp32 DNA	CCAAAGATAATGTTG
rev06 (*blyB* probe: B)	cp32 DNA	GATCTATGTTTGTATC

[1] designations in parentheses are the names used for the probes generated from those primers (refer to text)

Chapter 3

Identification of a new phage of *Borrelia burgdorferi*

[adapted from Eggers and Samuels, 1999 (63)]

We recovered extracellular nucleic acid from cultures of a California strain of *B. burgdorferi*. This nucleic acid had properties characteristic of a genome packaged within a bacteriophage capsid. Consistent with this hypothesis, electron micrographs of supernatant material containing the extracellular nucleic acid exhibited characteristic bacteriophage-like particles. We report here the physical properties of the packaged nucleic acid, the structural features of the bacteriophage capsid, and the induction of a previously unreported lysogenic prophage. Based upon our molecular characterization we have named this bacteriophage ϕBB-1.

Isolation of extracellular DNA. Nucleic acid was recovered from PEG-precipitated cell-free supernatants of late log phase cultures of *B. burgdorferi* strain CA-11.2A (Figure 2). This nucleic acid was protected from DNase through two chloroform treatments (Figure 2, lane 1). When precipitated samples containing the nucleic acid were first treated with PK and SDS, and extracted with organic solvents prior to DNase addition, the nucleic acid became sensitive to DNase digestion (Figure 2, lane 2). This protein-mediated nuclease protection would be expected of a bacteriophage capsid. The extracellular nucleic acid is resistant to RNase (data not shown). The nucleic acid migrates as an approximately 32-kb molecule when resolved by either field inversion (Figure 2, lane 1; black arrow) or conventional (Figure 3, lane 1) gel electrophoresis. Circular molecules migrate differently under these two conditions. During conventional field gel electrophoresis, supercoiled circular molecules migrate faster than linear

+	+	pre-DNase
+	+	SDS/PK
-	+	post-DNase

48.5 -
38 -
33.5 -

24 -

17 -
15 -

10 -

1   2
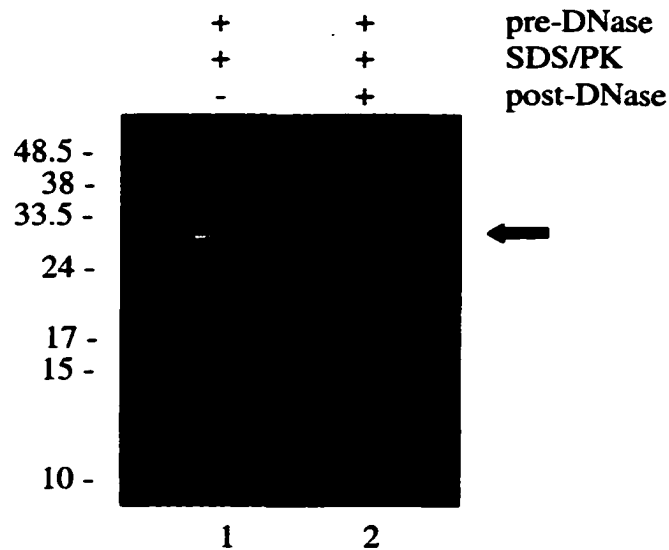
Figure 2. Protein-mediated protection of extracellular nucleic acid from DNase. Cell-free supernatants of *B. burgdorferi* strain CA-11.2A cultures were PEG-precipitated and treated twice with chloroform. Samples of these precipitates were subjected to digestion with DNase I prior to DNA extraction (lanes 1 and 2). The proteins were then degraded by adding SDS and PK (lane 1 and 2). The DNA was extracted with organic solvents, precipitated and either loaded directly onto a 0.8% agarose gel (lane 1) or subjected to another digestion with DNase I and then loaded onto the agarose gel (lane 2). The DNA was resolved by FIGE and visualized by EtBr-staining. The arrow indicates the ~32-kb linear double-stranded DNA. Molecular sizes are in kilobase pairs.

equivalents, but the migration of these circular molecules is retarded when subjected to field inversion electrophoresis (80, 155). Because of the similarity of the electrophoretic mobility under these two conditions, the resistance to RNase-digestion and the conditional susceptibility to DNase, we have concluded that the extracellular nucleic acid is a double-stranded, linear DNA molecule. In addition, when observed by electron
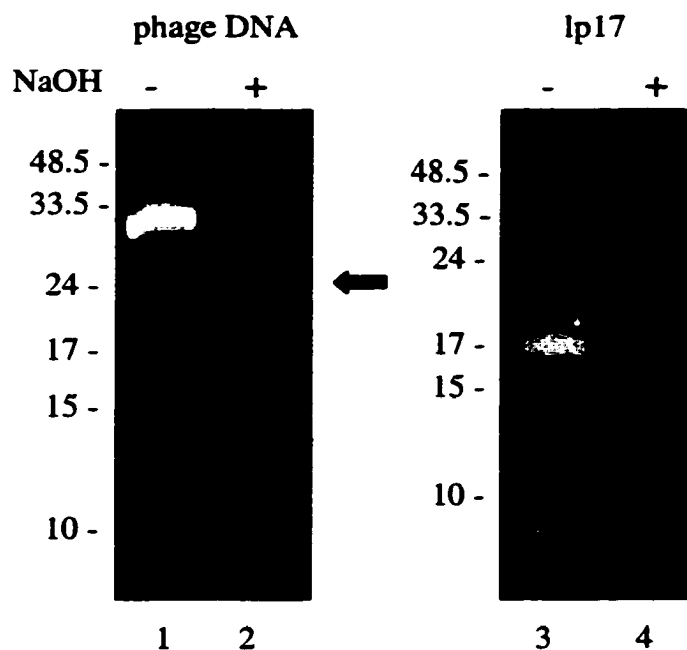
Figure 3. Denaturation of extracellular phage DNA. DNA denatured with 0.2 M NaOH (+) and an untreated control (-) were resolved on a 0.5% agarose gel by conventional field electrophoresis. The arrow indicates single-stranded DNA products generated by the denaturation of non-covalently closed double-stranded phage DNA (lane 2). The control molecule, lp17, contains covalently closed ends and reanneals to regenerate a double-stranded DNA molecule (lane 4). The gel was stained with EtBr. Molecular sizes are in kilobase pairs.

microscopy, the nucleic acid appears to be a double-stranded, linear ~32-kb DNA molecule with no gross secondary structure (102). We have proposed that this DNA is the genome of a temperate bacteriophage of *B. burgdorferi*.

All of the linear DNA molecules of *B. burgdorferi* have covalently closed ends (Figure 1) (18, 41, 68, 81, 83, 84). To characterize the ends of the linear bacteriophage DNA, a sample was denatured with NaOH, producing single-stranded products (Figure

3, lane 2). When DNA lacks covalently closed ends, the single stranded molecules generated during denaturation cannot "snap back" and regenerate a double-stranded DNA molecule (Figure 3, lane 2; black arrow). As a control, the small linear plasmid of the *B. burgdorferi* genome, lp17, was exposed to the same conditions (Figure 3, lane 4). lp17 has covalently closed ends (18, 84) and reannealing occurred rapidly during a brief recovery period after denaturation (Figure 3, lane 4). The DNase-protected phage DNA did not rapidly reanneal, indicating both the double-stranded nature of the molecule and the lack of covalently closed ends.

Visualization of bacteriophage particles. Phage ultrastructure was examined by TEM (Figure 4). The phage heads appeared isometric with a diameter of 46 ± 1.4 nm. The contractile tails were approximately 92 ± 4 nm × 10 ± 0.9 nm. In the PEG-precipitated preparation (Figure 4A), both empty (darkly stained) and intact heads (lightly stained) were observed. A large percentage of the observed particles were no longer intact. The empty heads could be due to inefficient packaging into the procapsid or this phenomenon may be an artifact of purification and staining. After further purification on CsCl gradients, preparations that contain only full heads were recovered (data not shown). However, the extra purification step sharply decreases the yield of phage DNA recovered per ml of original supernatant. The contractile tail was observed in both the extended and contracted conformation (Figure 4B). The bacteriophage we report here has not yet been seen in association with *B. burgdorferi* cells. We have designated this bacteriophage φBB-1.

A.   B.
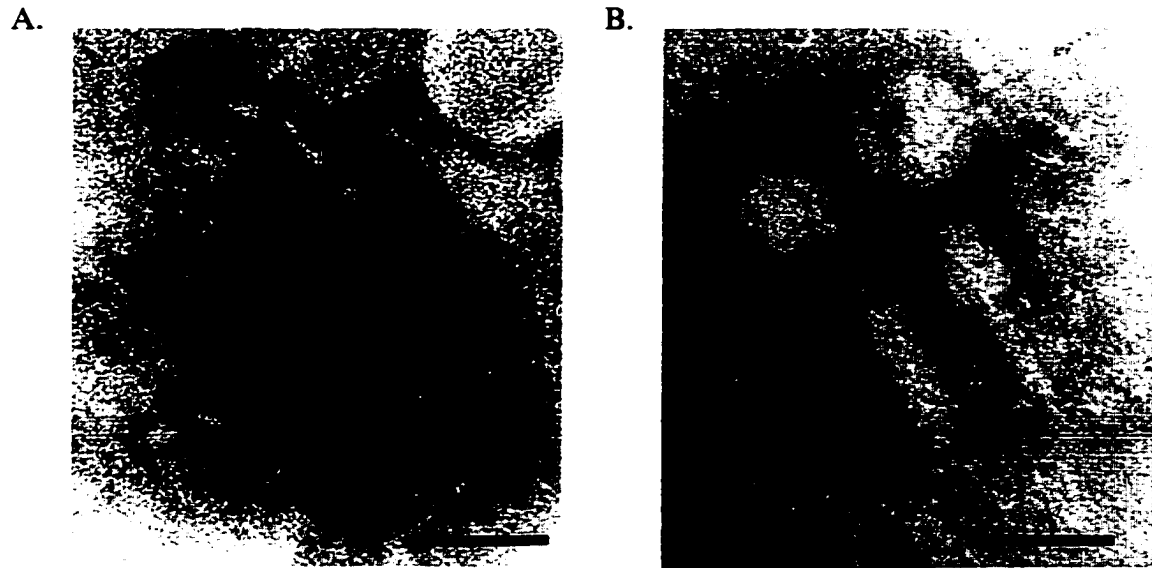
Figure 4. *B. burgdorferi* phage particles. Samples were collected from PEG-precipitated cell-free supernatants of an induced culture of *B. burgdorferi* CA-11.2A and viewed by TEM. (A) Both tailless and complete phage particles were visible, including intact heads. Phosphotungstic acid stain; magnification, ×175,000 (bar = 115 nm). (B) High magnification of the intact phage particles. The contractile tail is either extended (left) or contracted (right). Phosphotungstic acid stain; magnification, ×270,000 (bar = 45 nm).

The lysogenic prophage. To identify the genomic location of the φBB-1 prophage within the *B. burgdorferi* genome, total cellular *B. burgdorferi* CA-11.2A DNA was resolved by two-dimensional agarose gel electrophoresis (Figure 5, left). The DNA was electrophoresed in the presence of chloroquine, a DNA intercalater, in the second dimension. This is an effective technique for differentiating between the circular and linear elements of the *B. burgdorferi* genome. Chloroquine introduces positive writhe,
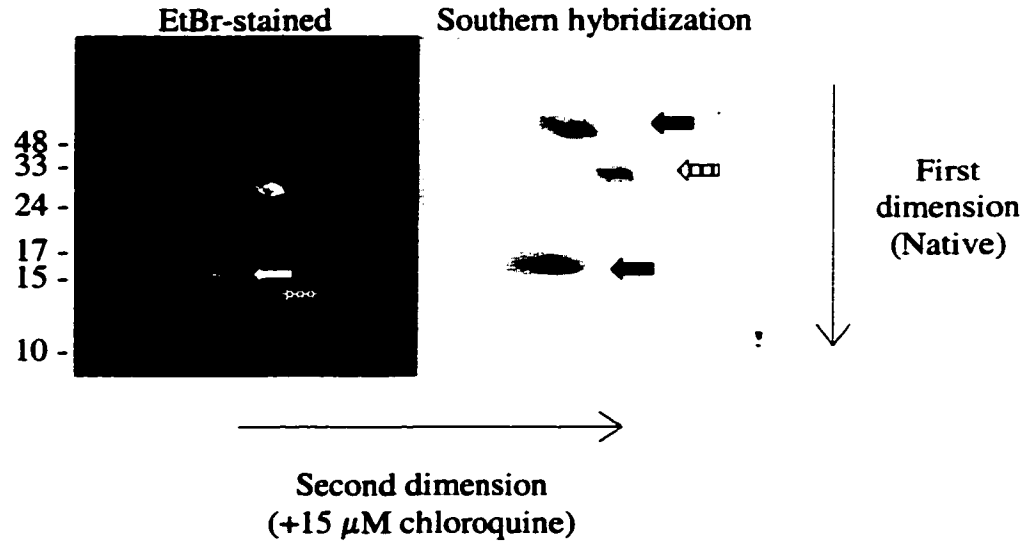
Figure 5. Genomic location of the φBB-1 prophage. Total cellular DNA from *B. burgdorferi* CA-11.2A was resolved by two-dimensional gel electrophoresis (left panel). The large circular plasmid (white arrow) was retarded in its migration in the second dimension, while the migration of the linear DNA elements was unaffected. A Southern blot of the gel (right panel) was probed with total phage DNA that was extracted and radiolabeled. The phage DNA hybridized to the circular 32-kb plasmid (black arrow). Additionally, the phage DNA hybridized to the nicked (gray arrow) and linearized (hatched arrow) forms of cp32. The location of cp26 is indicated by the speckled arrow. Molecular sizes are in kilobase pairs.

relaxing negatively supercoiled circular DNA molecules (138) and retarding the migration of these molecules in the second dimension (Figure 5, white and speckled arrows). The migration of linear DNA molecules is unaffected by the presence of chloroquine.

Total phage DNA was hybridized to a blot of the two-dimensional gel (Figure 5, right panel). The phage DNA hybridized with the supercoiled circular (Figure 5, black arrow), linearized (Figure 5, hatched arrow) and nicked forms (Figure 5, gray arrow) of the cp32. The hybridization to the nicked DNA (Figure 5, gray arrow) may also mask or include hybridization to lp56, which has sequence homology to the cp32s and co-migrates with the nicked DNA under these conditions.

The pattern of hybridization of a small probe specific to the 26-kb circular plasmid, cp26 (Figure 5, speckled arrow), was used to differentiate these large circular plasmids and to determine that this similarly-sized molecule was not packaged within the phage capsid (data not shown).

In addition to the hybridization of total phage DNA to cp32, several different cp32-specific probes hybridize to total phage DNA (see Figure 11). No DNA other than cp32 DNA has been found within the ϕBB-1 capsid by either hybridization or PCR amplification.

Several fragments generated by *Hind*III-digestion of genomic ϕBB-1 DNA from *B. burgdorferi* CA-11.2A have been partially sequenced. The sequences from these fragments were analyzed by BLAST search for sequence similarity (114, 176). When compared to the known *B. burgdorferi* B31 cp32 sequences, all of the cloned fragments from the CA-11.2A ϕBB-1 genome had ≥85% sequence identity to at least one *B. burgdorferi* B31 cp32 (Table 2). Using the known B31 cp32 sequences, we have also identified the approximate location of the sequenced end of each CA-11.2A ϕBB-1 fragment (Table 3). Fragments 7, 8, and 9 each have homology to several different cp32s

and map to a highly conserved region. Fragments 6, 12, 14, 23, and 25 are homologous

to the more variable regions of the cp32s, and accordingly, each share sequence similarity

with fewer cp32s (42, 176) (see Figure 28 and discussion).

Table 2. Sequence identity between CA-11.2A phage DNA fragments and the B31 cp32s.

ϕBB-1 fragment	cp32-1	cp32-3	cp32-4	cp32-6	cp32-7	cp32-8	cp32-9
6-SK	63.3%	91.4%	<54%[1]	<54%	63.3%	61.7%	<54%
7-SK	99.1%	99.1%	86.1%	89.6%	99.1%	99.1%	87.5%
8-SK	98.7%	98.6%	87.8%	92.9%	98.7%	98.7%	89.9%
9-SK	94.8%	94.8%	94.4 %	94.6%	93.9%	94.8%	94.8%
12-SK	65.2%	89.1%	54.9%	60.8 %	63.4%	63.2%	<53.1 %
14-SK	90.5%	64.1%	89.3%	89.5%	90.3%	86.8%	70%
23-SK	66.0%	76.1%	85.6%	84.6%	70.6%	65.6%	84.9 %
25-SK	<55.1%	<55.1%	65.1%	98.1%	<55.1%	<55.1%	<55.1 %

[1] Sequence identity of the CA-11.2A phage DNA fragments to the B31 cp32s reported as <X% are not

within the top 20 reported scores for which percentages are given, but are within the top 50 best scores

Table 3. Approximate location of sequenced CA.11-2A ϕBB-1 fragments on the cp32 molecule

ϕBB-1 fragment (size)	B31 plasmid with highest sequence identity	Approximate location on cp32[1]
6-SK (3.5 kb)	32-3	~22000
7-SK (1.5 kb)	32-1,3,7,8	~1800
8-SK (1.7 kb)	32-1,7,8	~1500
9-SK (2 kb)	32-1,3,8,9	~6000
12-SK (3.5 kb)	32-3	~21800
14-SK (2 kb)	32-1	~22600
23-SK (400 bp)	32-4	~22200
25-SK (800 bp)	32-6	~27000

[1] approximate map location was determined by comparing ~400-bp of sequence from CA-11.2A ϕBB-1 to

the known B31 cp32s (42)

Induction of the lysogenic ϕBB-1 prophage. Quantifying the phage titer

released from *B. burgdorferi* cultures is technically difficult. *B. burgdorferi* cells can be

grown in solid medium, but they do not readily form a lawn (unpublished observations),

and plaque assays are not feasible. The most efficient way of detecting the presence and

amount of phage in a sample is by determining the concentration of the extracted

extracellular DNA from cell-free supernatants. The concentration of the DNA can be

evaluated by agarose gel electrophoresis or by the optical density at 260 nm. By these

methods, the upper limit of the number of full phage heads in an uninduced culture can

be determined as approximately 10^6 phage ml^{-1} of original culture. This is at the lower

limit of detection by EtBr-staining of an agarose gel or visualization by electron

microscopy. Unfortunately, this method does not assess the number of infective ϕBB-1

particles in a sample. The assessment of the total number of infective particles is

currently beyond the scope of the experimental system.

Both mitomycin C and ciprofloxacin had been used previously to induce

prophages from spirochetes (33, 87, 110, 117), but neither of these chemicals nor UV

light consistently induced the ϕBB-1 prophage from *B. burgdorferi* CA-11.2A. We have

seen isolated incidents of increased ϕBB-1 release from mitomycin C-treated cells, but

this method does not reliably generate higher phage titer.

Preliminary evidence suggested that the lysogenic ϕBB-1 prophage of *B.

burgdorferi* CA-11.2A was consistently inducible with MNNG. The concentration of

MNNG required for induction was evaluated over a range from 0 to 50 µg ml^{-1}, with 10

µg ml^{-1} producing the largest phage release (Figure 6A). The time of MNNG treatment
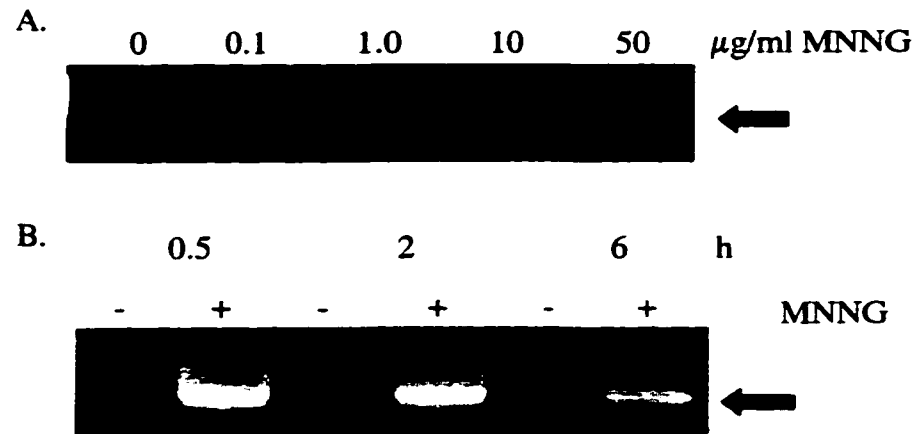
Figure 6. Developing a standard protocol for φBB-1 prophage induction from *B. burgdorferi* CA-11.2A. The induction of the φBB-1 prophage was evaluated over a range of 0 to 50 μg ml^{-1} MNNG by the presence of phage DNA (A). After determining that 10 μg ml^{-1} MNNG was the most effective concentration for prophage induction, the effect of the time of exposure to this concentration of MNNG was also assayed (B). Phage DNA was collected from supernatants of untreated cultures (-) and cultures exposed to 10 μg ml^{-1} MNNG for increasing amounts of time (+). Phage release was similar when the cells were treated from 0.5 to 2 h, but decreased with longer exposures to MNNG. Samples were electrophoresed on 0.5% agarose gels and stained with EtBr. 32-kb linear phage DNA is indicated by the black arrow.

was evaluated from 0.5 to 6 h, with the number of phage released decreasing dramatically when cells were exposed to the mutagen for longer than 2 h (Figure 6B).

φBB-1 released by recovering CA-11.2A cells (both untreated and MNNG-treated) was assayed over a course of about ten doubling times (14) (Figure 7). Although
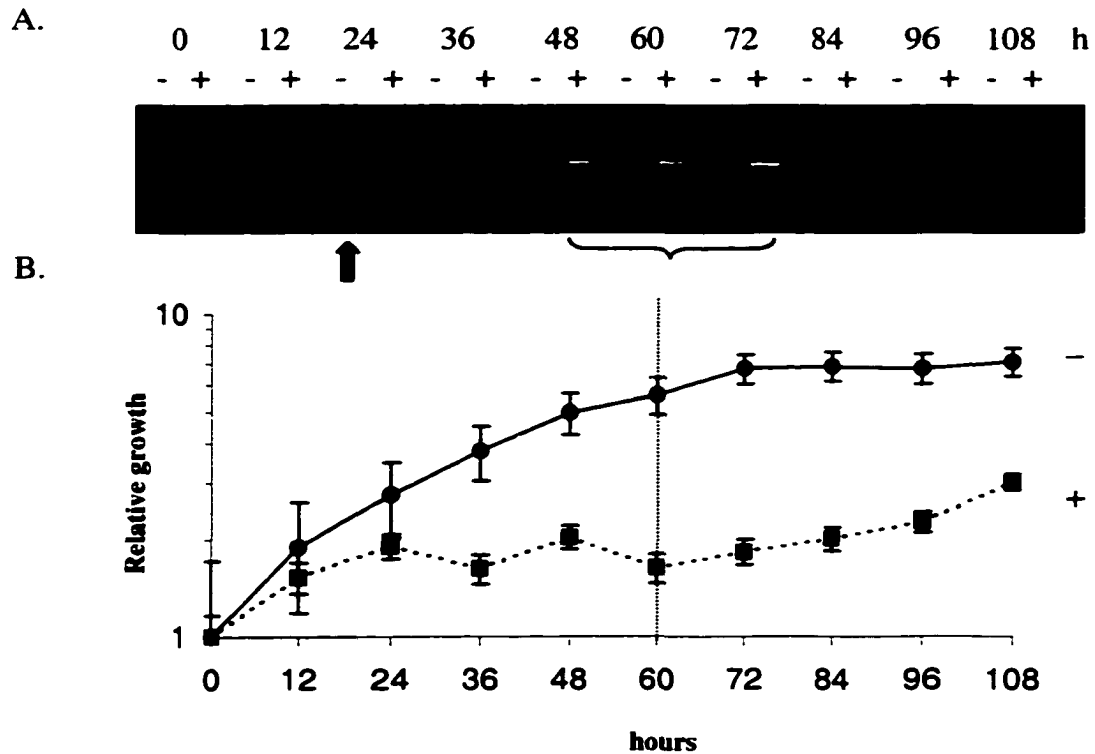
Figure 7. Phage release and *B. burgdorferi* CA-11.2A cell density after MNNG treatment. Aliquots from both a treated (+) and an untreated (-) batch culture were analyzed for phage every 12 hours (A). DNA was resolved on a 0.5% agarose gel and stained with EtBr. The black arrow indicates the first appearance of phage in the untreated culture. The CA-11.2A cell density of aliquots from both the treated (■; +, dashed line) and untreated (●; -, solid line) culture was measured at the same 12 hour time points to correlate cell density with phage release (B; error bars represent the standard error of the mean from four independent experiments). The vertical dotted line indicates the median time (60 h) at which the highest amount of phage DNA is present in the MNNG-treated culture (A; bracket). Relative growth was determined as the percentage of growth above the cell density at time point 0.

phage is first released from untreated cells after 24 h (Figure 7, -, black arrow), the amount of phage released from the MNNG-treated culture is higher as the recovery is extended. The amount of phage present in the treated sample was highest from 48 to 72 h after recovery (Figure 7A, +, bracket) and decreased at a much slower rate than the phage released by the untreated cells over the next 36 h. In the experiment shown in Figure 7A, the amount of phage DNA recovered between 48 and 72 h from the treated culture was approximately three-fold that of the phage DNA recovered from the untreated culture during the same time period.

The density of the recovering *B.burgdorferi* CA-11.2A cells was also evaluated over the same time period (Figure 7B). Although MNNG-treated cells did not appear as viable as untreated cells, there was no evidence of a dramatic culture-wide cell lysis associated with phage release in an MNNG-induced culture of *B. burgdorferi*. There was a 16% decrease in cell density between 24 and 36 h, and a 20% decrease between 48 and 60 h (Figure 7B). Each observed decrease was relative to the previous time point; the cell density never decreased below the original number of cells in the culture.

The φBB-1 prophage could be induced from high passage *B. burgdorferi* B31-UM (Figure 8, lanes 1 to 3), and *Borrelia bissettii* DN127 (Figure 8, lanes 7 to 9) as well as *B. burgdorferi* CA-11.2A (Figure 8, lanes 4 to 6) when cells were treated with 10 μg ml⁻¹ of MNNG for 2 h. The induction of prophage from *B. burgdorferi* B31-UM is notable because this strain rarely produces phage spontaneously (Figure 8, lanes 2 and 3). *B. bissetii* DN127 is a California tick isolate closely related to *B. burgdorferi* (26, 122, 149). DN127 released low levels of phage when uninduced and could be treated with

B31			CA11-2A			DN127		
1	2	3	4	5	6	7	8	9

| pre | - | + | pre | - | + | pre | - | + |
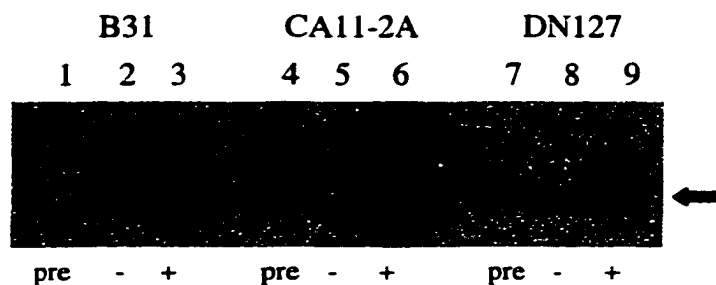
Figure 8. Induction of the φBB-1 prophage from different *Borrelia* strains. Cell-free supernatants from 10 ml cultures of *B. burgdorferi* B31 (lanes 1 to 3), *B. burgdorferi* CA-11.2A (lanes 4 to 6) and *B. bissettii* DN127 (lanes 7 to 9) were analyzed for DNA content. The supernatants were collected from log phase starter cultures (pre; lanes 1, 4, and 7), untreated controls (-; lanes 2, 5, and 8) and cultures treated with 10 μg ml^{-1} MNNG (+; lanes 3, 6, and 9). The DNA was resolved on a 0.5% agarose gel. The gel was blotted and probed with a cp32-specific probe to enhance detection. The black arrow indicates the 32-kb linear phage DNA.

MNNG to consistently produce slightly higher levels (Figure 8, lanes 8 and 9). When treated with MNNG, *B. burgdorferi* CA-11.2A produced a much higher titer of phage than was naturally released (Figure 8, lanes 5, and 6). After MNNG-treatment, phage titer from a *B. burgdorferi* CA-11.2A culture can sometimes approach 10^{9} phage per ml of original culture supernatant.

We have assayed several other *B. burgdorferi* isolates, as well as other *Borrelia* species, for phage production from cells treated with MNNG (Table 4). We have seen no evidence of either spontaneous production of phage or MNNG-induction of the cp32 prophage from any of these isolates. Supernatants of both untreated and MNNG-treated

Borrelia anserina, the causative agent of avian spirochetosis, and MNNG-treated

Borrelia coriaceae, the causative agent of epizootic bovine abortions (19), did contain

DNase-protected extracellular DNA.

B. anserina has a genome that apparently lacks circular DNA [data not shown,

(106)], suggesting that the DNA released from this species and the genome of φBB-1 are

different. Furthermore, the DNA isolated from the supernatant of *B. anserina* cultures

has been sized at approximately 42 kb (data not shown). Neither *B. burgdorferi* phage

DNA nor the cp32-specific probe 4, highly conserved among the Lyme disease

spirochetes (43), hybridizes to the DNA released from either *B. anserina* or *B. coriaceae*.

The DNA isolated from the supernatants of these two species was detected by staining

with EtBr or GelStar.

Table 4. *Borrelia* isolates assayed for MNNG-induction of the φBB-1 prophage

Spontaneous/ Inducible (see Figure 8)	No Detectable φBB-1 Production
B. burgdorferi sensu stricto	*B. burgdorferi* sensu stricto
B31-UM[1] (high passage)	B31-CDC (low passage)
CA-11[2]	B31-1M1T (low passage)
CA-11.2A	297
CA-11.2B	1A7 (high passage clone of SH2-82)
CA-11.2G	CA-2
CA-11.4	HB19 (low passage)
CA-11.2A/R133I (coumermycin A_1-resistant clone;	CA-9
gyrB locus)	N40 (cloned)
B. bissettii (DN127)	NGR (coumermycin A_1-resistant
	clone; *gyrB* locus)
	B31-3 (coumermycin A_1-resistant
	clone; cp26 location)
	B. burgdorferi sensu lato
	Borrelia afzelii (IP21)
	Borrelia garinii (G2)
	Borrelia andersonii (21038)
	Borrelia bissettii (CA-55)
	Borrelia valaisiana (VS116)
	Borrelia japonica (HO14)
	Relapsing fever spirochetes
	Borrelia hermsii (HS1)
	Borrelia parkeri
	Borrelia turicata
	Borrelia anserina[3]
	Borrelia coriaceae (CO53)[3]

[1] –UM designates the strain that is used in our laboratory; [2] low passage isolates of uncloned CA-11 are not inducible, but as the strain is passaged, phage release is observed more often, though not consistently; [3] *B. anserina* and *B. coriaceae* produce DNase-protected extracellular DNA that are apparently unrelated to φBB-1 (see text)

Chapter 4

Characterization of the genome of φBB-1

Having demonstrated the relationship between the lysogenic prophage of φBB-1 and cp32, we now present more data on the genomic content of the phage head. φBB-1 released from *B. burgdorferi* CA-11.2A packages at least three cp32s, although one is more abundant in the phage population. Restriction analysis of the phage genome yields a circular molecule, suggesting that the φBB-1 genomic DNA is circularly permuted.

Determining the number of cp32s. Specific probes to individual *B. burgdorferi* B31 cp32s (43) do not hybridize to *B. burgdorferi* CA-11.2A cp32s (data not shown). To determine the number of cp32s in both *B. burgdorferi* cells and φBB-1, oligonucleotides that flank a diagnostic variable region (designated VR1) were designed. VR1 encompasses a portion of each cp32 where the *ospE/ospF/elp* (*erp*) genes are found (see Figures 12B and 28) (5, 32, 42, 107, 121, 169, 176). PCR amplification of VR1 with these oligonucleotides generates products of different sizes for several of the *B. burgdorferi* B31 cp32s whose sequences are available (Table 5).

Using the VR1 primers and FIGE for maximum resolution, we have identified a minimum of four different cp32 molecules present in *B. burgdorferi* CA-11.2A (Table 6; Figure 9, lane 1). We have also identified a minimum of four different cp32s present in *B. burgdorferi* strain B31-UM (Table 6; Figure 9, lane 3). The φBB-1 phages released from CA11-2A and B31 cells package cp32s that are represented by only three (Figure 9, lane 2; Figure 9, lane 4) of the variable regions amplified from the respective hosts. The absence of the ~2.8-kb band from both φBB-1 samples suggests that the phage does not package the cp32 that is integrated into lp56 (Tables 5 and 6).

57

Table 5. Predicted fragment sizes of variable region 1 of the B31 cp32s[1]

B. burgdorferi B31 plasmid	amplicon size (bp)
cp32-1	3429 ←
cp32-3	2442
cp32-4	3377 ⇐
cp32-6	2507
cp32-7	3575
cp32-8	3429 ←
cp32-9	3367 ⇐
lp56	2796

[1]as determined by the MacVector program using the published cp32 sequences (42, 114, 176); black arrows and hatched arrows indicate two pairs of variable regions indistinguishable by our methods

Table 6. Amplification of the VR1s of CA-11.2A, B31 and φBB-1[1]

CA-11.2A total DNA	CA-11.2A phage DNA	B31-UM total DNA	B31-UM phage DNA	Predicted B31 cp32[2]
		3426	3426	cp32-1 or 8
		3343	3343	cp32-9 or 4
3047	3047			
2819		2828		lp56
2537	2537			
		2484[3]	2484	cp32-3[3]
2455	2455			

[1]sizes (in bp) determined by regression using Multi-Analyst software; [2]predictions based on size estimates from ≥3 trials and applicable only to the B31 fragments; [3] prediction confirmed by sequencing of VR1

The proportion of each variable region within a population of *B. burgdorferi* CA-11.2A cells and φBB-1 phage heads was estimated by semi-quantitative PCR (Figure 10). Three samples were assayed: total DNA from CA-11.2A cells (Figure 10, lanes 1-8), total DNA from MNNG-treated CA-11.2A cells (Figure 10, lanes 9-16), and DNA extracted from φBB-1 produced from MNNG-treated CA-11.2A cells (Figure 10, lanes 17-24). The cp32 containing the 2537-bp variable region is the dominant species in all three CA-11.2A DNA populations (Figure 10, hatched arrow). In all three DNA sources,
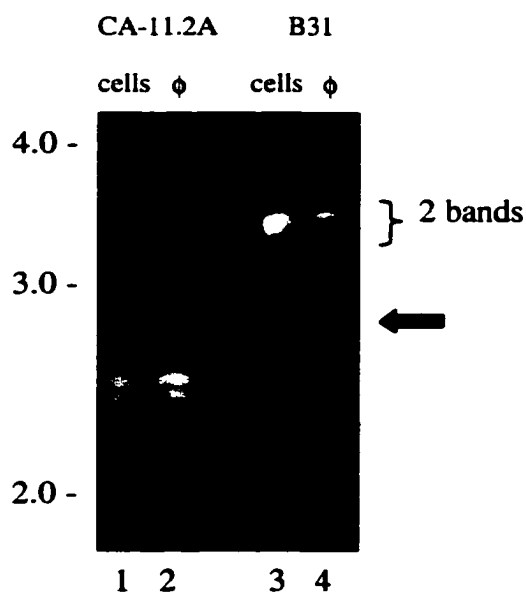
Figure 9. Determining the number of cp32 molecules in *B. burgdorferi* cells and φBB-1 by amplification of VR1 by PCR. Highly conserved primers that flank a variable region (VR1) of cp32 amplify four different size products representing a minimum of four different cp32s and homologous molecules (i.e., lp56) from *B. burgdorferi* strains CA.11-2A and B31. The two variable regions from the cp32s of B31 at ~3.3 kb can be resolved with extended electrophoresis times. The φBB-1 released from both of these strains package three of these cp32s (lanes 2 and 4), but do not package the molecule that generates the ~2.8-kb band, which corresponds to the cp32 integrated into lp56 (black arrow). Fragments were resolved on a 0.8% agarose gel by FIGE and stained with EtBr. Molecular sizes are in kilobase pairs.

the ~2.5-kb fragment is visible by EtBr-staining about three cycles before the other fragments (Figure 10, black arrows), which suggests that theconcentration of this cp32 species is ~8-fold greater concentration of this cp32 species than the other cp32s in the
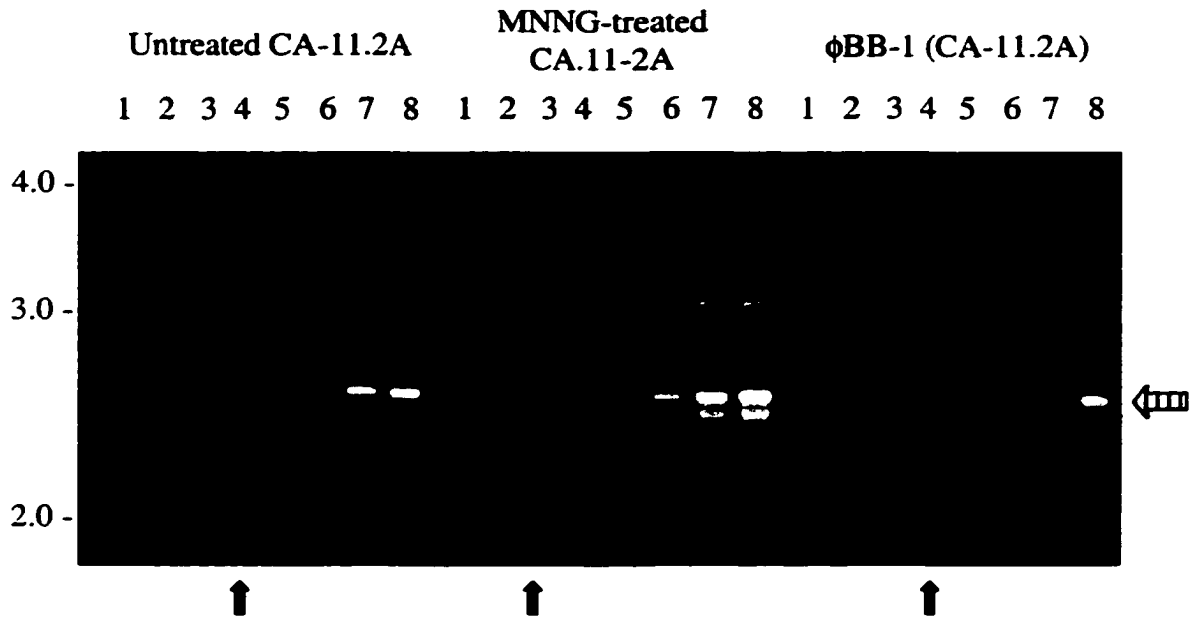
Figure 10. Semi-quantitative analysis of the population of cp32s of *B. burgdorferi* CA-11.2A. The VR1s of untreated and MNNG-treated CA-11.2A, as well as φBB-1 DNA from MNNG-treated CA-11.2A supernatants, were amplified with the VR1 primers. Samples were collected every three cycles, starting with cycle 6 (lane 1) through cycle 27 (lane 8). Products were resolved on 0.8% agarose gels by FIGE. The ~2.5-kb fragment (hatched arrow) is the dominant species in all three samples. For each sample, the first cycle in which this band is visible is marked with a black arrow. Molecular sizes are in kilobase pairs.

population. This 2.5 kb band corresponds to the dominant phage genome detectable by restriction mapping and Southern hybridization (see below).

Mapping the dominant phage genome. φBB-1 genomic DNA was digested with several different restriction enzymes. Data from the digestion of phage DNA with

A.

*Nhe*I digest

φ 4 2 N

48.5 -
33.5 -
15 -
9.6 -
6.6 -
4.4 -
2.3 -

B.

*Pst*I digest

φ 4 2 N B V

48.5 -
33.5 -
17.1 -
9.6 -
6.6 -
4.4 -
2.3 -
2.1 -

C.

*Sac*I digest

φ 4 2 N B V

48.5 -
33.5 -
23.1 -
9.6 -
6.6 -
4.4 -
2.3 -
2.1 -

D.

*Spe*I digest

φ 4 2 N

48.5 -
33.5 -
15 -
9.6 -
6.6 -
4.4 -
2.3 -
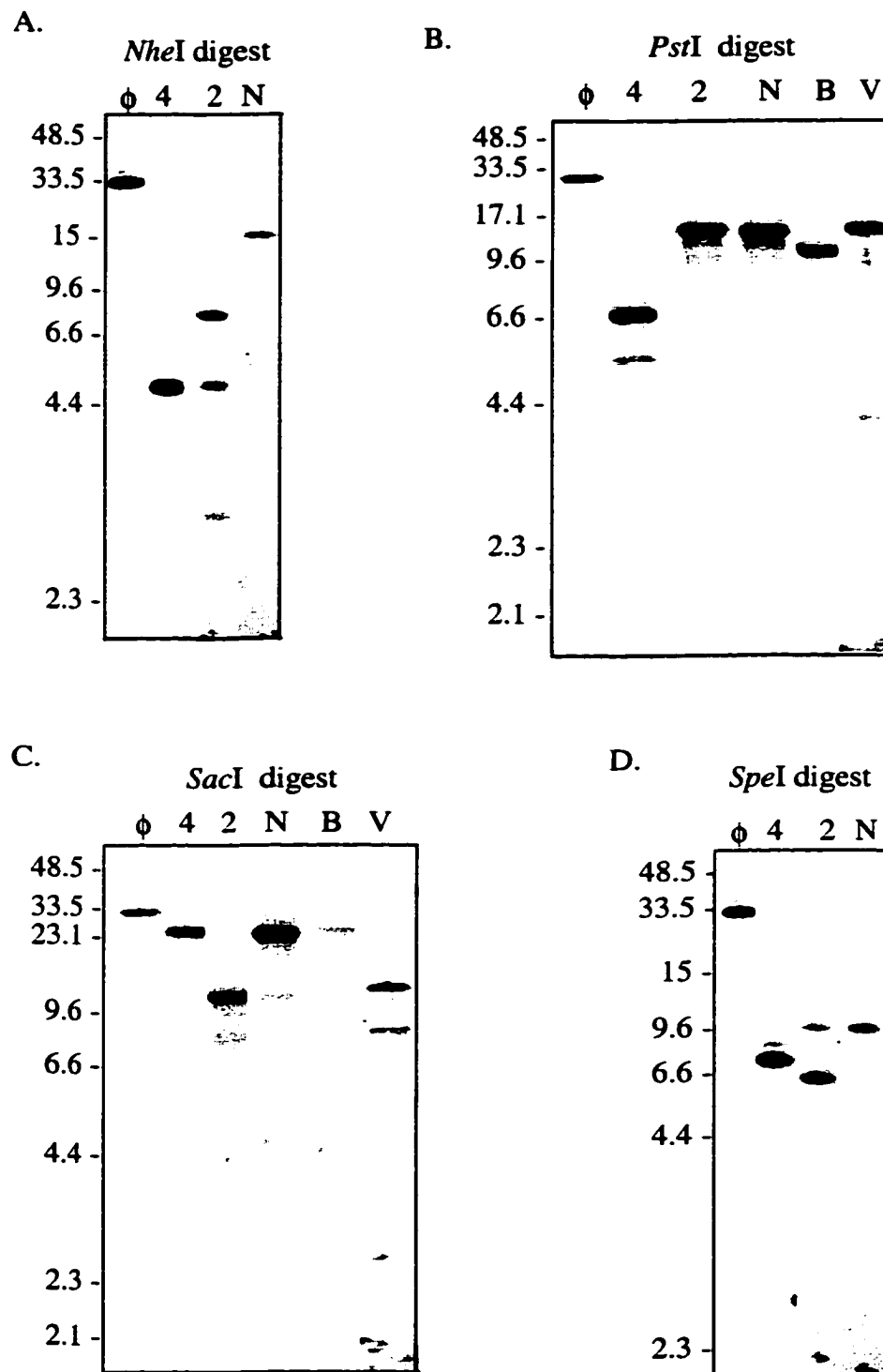
Figure 11.

Figure 11 (previous page). Restriction digests of φBB-1 DNA. Phage genomic DNA

digested with *NheI* (A), *PstI* (B), *SacI* (C), or *SpeI* (D) was resolved on 0.8% agarose gels

by FIGE. The gels were blotted to nylon membranes and probed individually with

probes 2 and 4, two cp32-specific probes (43), B, a probe to the *blyB* gene on cp32 (75),

N, a probe that encompasses an *Nde* I site on the dominant φBB-1 genome, and V, a

probe to the VR1s. Uncut phage DNA is shown as a control (φ). Molecular sizes are in

kilobase pairs.

Table 7. Restriction fragment sizes[1] of the dominant φBB-1 genome

	Probe 4	Probe 2	*Nde* I probe	*blyB* probe	VR1 probe
Nhe I	5.5	7.7	15.1	-	-
Pst I	7.1	13.9	13.9	9.0	13.9
Sac I	19.7	9.9	19.7	19.7	9.9
Spe I	7.3	5.8	9.6	-	-

[1] approximate sizes in kb; - data for these fragments not available

four enzymes is presented in Figure 11, although more than 10 enzymes have been used.

The digestions of the phage DNA with *PstI* and *SacI* were the most informative and we

present mapping data for these enzymes using five different conserved cp32 probes

(Figure 11, B and C, respectively). The digestions with two other enzymes, *NheI* and

SpeI, are shown with only three different probes (Figure 11A and D). The sizes of the

dominant fragments are listed in Table 7.

Using single (Figure 11) and double digests (data not shown) and the five

available probes, we were able to generate a partial restriction map of the dominant phage

genome released from *B. burgdorferi* CA-11.2A cells (Figure 12). Although the phage

genome is linear (Figures 2 and 12A), the mapping data are consistent with a circular

A.

B.
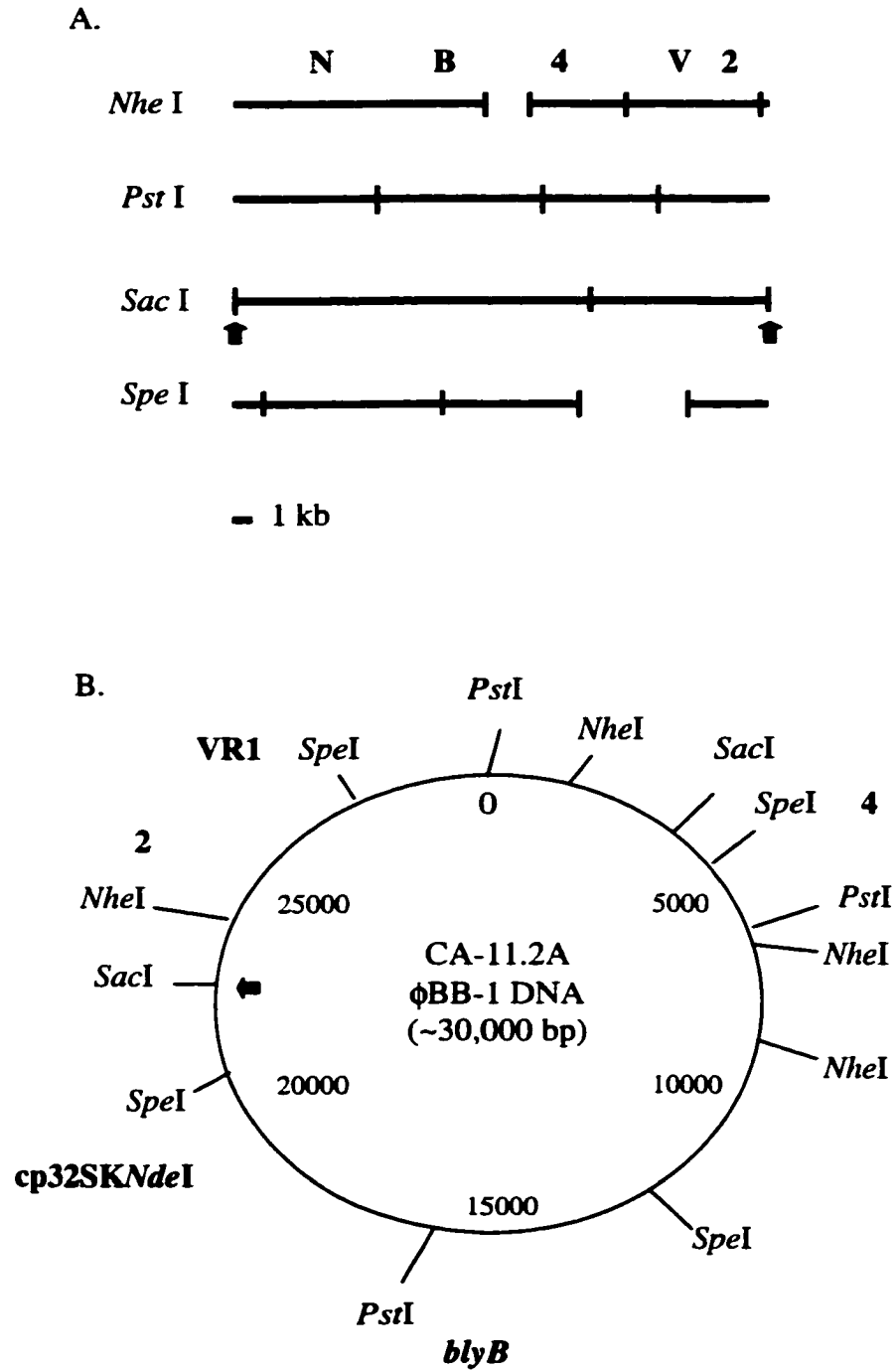
Figure 12.

Figure 12 (previous page). Partial restriction map of the dominant φBB-1 genome.

Using information from single and double digests with selected restriction enzymes,

linear maps of the dominant phage genome were drawn (A). A gap in the linear map

indicates that we have no probe for visualizing those fragments, although total φBB-1

DNA hybridizes to fragments of appropriate sizes (data not shown). The black vertical

lines indicate cut sites of the specific enzyme. The black arrows indicate the same *Sac*I

cut site (the ends join at that cut site, see 12B). No vertical line at the end of a fragment

on the linear diagram indicates that the fragment is continued on the other side of the

linear molecule (as for *Nhe*I, *Pst*I, and *Spe*I), consistent with a circular molecule. A more

accurate representation of the phage genome is a circular map (B). In both maps, the

approximate locations of the hybridization probes are shown in bold (N: cp32SK*Nde*I, B:

blyB probe, V: VR1 probe). The circular plasmid diagram was created with the Plasmid

Artist Demo (GeneSystems Computer Software).

molecule (Figure 12B). The map is shown with the cut sites of only the four restriction

enzymes shown in Figure 11. We also have incomplete mapping data for several other

enzymes, including *Eco*RV, *Eco*RI, *Hind*III, and *Nde*I (data not shown). The restriction

map of the dominant CA-11.2A cp32 is different from those of the B31 plasmids;

however the location of the probes, thus the gene order, is highly conserved (Figures 12

and 29). A circular restriction map generated from a linear molecule (the φBB-1

genome) is indicative of circular permutation (see below and Figure 29).

Possible terminal redundancy of the φBB-1 genome. Because of the

mechanism by which they are packaged, circularly permuted phage genomes are

terminally redundant. This terminal redundancy makes the phage genome in the virion

larger than the lysogenic prophage equivalent. Several methods have been used to

determine the size of the φBB-1 genome. The phage DNA has been previously sized at

32.7 kb by electron microscopy (102) and 32.3 kb by conventional gel electrophoresis

(137). Using the same method of regression analysis of DNA resolved by conventional

gel electrophoresis, the circular cp32s were previously determined to be 29.3 kb (137).

The actual sizes of the B31 cp32s range from 29.8 to 30.9 kb (176).

We have directly compared the size of φBB-1 DNA and linearized cp32

molecules from CA-11.2A (Figure 13). The phage DNA was sized at 31.3 kb (Figure 13,

lane 1) and the linearized CA-11.2A cp32s were sized at 29.9 kb (Figure 13, lane 2, black

arrow).

The size range of the CA-11.2A cp32s, while predicted to be similar to that of the

B31 cp32s, is not known, and there is likely overlap between the cp32-sizes and the

lower limit of our measurements, but the size difference is visually apparent (Figure 13).

By three means (electron microscopy, regression analysis of DNA resolved by

conventional gel electrophoresis, and regression analysis of DNA resolved by field-

inversion gel electrophoresis) we have sized the φBB-1 genome as larger than the

predicted cp32 sizes. We anticipate that the size difference ($\geq$1.4 kb) between the phage

DNA and the lysogenic prophage is likely due to terminal redundancy at the end of the

DNA packaged into the virion.
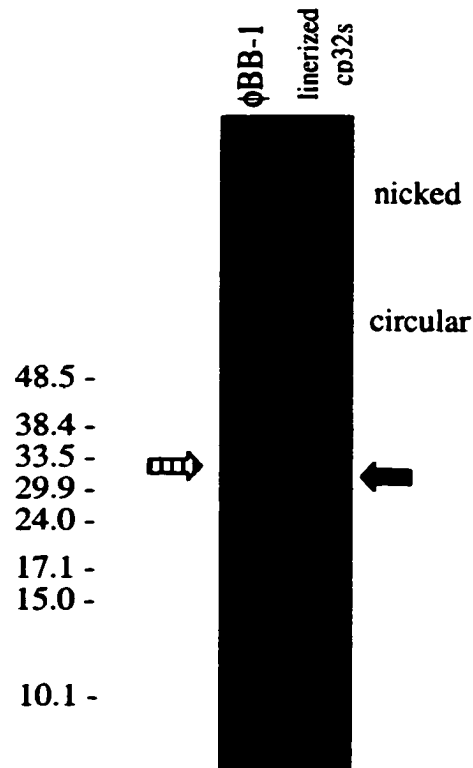
Figure 13. Size comparison of φBB-1 DNA with linearized cp32s/prophages.

Undigested phage DNA and *B. burgdorferi* CA-11.2A plasmid DNA that had been

digested with *Bsu*36I, an enzyme that cuts the CA-11.2A cp32s once or not at all (data

not shown), were resolved on 0.8% agarose gels by FIGE, and the gel was stained with

EtBr. The phage DNA (lane 1, hatched arrow) is larger than the linearized cp32

molecule(s) (lane 2, black arrow). The location of the linearized cp32 molecule was

confirmed by Southern hybridization with a cp32-specific probe (data not shown). The

size of the phage DNA is ~31.3 kb and the size of the linearized cp32(s) is ~29.9 kb as

determined by regression using the Multi-Analyst software. The molecular sizes are in

kilobase pairs.

Cyclical permutation of the linear phage genome. The conversion of a circular molecule like cp32 to a linear phage genome that is packaged into a procapsid requires a processing step. Using restriction digests (Figure 11) we have determined that the φBB-1 genome is circularly permuted. That is, there is more than one cut site at which the processing occurs on the phage genome (see Figure 29). There are two types of permutation possible: (1) restricted permutation with the processing site within a small portion of the total genome, or (2) random permutation with the processing site anywhere within the genome (see Figure 30). To distinguish the two possibilities, *Hind*III-digested end-labeled phage DNA was hybridized to phage DNA that had also been digested with *Hind*III (Figure 14, lane 1). The amount of hybridization (Figure 14, lane 2) appears equal between all of the fragments, suggesting that all the fragments contain an end that can be labeled, which might indicate random circular permutation of the φBB-1 genome.
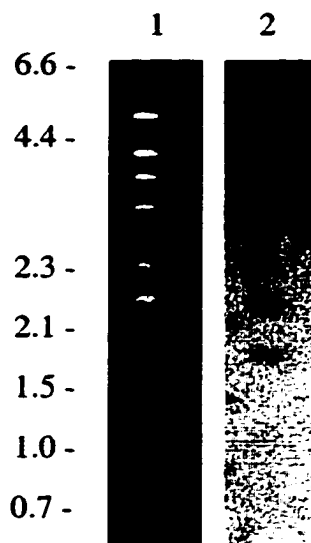
Figure 14. Circular permutation of the φBB-1 genome. Phage DNA was digested with

*Hind*III and subjected to FIGE (lane 1). The gel was blotted and probed with phage DNA

that was end-labeled and then digested with *Hind*III (lane 2). The amount of label

hybridized to each fragment appears to be approximately equal in intensity to the EtBr-

stained DNA. Molecular sizes are in kilobase pairs.

Chapter 5

The search for phage proteins

Here we present our efforts to identify and characterize the proteins of φBB-1 as isolated from the cell-free supernatants of *B. burgdorferi*. Two approaches have been taken to reduce the number of non-specific proteins from PEG-precipitated phage samples. Using these methods, we have identified two proteins that could be phage-related structural proteins. In collaboration with Don Oliver and Chris Damman from Wesleyan University, we have also characterized two putative non-structural phage proteins encoded on cp32.

Structural phage proteins from CsCl purified φBB-1. BSK-complete is a protein-rich, serum-based medium (14) (Table 8). Concentrating phage particles with PEG also precipitates a large number of other medium proteins non-specifically (Figure 15A, Str lane). We have used successive CsCl-gradients as a means of removing some of the background proteins (Figure 15). Phage-containing samples, as assayed by the presence of φBB-1 DNA, were ultracentrifuged through three CsCl-gradients. After each gradient, phage-containing fractions (fraction 5) were pooled from multiple samples and dialyzed.

A small portion of the dialyzed sample was saved from each gradient for the analysis of protein (Figure 15A) and phage DNA content (Figure 15B). The 3X fraction 5 sample was also viewed by electron microscopy and intact phage-heads (without tails) were observed (data not shown). Purifying the phage by several CsCl-gradients was also a reliable method for producing phage DNA suitable for restriction digestion (data not shown).

69
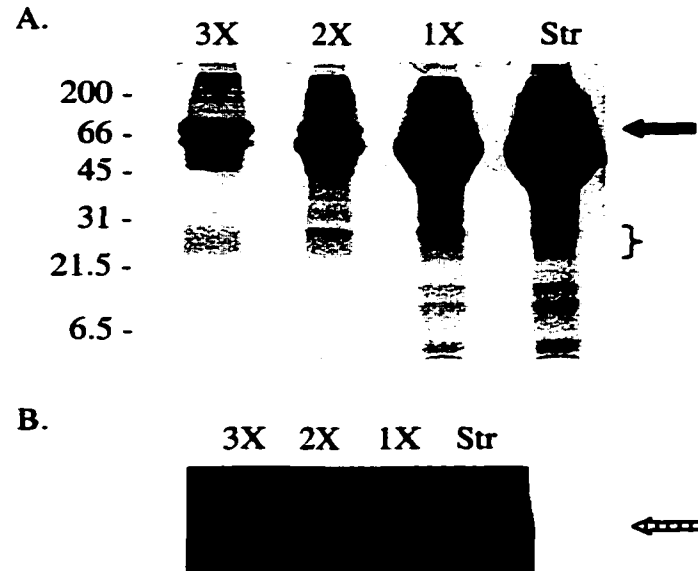
Figure 15. Analysis of phage samples purified by multiple CsCl-gradient centrifugation. PEG-precipitated supernatant from CA-11.2A cultures was applied to a CsCl-gradient (Str). After ultra-centrifugation the fractions were collected in 400 µl aliquots from the top, and the fifth fraction, which contained the phage DNA (B; hatched arrow), was collected and dialyzed against SM (1X). This step was repeated twice more, with the fifth fraction being retained each time (2X, 3X). A sample from each step was resolved on a 12.5% SDS-PAGE gel and stained with CBB (A). A number of small proteins (bracket) seem to increase, but there are no distinct bands that emerge from this one-dimensional analysis. Additionally, a large ~70 kDa band (black arrow) appears to increase as the amount of BSA decreases. We are currently purifying this protein for N-terminal sequencing or MALDI mass spectrometry. Molecular sizes in kDa are shown.

Most head proteins of tailed-bacteriophage are between 30 and 40 kDa (37).

There was no dramatic increase of proteins of this size despite the presence of intact

phage heads, as assayed by DNA presence (Figure 15B) and electron microscopy (not

shown). There is a small increase in a number of indistinguishable proteins of 24 to 28

kDa, but no discrete bands (Figure 15A, bracket) and obtaining sequence from what

appears to be multiple proteins would be difficult. The resolution of the proteins within

this grouping might require two-dimensional gel electrophoresis.

As the amount of BSA diminishes, there is also an increase of a larger protein,

~70 kDa, visible in fraction 5 (Figure 15A, black arrow). This is consistent with the sizes

of some tail proteins, however electron micrographs of phage purified from CsCl-

gradients suggest that the tails are missing from the phage heads. The head protein may

be covalently modified, possibly linked as a dimer by a reducing agent-resistant and heat-

stable bond, causing the protein to migrate as a much larger molecule. We are currently

purifying this protein for N-terminal sequencing.

A low-protein medium. There are two major protein components to BSK-

complete: BSA and rabbit serum (Table 8). We have attempted to substitute these

elements with cell culture media enhanced with lipids or Excyte VLE (Bayer), a lipid

supplement. In many cases, relatively high density growth ($\sim 10^7$ cells ml^{-1}) of B.

$burgdorferi$ could be achieved for the first two or three passages, but these cells no longer

released ϕBB-1 (data not shown).

To lower background proteins from induced phage preparations, a low-protein

medium that was suitable for phage induction was formulated. BSK medium that

contained no rabbit serum was prepared and rabbit serum was added to aliquots of the

Table 8. Components of the standard *B. burgdorferi* culture medium

BSK-complete
CMRL-1066 (w/o L-glutamine and sodium bicarbonate)
neopeptone
bovine serum albumin (47 g L^{-1})
HEPES
glucose
sodium citrate
sodium pyruvate
N-acetyl-D-glucosamine
sodium bicarbonate
rabbit serum (6.6%)

Bold: components that contain the most proteins

serum-free medium in increasing quantities. The final concentration of rabbit serum in the media ranged from 0 to 8%. Phage production by CA-11.2A cells after MNNG-treatment required a minimum serum content of 3% and did not appear to improve significantly with an increase in the serum percentage (data not shown).

BSK medium containing 3% rabbit serum and no BSA was prepared. Fraction V BSA was added back into aliquots of the media so that the final concentrations ranged from 0 to 40 g L^{-1} BSA. ϕBB-1 release after MNNG-treatment did not appear to require exogenous BSA being added, although the amount of phage released appeared to increase modestly with an increase in exogenous BSA (Figure 16; black arrow). Whether the serum albumin present in 3% rabbit serum is sufficient for the physiological requirements of phage release, or whether phage release is independent of the presence of any serum albumin has not been explored.

We have designated the low-protein medium containing 3% rabbit serum and no exogenous BSA as BSK-che1. *B. burgdorferi* CA-11.2A cells were grown to log phase in BSK-complete, treated with MNNG and recovered in BSK-che1. After recovery,

neg 0 5 10 15 20 25 30 40   g L⁻¹ BSA

48.5 -
33.1 -
24 -
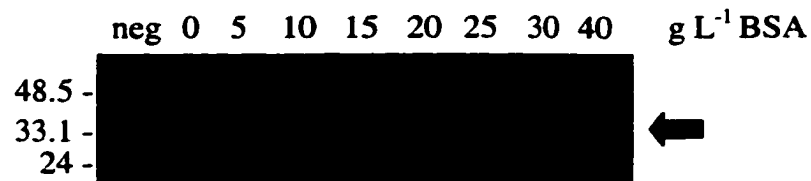
Figure 16. The effects of BSA concentration on φBB-1 release. MNNG-treated *B. burgdorferi* CA-11.2A cells were recovered in samples of BSK medium that had 3% rabbit serum and BSA concentrations ranging from 0 to 40 g L⁻¹. The amount of phage released from these cells was analyzed by DNA extraction (black arrow) and resolution on a 0.8% agarose gel by FIGE. The gel was stained with EtBr. As a control, a culture was left untreated with MNNG and recovered in BSK-complete (neg). Molecular sizes are in kilobase pairs.

phage particles were collected by PEG-precipitation. BSK-che1 that contained no cells was also precipitated as a control to evaluate protein background. An aliquot of the PEG-precipitated sample was analyzed for the presence of phage DNA as described above (data not shown). A portion of the sample that contained phage DNA was then resolved on a 12.5% SDS-PAGE gel (Figure 17). The sample loaded in Figure 17 is at least three times more concentrated than the samples in Figure 15A (Str). Although the background has been significantly reduced, the only protein that is increased in the phage–containing sample (Figure 17, lane 2), but not the low-protein medium control (lane 1), is an ~25-kDa protein (black arrow).

Because of the difficulties involved in resolving this protein in one dimension, we have been unable to obtain N-terminal sequence of the 25-kDa protein. Recently, we have excised this band and attempted a second SDS-PAGE purification that has yielded
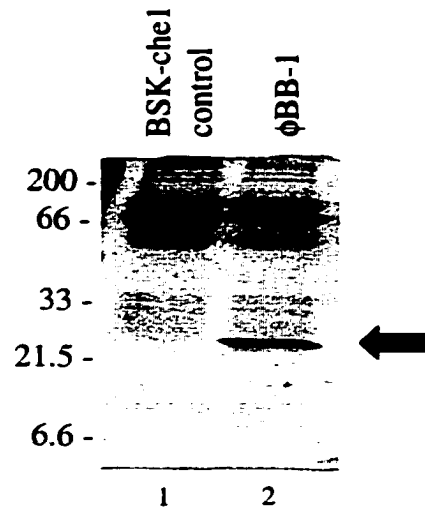
Figure 17. A possible φBB-1 phage protein shed into a low-protein medium. A sample of precipitated phage particles collected from a low-protein medium was resolved on a 12.5% SDS-PAGE gel (φBB-1; lane 2). A negative control of PEG-precipitated low-protein medium was also resolved (BSK-chel control; lane 1). The gel was stained with silver. There was one distinct ~25-kDa protein present in the phage sample, but not in the control (black arrow). The protein was not resolved enough to obtain useful N-terminal sequence data. Molecular weights are in kDa.

promising preliminary results, but we have not yet concentrated enough protein by this method for sequence analysis.

Non-structural phage proteins. Don Oliver and Chris Damman have proposed that two proteins encoded on cp32, BlyA and BlyB, comprise a holin-like system (50), a component of the lysis mechanism for all known tailed-phages (191, 192). In collaboration with these researchers, we have characterized this holin-like system with

relation to φBB-1 prophage induction. In this system, *blyA* encodes a putative holin, while the function of the *blyB* gene product remains unclear, but is postulated to be involved in cell lysis.

To examine the synthesis of BlyA and BlyB in *B. burgdorferi* B31, CA-11 and CA-11.2A, cells were left untreated (Figure 18, uninduced; -) or were treated with MNNG (Figure 18, induced; +). After the appropriate recovery time, the level of synthesis of BlyA and BlyB proteins was determined by Western analysis (Figure 18A) and the expression of the *blyAB* transcript was analyzed by Northern hybridization (Figure 18C). The PEG-precipitated samples were also analyzed for the presence of phage DNA (Figure 18B).

There is a dramatic increase in the amount of both BlyA (7.4 kDa) and BlyB (13 kDa) in all three strains (Figure 18A), correlated with the induction of φBB-1 DNA (Figure 18B). The uninduced CA-11.2A cells produced BlyA at low levels (Figure 18A, -), as expected, since this culture was also producing phage (Figure 18B, -). Protein extracts from *E. coli* cells expressing *blyA* and *blyB* were also probed with the antibodies as a positive control (data not shown).

To evaluate the synthesis of another plasmid-encoded protein after MNNG-treatment, protein extracts from induced and uninduced cultures were also probed with an OspC antibody (Figure 18A; OspC control). *ospC* is a differentially-expressed gene on cp26 that encodes an outer surface protein of *B. burgdorferi* (6, 26, 70, 96, 148, 177, 185-187). The amount of the OspC protein appears relatively constant in both uninduced (Figure 18, -) and induced cultures (Figure 18, +) of the major phage producing strains, B31 and CA-11.2A, suggesting that the increase in BlyA and BlyB synthesis is not just
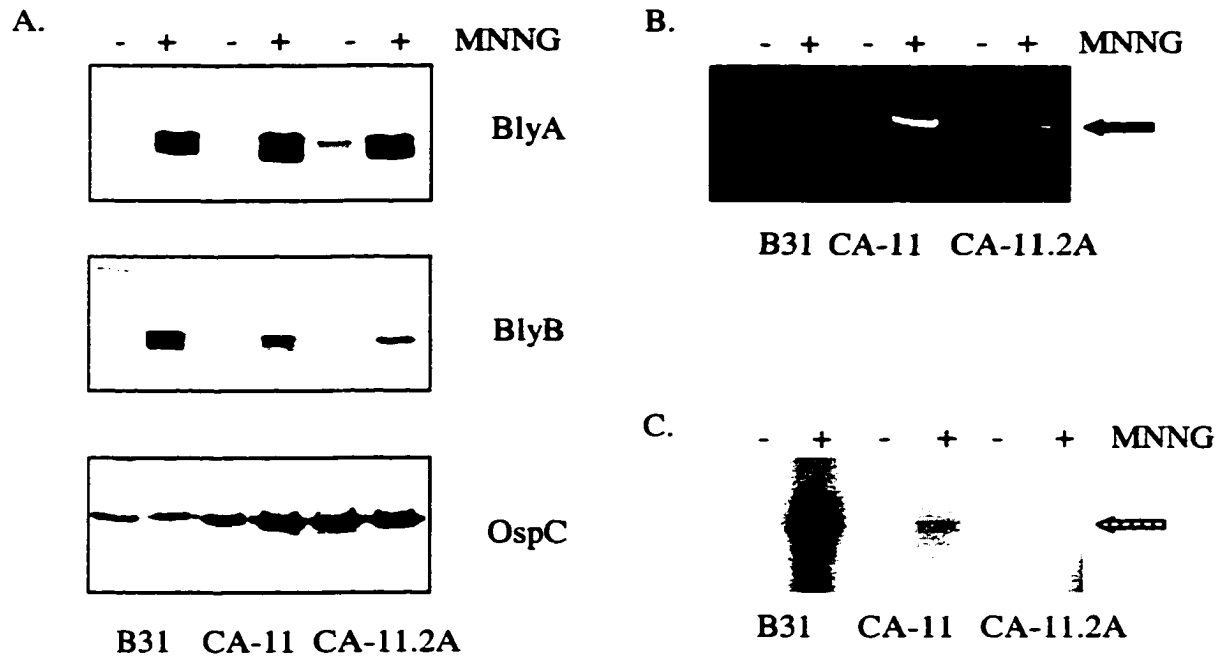
Figure 18. Induced expression of a possible holin-like protein. Protein extracts from

MNNG-treated cells (+) and untreated controls (-), were resolved on 17.5%

polyacrylamide gels and analyzed by Western blotting with the appropriate antibody for

BlyA and BlyB, as well as a control, OspC (A). The increase in the synthesis of the

BlyA and BlyB proteins correlates well with the increase in phage release (B, black

arrow). The expression of the *blyAB* transcript RNA from these cells was analyzed by

Northern hybridization (C, hatched arrow). The Northern blot was probed with the ~400

bp *blyB* probe [as well as the ~175 bp *blyA* probe (data not shown)].

due to the global upregulation of all protein synthesis in response to the stress of MNNG

treatment.

blyA and *blyB* are on the same operon and they are co-transcribed on the same RNA transcript (75, 121). Northern analysis of the RNA from uninduced (-) and induced (+) cultures indicates that the expression of the *blyAB* transcript is also increased in all three MNNG-treated cultures (Figure 18C).

Damman and Oliver have shown that in *E. coli* expressing *B. burgdorferi blyA* and *blyB*, the majority of the BlyA protein was found in the membrane and the majority of the BlyB protein was found in the soluble fraction (50). We assessed the subcellular location of these proteins in MNNG-treated *B. burgdorferi* cells (Figure 19). The treated cells were sonicated and the lysate was ultracentrifuged. Proteins from the pellet (P100) and from the supernatant (S100) were resolved by SDS-PAGE and blotted with the BlyA and BlyB antibodies (Figure 19). All of the BlyA was found in the pellet fraction, containing the membrane-bound proteins, and most of the BlyB was found in the supernatant fraction, containing the soluble proteins. These data indicate that the subcellular location of these two proteins was the same in *B. burgdorferi* as in *E. coli*. The location of BlyA in *B. burgdorferi* is also consistent with the proposal that this protein is a membrane-bound bacteriophage holin (191). Taken together, these data, along with previous structural and functional data (50), suggest that the BlyA and BlyB proteins may play an important role in cell lysis during the last stage of the ϕBB-1 lytic cycle.

Chapter 6

Transduction by φBB-1

Here we demonstrate that φBB-1 is capable of transducing an antibiotic-resistance marker between *B. burgdorferi* cells. We have constructed a recombinant cp32 (φBB-1 prophage) carrying a kanamycin-resistance cassette (provided by J. Bono) and transformed *B. burgdorferi* CA-11.2A. φBB-1 shed from the transformant was used to transduce the antibiotic-resistance marker to susceptible CA-11.2A cells as well as cells from other strains of *B. burgdorferi*.

Inserting the kanamycin-resistance cassette into a cp32. pCE210 was constructed by cloning the kanamycin-resistance (kan^R)-cassette expressed from the *B. burgdorferi flgB* promoter (28) into a plasmid containing ~3.5 kb of phage DNA. This plasmid was linearized and transformed into competent *B. burgdorferi* CA-11.2A cells. Colonies selected in 500 μg ml⁻¹ kanamycin were screened by PCR primers that flank the site into which the kan^R-cassette had been inserted (Figure 20A). The ~1.4-kb product (Figure 20A, hatched arrow) contains the kan^R-cassette. The ~100 bp product (Figure 20, black arrow) was amplified from the other homologous cp32 loci in the cell that did not contain the insert. Both products are expected in a population of *B. burgdorferi* cells containing more than one homologous cp32 if the kan^R-cassette recombines into only one of them. Our mapping data show that the site of the kan^R-cassette insertion (on fragment 12SK) is located within or near one of the variable regions (not VR1) of the cp32 molecule (Figure 25 and Table 3).

79
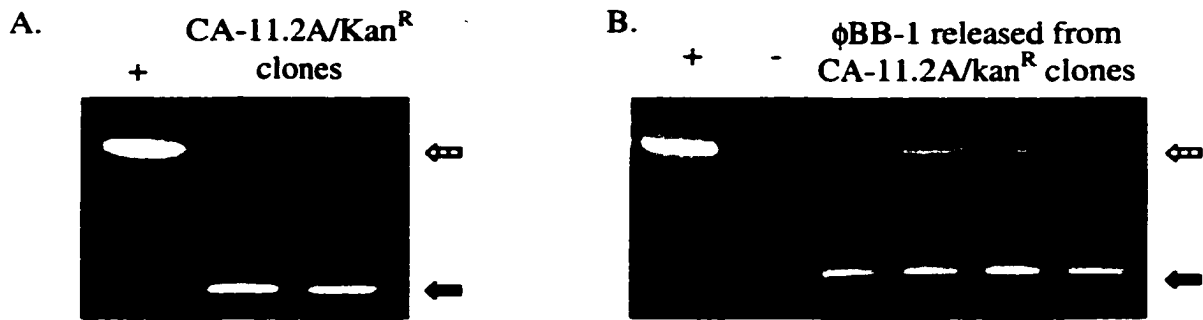
Figure 20. Kanamycin-resistant transformants of *B. burgdorferi*. Transformed CA-11.2A cells were selected with 500 µg ml^{-1} kanamycin and colonies were screened by PCR using the cp32SK*Nde*I primers that flank the *kan^R*-cassette insertion site (A). The PCR products were resolved on a 1% agarose gel and stained with EtBr. Both of the clones shown here contain two products, a small product that is the result of PCR from wild-type (uninserted) DNA (~100-bp; black arrow) and the larger product that contains the *kan^R*-cassette (~1.4-kb; hatched arrow). Phage released from several CA-11.2A/*kan^R* transformants were assayed for the kanamycin-resistance cassette by PCR (B). The phage DNA also contains both inserted (hatched arrow) and uninserted (black arrow) cp32s. pCE210 DNA was amplified as a positive (+) control and wild-type CA-11.2A phage DNA was used as a negative (-) control.

Phage collected from the supernatants of these transformants contain the *kan^R*-insertion, as well as parental phage genomes (Figure 20B), consistent with the results from the variable region analysis indicating that more than one cp32 is packaged in a population of φBB-1 phage heads (Figure 9). In all cases, PCR performed on the transformed strain and phage using an internal *kan^R*-primer (Kan1207F) and the

cp32SK*Nde*IF primer generates a single positive product of ~150 bp (for example see

Figure 23B).

The cellular location of the integrated kanamycin cassette was determined by

Southern hybridization (Figure 21B and C) of total cellular DNA resolved by two-

dimensional electrophoresis (Figure 21A). The blot of the gel was probed with the cp32-

specific probe 4 to localize the circular 32-kb molecules (Figure 21B). The membrane

was also probed with pOK12, the original source of the kanamycin-resistance gene (28,

181) (Figure 21C). The kan^R-probe hybridizes only to the CA-11.2A/kan^R transformant,

and has the same hybridization pattern as probe 4, locating the insertion on a cp32.

Extracted phage DNA (Figure 22A) was also probed with probe 4 (Figure 22B), which

hybridizes to phage DNA released from both the parental and the transformed CA-11.2A.

The kan^R-cassette probe hybridizes to only the φBB-1 DNA packaged and released by

CA-11.2A/kan^R (Figure 22C).

Transduction. To evaluate the ability of φBB-1 to introduce the kan^R-gene into

kanamycin-susceptible cells, bacteriophage from the CA-11.2A/kan^R-transformant were

Figure 21 (over). Analysis of the genomic location of the kanamycin-resistance cassette.

Total DNA from both parental CA-11.2A and transformed CA-11.2A/kan^R was extracted

and resolved by two-dimensional gel electrophoresis. The gel was stained with EtBr (A)

then blotted to nylon and probed with the cp32-specific probe 4 (B) or pOK12, the source

of the kan^R gene (C). The kan^R-probe has the same hybridization pattern as the cp32

specific probe, indicating that the integration of the cassette was into a cp32/prophage

(circular form; black arrow). Molecular sizes in kilobase pairs are indicated.

Figure 21.

A.

EtBr stain

48.1 -
33.5 -

17.1 -

10.1 -

CA-11.2A   CA-11.2A/
kan^R

B.

conserved cp32 probe

48.1 -
33.5 -

17.1 -

10.1 -

CA-11.2A   CA-11.2A/
kan^R

C.

kan^R probe

48.1 -
33.5 -

17.1 -

10.1 -
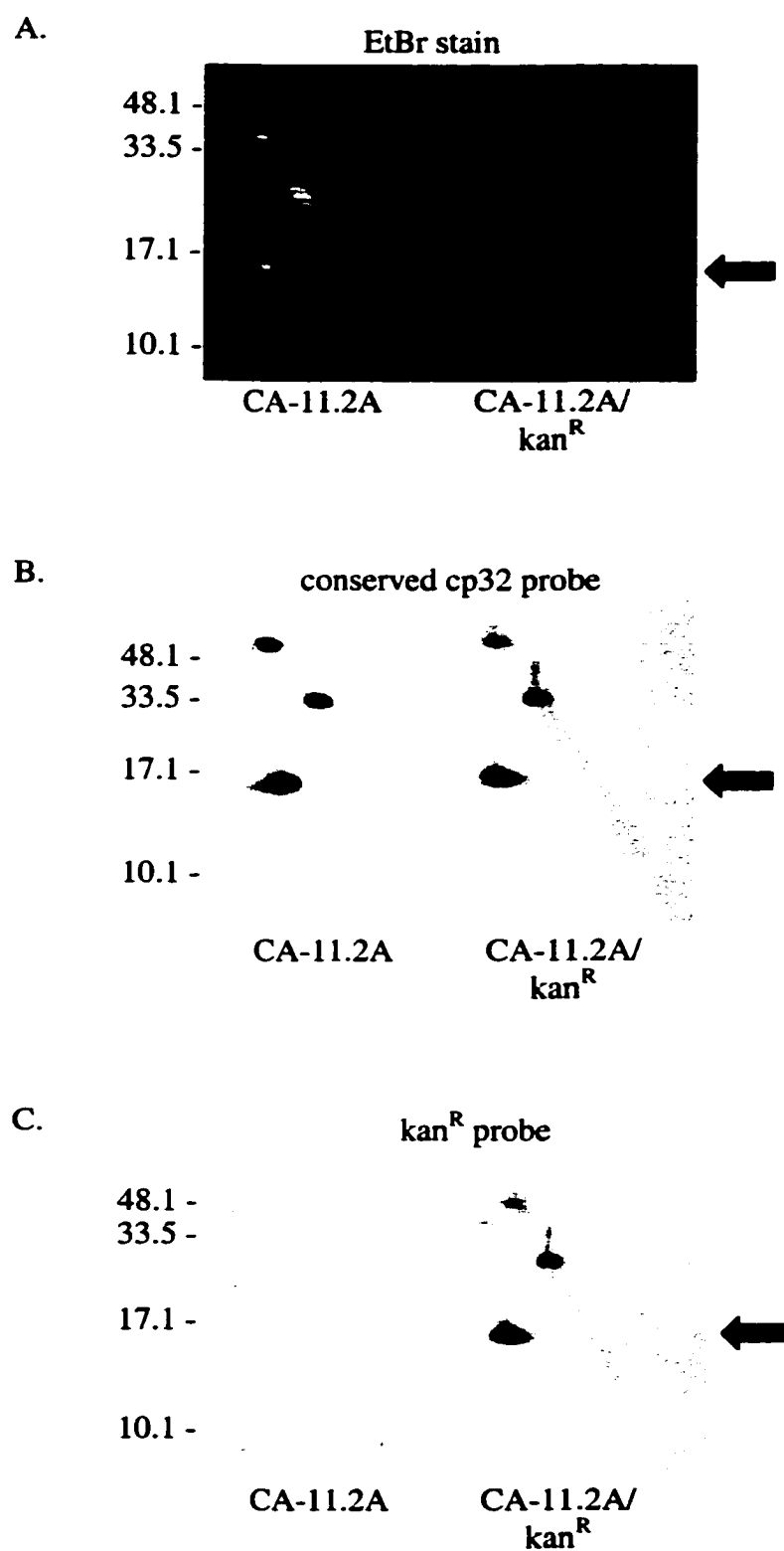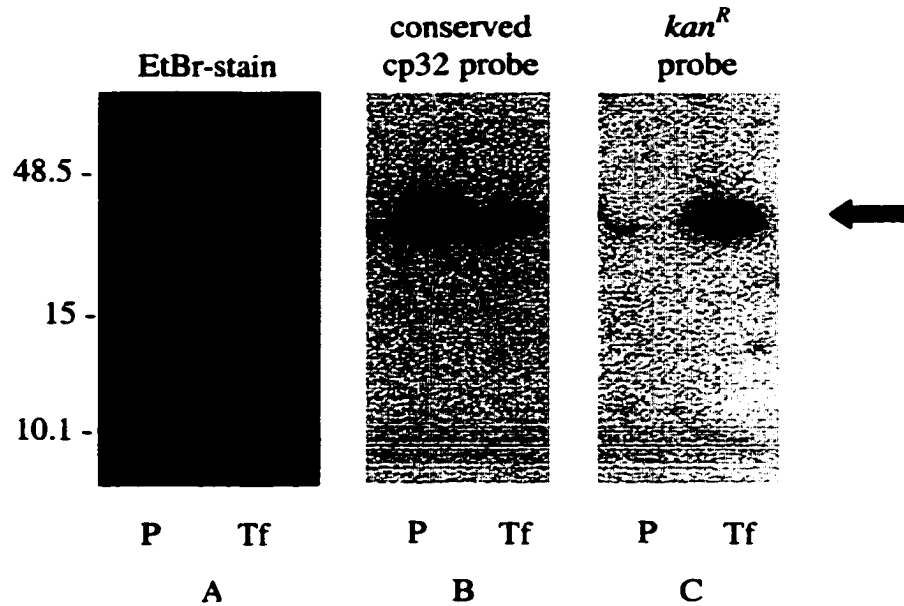
CA-11.2A   CA-11.2A/
kan^R

Figure 22. Analysis of the packaging of the *kan*^{R}-cassette by φBB-1. Phage particles

were precipitated from both parental (P) and transformed (Tf) CA-11.2A cells. The DNA

was extracted and resolved on a 0.5% agarose gel by conventional field electrophoresis.

The gel was stained with EtBr (A), then blotted and probed with either probe 4 (B) or the

kan^R-probe (pOK12; C). The conserved cp32 probe hybridizes to both the parent and the

transformant (black arrow), but the *kan*^{R} probe hybridizes to only the transformant. Thus,

the ~1.3 kb antibiotic-resistance marker was inserted into the lysogenic prophage and is

packaged by φBB-1. Molecular sizes are in kilobase pairs.

incubated with CA-11.2A cells at a ratio of approximately 1000:1. After an overnight

incubation, the cells were plated in 500 μg ml^{-1} kanamycin. We screened 10 of ~100

colonies by PCR. All of the *kan*^{R} colonies contained the *kan*^{R}-gene integrated into a

cp32.

The efficiency of transduction of φBB-1 between CA-11.2A cells is about 1 ×

10^{-5}. Plates containing no phage and CA-11.2A cells, or plates with phage but no cells

had no colonies. The addition of PK to the φBB-1/kan^R prior to incubation with cells

abrogated the transduction of the antibiotic-resistance marker. Incubating washed,

chloroform-killed CA-11.2A/kan^R cells with live CA-11.2A cells resulted in 0 to 3

colonies. No colonies grew when PK was added to the dead transformant cells prior to

mixing them with susceptible cells. This implies that even the small amount of transfer

between dead CA-11.2A/kan^R cells and live CA-11.2A cells requires protein. These data,

taken together, suggest that the lateral genetic transfer is mediated by phage φBB-1.

φBB-1/kan^R from the CA-11.2A transductant (CA.11-2A TR3) was incubated

with several other isolates of *B. burgdorferi* (Table 4). We have demonstrated

transduction of the kan^R-cassette by φBB-1/kan^R (CA-11.2A) into *B. burgdorferi* strains

B31 and 1A7 (a high passage clone of *B. burgdorferi* SH2-82) (Figure 23). The

efficiency of transduction by φBB-1/kan^R (CA-11.2A) into other strains is much lower, at

about 1 × 10^{-7}, or 100-fold less efficient than into CA-11.2A cells. Neither the 1A7

transductant (1A7 TR5) nor the B31 transductant (B31 TR1) assume the CA-11.2A

phage-producing phenotype. No demonstrable DNA transfer occurred when dead CA-

11.2A/kan^R cells were incubated with 1A7 and B31 cells.

To verify that TR3 and TR1 were CA-11.2A and B31, respectively, the first 300

bp of the polymorphic outer surface protein, *ospC*, were sequenced. The sequences,

which are strain-specific and diagnostic (105, 185, 186), were consistent with the *ospC*

sequences expected from each strain.

A. cp32SK*Nde*I primers

B. Kan^{R}1207F/cp32SK*Nde*IF primers

CA-11.2A B31 1A7

P Tf Td P Td P Td

CA-11.2A B31 1A7

P Tf Td P Td P Td

+ 1 2 3 4 5 6 7

+ 1 2 3 4 5 6 7
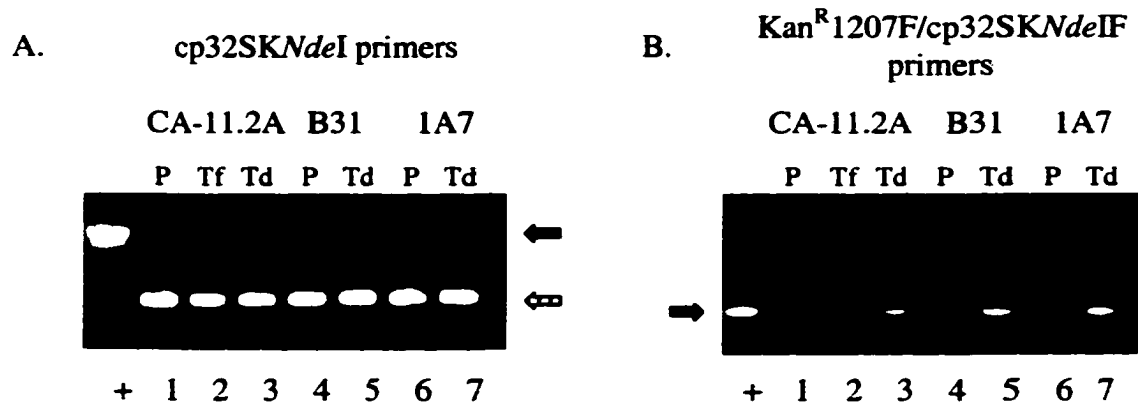
Figure 23. PCR analysis of *kan*^{R}-transductants of *B. burgdorferi*. *B. burgdorferi* strains CA-11.2A, B31, and 1A7 (a high passage SH2-82 clone) were incubated overnight with φBB-1/*kan*^{R} (CA-11.2A) and the cells were plated in 500 μg ml^{-1} kanamycin. Colonies were screened by PCR using the cp32SK*Nde*I primer pair that flank the *kan*^{R}-insertion site (A). Transductants (Td) contain both the ~100 bp negative product (all lanes, hatched arrow) and the ~1.4-kb band that contains the *kan*^{R}-cassette (black arrow; lanes 3, 5 and 7). pCE210 was amplified as a positive control (+), while the parental cells (P) of each strain served as negative controls (lanes 1, 4, 6). Lane 2 is the CA-11.2A/*kan*^{R} transformant (Tf). The transduction was verified by PCR using the Kan^{R}1207F/ cp32SK*Nde*IF primer pair (B), which yields an ~ 125-bp product from DNA containing the *kan*^{R}-cassette (B; black arrow, lanes 2, 3, 5, and 7). pCE210 was amplified as the positive control (+). No product was amplified in the parental strains (lanes 1, 4, and 6) when the junction between the cp32 sequence and the *kan*^{R}-cassette was the target of the PCR. The products were resolved on a 1% agarose gel and stained by EtBr as described above. The *kan*^{R}-integration site in each transductant was also verified by long range PCR using the Kan^{R}1207F/VR1R primers (data not shown).

ϕBB-1/*kan^R* (B31) also packages the *kan^R*-cassette (data not shown). We were

able to efficiently transduce the *kan^R*-marker into B31 using ϕBB-1/*kan^R* (B31), but we

have not yet been able to transduce the gene back into susceptible CA-11.2A cells using

ϕBB-1/*kan^R* (B31).

Variable region analysis of the transduced cp32s. We have demonstrated a

possible mechanism for lateral gene transfer in *B. burgdorferi* via transduction by ϕBB-1.

To determine if the *kan^R*-cassette of ϕBB-1 was introduced as a discrete plasmid or by

recombination, the VR1s of the parent strains, CA-11.2A, B31 and 1A7, as well as the

transduced strains, CA-11.2A TR3, B31 TR1 and 1A7 TR5 were amplified and resolved

by FIGE (Figure 24). The variable region VR1 is located ~5-kb from the site of the *kan^R*-

insertion (Figure 25). The fragments generated by PCR from the VR1 regions of the CA-

11.2A transductant, TR3 (Figure 24, lane 2), are identical to those of parental CA-11.2A

(Figure 24, lane 1; for sizes, see Table 6, Chapter 4). The B31 transductant (TR1; Figure

24, lane 4; for sizes, see Table 6), no longer has the smallest VR1 (2484 bp) of the

parental B31 (Figure 24, lane 3), but has now gained a VR1 that is the same size as the

second smallest CA-11.2A VR1 (2537 bp; Figure 24, black arrow). The B31

transductant has also lost the variable region corresponding to lp56, but whether this is a

result of the natural loss of the plasmid during cloning or due to the introduction of the

ϕBB-1/*kan^R* (CA-11.2A) prophage is unknown. 1A7 also has a small VR1 (2373-bp) that

is missing from 1A7 TR5, and the transductant has a VR1 that is also the same size as the

second smallest CA-11.2A VR1. This analysis suggests that the VR1 from the

introduced cp32, which contains the 2537-bp VR1 (data not shown), has replaced the
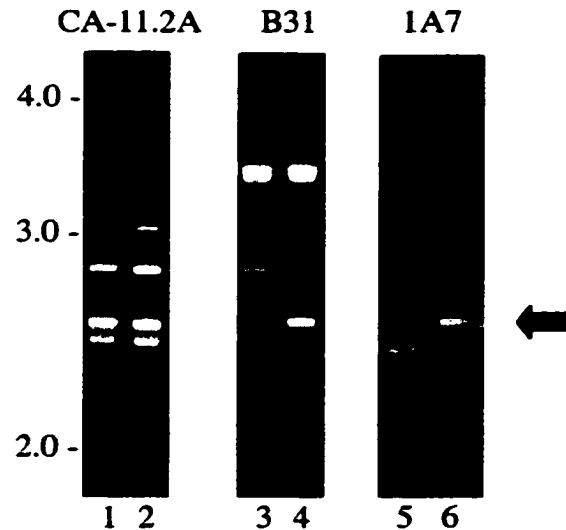
Figure 24. Amplification of VR1 from *B. burgdorferi kan^R*-transductants. The VR1

primers were used to amplify the cp32 VR1s of parental CA-11.2A (lane 1), B31 (lane 3),

and 1A7 (lane 5) as well as the variable regions of CA-11.2A TR3 (lane 2), B31 TR1

(lane 4), and 1A7 TR5 (lane 6). There are no changes in the plasmid complement

between the parental (lane 1) and transductant (lane 2) CA-11.2A strains, but both B31

TR1 (lane 4) and 1A7 TR5 (lane 6) have lost a variable region of the parental strains and

both have gained the ~2.5 kb VR1 (black arrow). Additionally, the B31 transductant has

lost the variable region corresponding to lp56. Amplification products were resolved on

0.8% agarose gels by FIGE and stained with EtBr. Molecular sizes are in kilobase pairs.

smallest VR1s of both B31 TR1 and 1A7 TR5. Whether the loss of the variable region

from the transductants is due to displacement of a resident plasmid, recombination by the

kan^R-gene into an extant plasmid, or due to the loss of a plasmid during cloning and

subsequent replacement with the φBB-1/*kan^R* (CA-11.2A) prophage is not known.
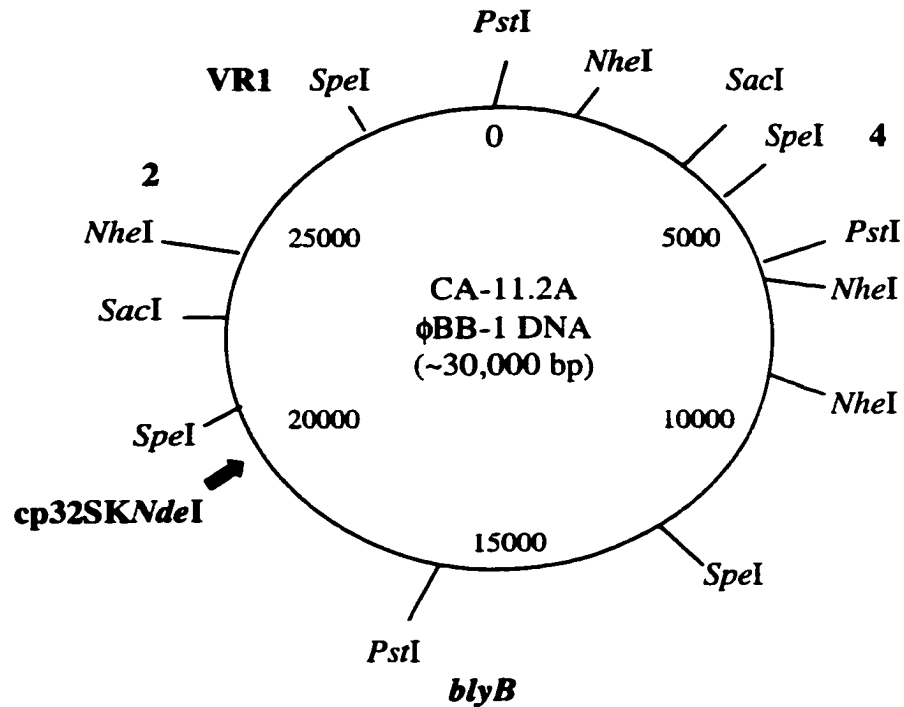
Figure 25. The insertion site of the kan^R-cassette. The circular phage map shows the approximate distances between the kan^R-cassette insertion site (black arrow) and the Southern hybridization probes used (probe 2: ~4000-bp, VR1 probe: ~5000-bp, probe 4: ~15,000-bp, *blyB* probe: ~5,000-bp). The kan^R-cassette is inserted in the middle of the BBP31 paralog present on the dominant φBB-1 genome.

Amplification of the VR1s from phage released from the B31 and CA-11.2A transductants was consistent with the results from the plasmid DNA. The VR1s not packaged by wild-type phage from parental cells are also not packaged by recombinantphage from transduced cells (data not shown). We are currently cloning and sequencing the 2537-bp VR1 from CA-11.2A and the transduced strains B31 TR1 and 1A7 TR5. Both the semi-quantitative PCR (Figure 10) and restriction mapping of the transductants indicate that the VR1 region that is introduced into B31 TR1 and 1A7 TR5

is from the dominant phage genome for which we have generated a partial restriction map (Figures 12 and 25). We have confirmed that the 2537-bp VR1 is linked to the kan^R-cassette on the transduced φBB-1/kan^R (CA-11.2A) genome by long-range PCR (data not shown).

Restriction mapping of transductants. Plasmid DNA from CA-11.2A, CA-11.2A/kan^R and CA-11.2A TR3 was extracted and digested with EcoRV to analyze the change in the cp32 molecules between the strains. We used Southern hybridization to map the location of the kanamycin-cassette on cp32 (Figure 26).

There are four hybridization sites in the cp32 population digested with EcoRV (Figure 26, left panel). This includes the ~6.6 kb band (hatched arrow) in the parental CA-11.2A (Figure 26, lane 1). This fragment is not present in either the CA-11.2A/kan^R transformant (Figure 26, lane 2) or the transductant, CA-11.2A TR3 (Figure 26, lane 3). In the latter two strains, there is an ~8-kb fragment (Figure 26, black arrow) that is not found in the parental strain. The size difference is the same size as the kan^R-cassette (~1.3 kb), suggesting the kan^R-cassette has been inserted into the 6.6 kb fragment. When the same blot is probed with the kan^R-marker, the ~8-kb fragments in the CA-11.2A/kan^R transformant and in CA-11.2A TR3 are the only hybridization sites (Figure 25, right panel, lanes 2 and 3, respectively). The ~6.6-kb fragment corresponds to the dominant band in an EcoRV digest of φBB-1 DNA probed with the cp32SKNdeI probe (data not shown).

To compare the kan^R-insertion site in the other transductants, plasmid DNA was extracted from the parental CA-11.2A, B31, 1A7 and the transductant CA-11.2A TR3, B31 TR1 and 1A7 TR5 cells. The plasmids were digested with XbaI and the DNA

cp32SK   Kan^R
*Nde*I

48.1 -

17.1 -

10.1 -

6.6 -

4.4 -

1 2 3   1 2 3
P Tf Td   P Tf Td
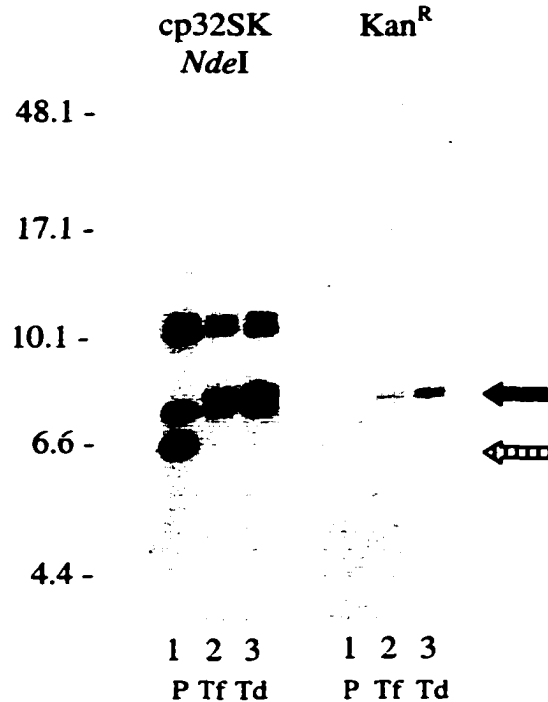
Figure 26. Restriction mapping of parental, transformant and transductant CA-11.2A

DNA. Plasmid DNA was extracted from CA-11.2A (lane 1, P), the CA-11.2A/*kan*^{R}

transformant (lane 2, Tf), and CA-11.2A TR3 (lane 3, Td), digested with *Eco*RV, and

resolved by FIGE. A blot of the gel was probed with either the cp32SK*Nde*I PCR

product (left panel), or with the *kan*^{R}-marker (right panel). Parental CA-11.2A has a ~6.6

kb fragment (hatched arrow) that is not present in either the transformant or the

transductant. Instead, these two isolates have an ~8-kb band (black arrow) that

corresponds to the ~6.6-kb band plus the 1.3 kb *kan*^{R}-insert. The restriction pattern of the

transformant and transductant cp32s are identical. Molecular sizes are in kilobase pairs.

resolved by FIGE. A blot of the gel was probed with both the cp32SK*Nde*I PCR product

and the *kan*^{R}-cassette (Figure 27). When probed with the cp32SK*Nde*I product (Figure

27, left panel), there is hybridization to a ~6.6-kb *Xba*I fragment that is found
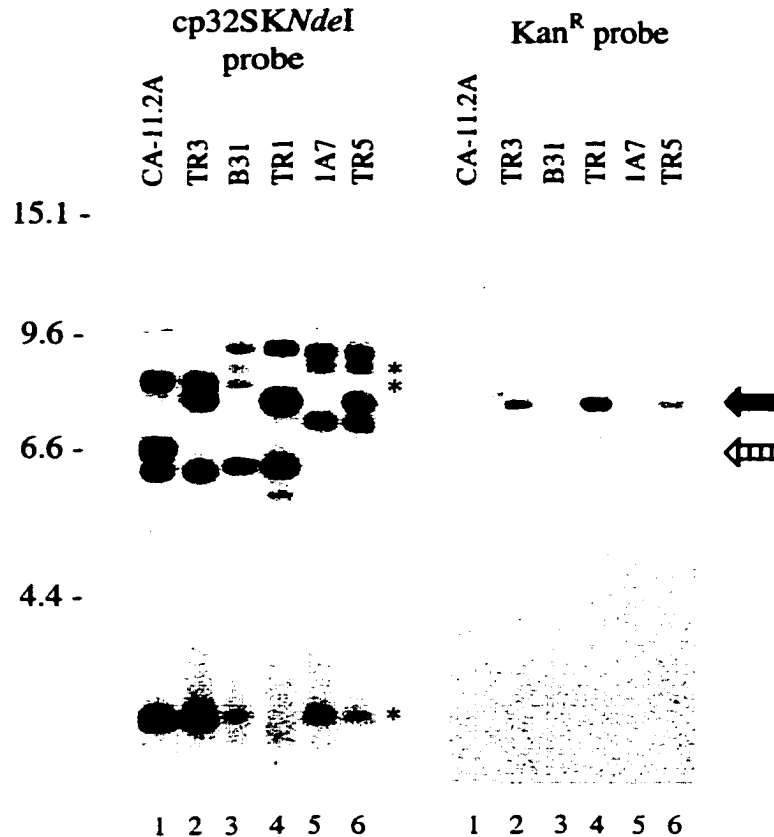
Figure 27. Comparison of the restriction maps of the cp32s of *B. burgdorferi* kan^R-transductants. Plasmid DNA from CA-11.2A (lane 1), CA-11.2A TR3 (lane 2), B31 (lane 3), B31 TR1 (lane 4), 1A7 (lane 5), and 1A7 TR5 (lane 6) was digested with *XbaI* and resolved by FIGE. A blot of the gel was probed with either the cp32SK*NdeI* probe (left panel) or the kan^R-probe (right panel). The 1A7 parent and the 1A7 transductant appear identical, except for the addition of an ~8-kb band. The B31 parent has three bands (lane 3; *) that do not appear in B31 TR1, possibly due to displacement of an under-represented cp32, or a loss of this plasmid during cloning.

exclusively in the parental CA-11.2A (Figure 27, lane; hatched arrow). An associated ~8-kb fragment is present in all the transductant lanes (Figure 27, lanes 2, 4, and 6; black

arrow). Hybridization with the kan^R-cassette (Figure 27, right panel) verified that the

~8 kb fragment contained the kan^R-cassette in all three transductants. There are also three

bands visible in the *Eco*RI-digest of parental B31 that are not present in the B31

transductant, TR1 (data not shown). The phage plasmid containing the kan^R-cassette was

either introduced into the transduced strains as a discrete plasmid, or the phage plasmid

recombines into an extant cp32 in a large stretch that encompasses both the variable

region and the *blyB* region (data not shown), a distance of almost 10-kb (Figure 25).

Chapter 7

Discussion

Thousands of bacteriophages have been identified in a large number of different bacterial species, yet their fundamental importance for the studies of molecular biology, genetics and epidemiology are reflected in the excitement still generated over the discovery of previously unidentified viruses. The importance of a new discovery is amplified when the bacteriophage that is characterized is from a species of bacterium that has previously had none described (3).

At what level of characterization is a new phage described? Most bacteriophage are identified primarily by their structural properties by electron microscopy, yet the ambiguity of sample contamination, staining artifact and relatively little molecular information gained from this technique (although electron microscopy remains a very powerful tool) has prompted most researchers to term viruses identified solely by microscopy as bacteriophage-like particles. Ackerman and colleagues, as members of the Bacterial Virus Subcommittee of the International Committee on Taxonomy of Viruses (ICTV), have proposed a series of traits that should be considered when determining whether a new phage has been described, including visual characterization, nucleic acid content, host range, and various chemical susceptibilities (3).

With these considerations, we now present evidence for a new bacteriophage of the Lyme disease agent, *B. burgdorferi*. This is the first molecular characterization of a bacteriophage from this genus. Based on our characterization we have assigned the name ϕBB-1 to the bacteriophage described here.

93

7.1 Structural features of φBB-1 particles.

A number of bacteriophage-like particles have been visualized in association with *B. burgdorferi* by electron microscopy (19, 77, 117, 144). The phage we describe here is structurally different from the elongated phages (19, 77) and one of the ciprofloxacin-inducible phages (117, 144) reported previously. φBB-1 may be structurally similar to the phage with A-1 morphology reported by Neubert *et al.*, but its capsid size is 1.5 times larger than that of the phage they visualized (30 nm) (117). φBB-1 also has an A-1 morphology, but the particle size is ~46 nm with a contractile tail of 90 × 10 nm (Figure 4). These structural characteristics place this newly described phage into the group of the tailed-bacteriophages, order *Caudovirales* (2). Characteristics of the bacteriophage in this order include a double-stranded DNA genome, an isometric capsid, and a tail that is involved in the injection of phage DNA into the host cell during infection (2).

The chloroform-resistance of the φBB-1 particle is consistent with a phage capsid that contains a protein coat and no lipid component. Additionally, the resistance to chloroform was an important consideration when identifying the particle as a possible bacteriophage. *B. burgdorferi* is a member of a group of bacteria, mostly Gram-negative, that package DNA into membrane-bound vesicles and release these vesicles into the culture milieu (56, 71). The DNA packaged in these 'blebs' appears to be non-specific genomic DNA of various sizes (56). Intercellular transfer of bleb DNA has been demonstrated in *Neisseria gonorrhoeae* (57), although not yet for *Borrelia*. Two important differences between blebs and the particle we have described are (1) the specific packaging of double-stranded 32-kb circular plasmid DNA by φBB-1 (Figure 5)

and (2) the chloroform-resistance of the particle, as evidenced by the continued DNase-protection after chloroform treatment (Figure 2), to which membrane-bound vesicles are susceptible but the majority of tailed bacteriophage particles are not (2, 3).

7.2 The 32-kb circular plasmid as the prophage.

After an extensive analysis of the conserved size of the linear chromosomes of *B. burgdorferi* sensu lato strains distributed world-wide, Casjens *et al.* concluded that any prophages in these bacteria were likely contained in the plasmids (38). The 32-kb circular plasmid was considered a good candidate for a temperate phage genome because of the ubiquity of the highly conserved molecule among the Lyme disease spirochetes and, indeed, many other members of the *Borrelia* genus (35, 42, 43, 68, 164).

There are many features of the cp32 family that are consistent with the hypothesis that these plasmids are prophage genomes (37, 42, 43). The conserved order of the genes of all known cp32s (37, 42) is similar to other phage families (39). The length of the DNA packaged into the procapsid of a tailed bacteriophage, as with some viruses, is restricted by the head size, and falls within a relatively narrow range (2, 55, 98, 112). The 32-kb circular molecules all fall within a range from 29.8 kb to 30.9 kb (mean = 30.5 kb) (37, 42, 43, 176). There is also evidence of recombination in at least one locus (containing the *ospE*, *ospF*, and *elp* homologs) on the cp32s (167, 172), suggesting lateral gene transfer has occurred among these plasmids. This gene transfer could be mediated from different cp32s within the same cell, by phage transduction of alternate cp32s within a population of cells, or by some other, as yet unknown, mechanism.

7.3 A model for the genomic structure of the prophage.

Using the data we have presented on φBB-1, the hypothesis that *blyA* encodes a holin (see below), and limited sequence homology with a known phage protein, Sherwood Casjens has proposed a model for the genetic organization of cp32 as a prophage [(37); refer to Figure 28]. Two genes on cp32, BBP42 and its paralogs and *blyA* (BBP23) and its paralogs, may be part of a phage late operon. P42 and paralogs are similar to *orf26* of the *Streptococcus thermophilus* temperate phage φO1205 (42, 156). The function of this gene has not been studied, but the gene lies between genes with homology to the small terminase subunit and portal genes of *Bacillus subtilis* phage SPP1 (47, 58, 74, 175), the locus that usually corresponds to the large terminase subunit in known tailed bacteriophage genomes (39, 78). These gene products play a role in the packaging of the DNA into the procapsid (74, 175). The *orf26* protein of the *Streptococcus thermophilus* temperate phage φO1205 and the P42 protein of *B. burgdorferi* cp32s are likely to encode the large terminase subunit. *blyA* (P23) and its paralogs encode a putative holin, as discussed below.

Both of these genes lie in locations on the cp32 plasmids that are consistent with a 'late operon' of a temperate phage. The longest contiguous block of genes on the cp32s without assigned function is from P41 through P26 (see Figure 28). This includes 28 genes, all transcribed in the same direction and each having a paralog on every cp32. P42 is the second gene in this regulon, exactly where it would be predicted to be based on the late operon gene orders of other bacteriophages (39, 78). *blyA* (P23) is at the 3' end of the gene cluster, again, in a predicted location (39, 191, 192). If these genes
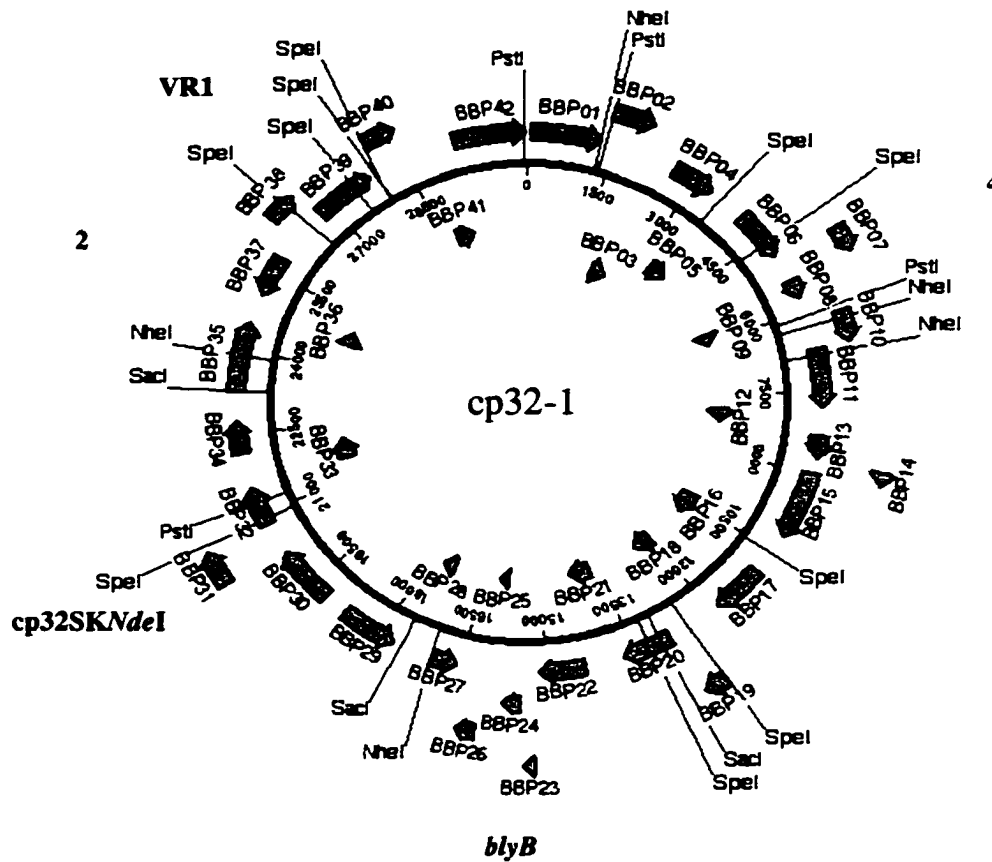
Figure 28. Map of cp32-1, a representative of the *B. burgdorferi* strain B31 32-kb

circular plasmids. The putative late operon of the bacteriophage runs from P41 clockwise

through P26. BBP23 is the *blyA* paralog and BBP42 has homology to *orf26* of *S.*

thermophilus φO1205. Both of these genes lie in their predicted locations based on the

late genes of other temperate bacteriophages. BBP32 has homology with partitioning

genes of other plasmids. The restriction map of cp32-1 and the dominant phage genome

of φBB-1 are different, although the gene order is the same. The positions of the probes

used on the dominant phage genome (Figures 11 and 12) are shown in their location on

cp32-1 in bold. The map was generated using MacVector based on sequences from the

complete genome (42, 68, 114).

are part of a late operon (or regulon) of the phage genome, then a prediction can be made that they would not be expressed during the lysogenic state. In fact, the very low levels of expression of the *blyA* gene and a P26 homolog from *B. burgdorferi* strain 297 (P26 and *blyA* are predicted to be on the same operon and they appear to be co-transcribed) during normal growth of *B. burgdorferi* has been demonstrated [(75, 121); Figure 18C]. We have also demonstrated an increase in the expression of this transcript after treatment with MNNG that is correlated with an increase in phage release (Figure 18C). Only 10^2 to 10^3 holin molecules are required for cell lysis, so tight regulation of the expression of these proteins is critical (191).

Other identified proteins encoded on the cp32s appear to be host-related. Those genes or gene families that appear to be expressed in culture (or in the host) include the *ospE*-paralogs, *ospF*-paralogs, *elp*, *rev*, *bdr*, and *mlp* genes (5, 32, 35, 64, 73, 107, 121, 128, 154, 166, 169, 172, 190, 194, 195). Bacteriophage often encode proteins that are synthesized during lysogeny and are involved in host pathogenesis, virulence or maintenance, and there are examples of bacteriophage that encode host genes as part of the late operon (49, 115, 116). The *ospE*/*ospF*/*elp* (*erp*) loci and some of the *bdr* genes are the only host-expressed genes that are in a location that could include them in the putative late regulon of the phage (35, 42, 128, 169, 176, 194).

There are also genes (BBP32 and heterogeneous paralogs) that are homologous to partitioning genes found on plasmids in other bacteria (16, 32, 42, 43, 167, 168, 176, 196). The only other extensively studied temperate phages with plasmid prophages, P1 and N15, both carry genes homologous to P32 of cp32 (1, 123). The heterogeneity associated with P32 and its paralogs may be a clue to the mechanism by which *B.*

burgdorferi can replicate and partition these homologous plasmids without incompatibility observed when homologous plasmids are replicated and partitioned in other bacteria (9, 22, 32, 167).

Comparing the maps of the φBB-1 genome from CA-11.2A (Figures 12B and 25) and cp32-1 from B31 (Figure 28) leads to a few provacative observations. The kan^R-gene has been inserted in the CA-11.2A paralog of BBP31, adjacent to the putative partitioning protein, P32. This is outside the putative late phage genes, and the disruption of this gene should have little effect on packaging and processing of the φBB-1 DNA. The most likely effect of the disruption of this protein would be in the partitioning of the plasmid during the lysogenic stage as partitioning genes are usually clustered together (9). We have observed no loss of this plasmid in transductants that have been passaged more than 20 times in the absence of selection (data not shown). Either this protein is not part of the partitioning apparatus, or the partitioning function associated with this protein can be provided in *trans* by one of the other cp32s that contain a functional paralog of P31.

There are also areas of remarkable similarity between the restriction maps of the two plasmids, particularly in the highly-conserved region. For example, the cp32-specific probe 4 is found on an identical-sized *PstI-SpeI* fragment on both cp32-1 (B31) and the dominant CA-11.2A cp32. As probe 4 is highly conserved on all known cp32s, the similarity is not surprising, but the fact that this region of high sequence similarity lies within the putative phage late genes does not escape our notice. Conversely, the inability of any of the specific B31 cp32-probes to hybridize with the CA-11.2A plasmids might be expected. The region of high diversity needed to segregate homologous B31 plasmids

from each other would be a region that is likely to be even more diverse in another strain. Most of these specific probes hybridize within the locus that encodes the variable OspE/OspF/Elp (Erp) lipoproteins (43, 169).

7.4 Processing of the lysogenic prophage.

We have demonstrated that the genome of φBB-1 is a linear double-stranded DNA molecule that arises from a circular lysogenic prophage (Figures 2 and 5). The mechanism by which this processing occurs for φBB-1 is not yet understood. Clues to the mechanism may lie in the ends of the phage genome, although the exact nature of these ends remains undefined for φBB-1.

There are three broad classes of double-stranded phage genomes: (1) molecules with unique ends and cohesive, single-stranded extensions, like those of coliphage λ (79); (2) molecules with unique ends with double-stranded terminal repetitions, exemplified by the T-odd phages like T1 (103); and (3) molecules with circularly permuted ends and terminal redundancy, such as phage P1 (89) and the *Salmonella* phage, P22 (124). Circular permutation means that, in a population of phage, every genome does not have the same processing site generating the packaged linear phage genome. Most tailed-bacteriophages fall into this third class (2).

Figure 29 is a diagram illustrating what would be expected of a restriction digest of a linear phage genome if the ends were (a) circularly permuted and non-specific (such as the coliphage P1) or (b) specific and unique ends (exemplified by λ phage). The ability to visualize overlapping fragments of the complete dominant φBB-1 genome demonstrates the absence of a specific, unique cut site generating the ends, consistent
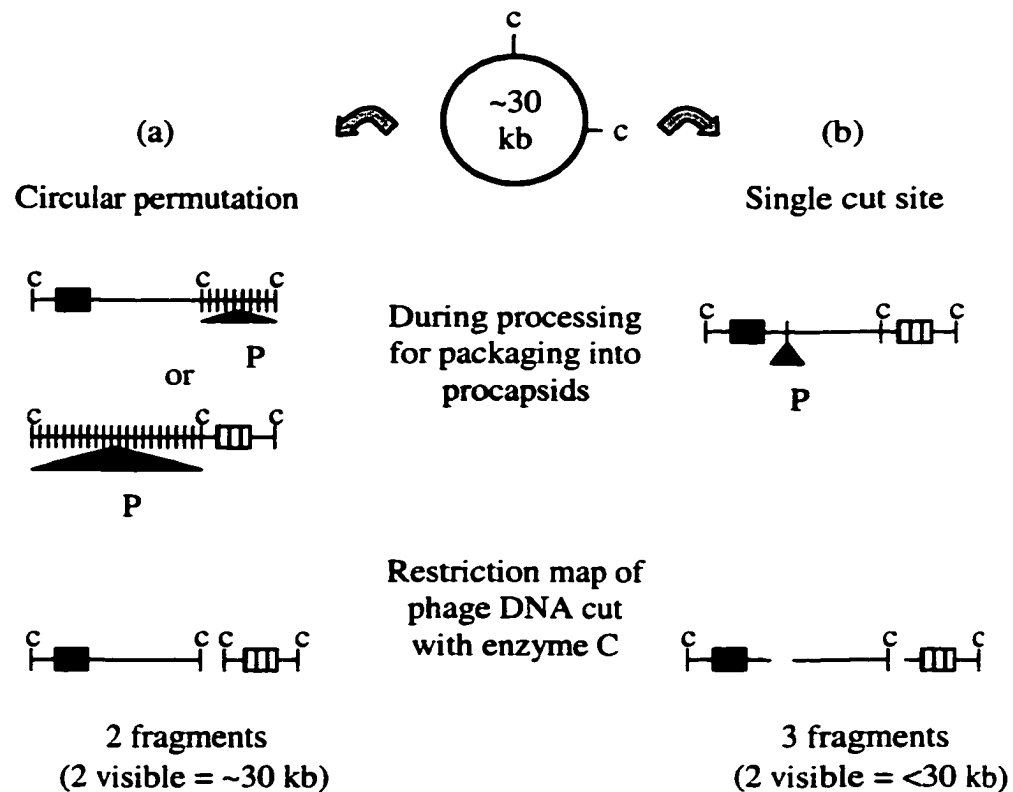
Figure 29. A model for using restriction digests to determine the processing of the prophage genome: circular permutation or a specific cut site? When digesting a linear molecule that has been generated by processing (P) from a circular molecule, if the processing is random (or semi-random) (a), then the restriction pattern (with enzyme c) will be consistent with a circular molecule (all fragments are visualized by the probes [black and hatched boxes], because none are preferentially absent due to non-restriction enzyme cutting). If the processing is specific (b), then hybridization with these probes will no longer be sufficient to visualize all of the joining fragments that generate a circular map. When the data from several digests are compiled, a unique cut site will be evident because all maps will align at the same site. If the processing is random, or semi-random, then the restriction maps will not align at a single cut site (see Figure 12A).

with the results from (a) (Figure 11). Additionally, the recapitulation of a 30-kb

circular molecule from the digest of linear phage DNA (Figure 12) indicates that the

φBB-1 genome is circularly permuted (2).

Based on the evidence, the genome of φBB-1 can be classified in the category of

the third type of double-stranded linear phage chromosomes and several generalizations

about φBB-1 may be true, based on what is known for other phages from this class. The

most well-defined model for a lysogenic prophage that is maintained as an

extrachromosomal element is bacteriophage P1 of *E. coli* (89). Bacteriophage P1 is one

of the largest phages known, with a genome of about 90 kb (89, 193). When packaged,

the DNA of infective virions possesses an ~10% terminal redundancy and is cyclically

permuted (89, 193). This cyclical permutation arises from processive 'headful'

packaging, the model that was first proposed for the packaging of T4 DNA (170). This

model has subsequently been used to explain the packaging of a number of viral DNAs.

The model involves several steps: (1) rolling circle replication late in viral infection

leading to concatemers of monomeric viral DNA; (2) initial cleavage of the concatemeric

DNA at a unique site [for P1 this occurs at the *pac* site (163)] or many different sites; (3)

packaging of the phage DNA from the cut end into the viral capsid until the head is full;

(4) cleavage of the packaged DNA from the rest of the concatemer; (5) reinitiation of a

second round of DNA packaging from the end generated by the headful-mediated cut

(163).

For bacteriophage P1, the processive headful packaging continues for three or

four viral units. Since each genome has ~10% terminal redundancy, the permutation of a

population of virion DNAs includes about 30 to 40% of the genome starting at the *pac*

site. That is, the processing site at which the circular P1 prophage is converted into a

linear phage genome occurs within ~30 kb of the *pac* site. In contrast, P22 has only ~2%

terminal redundancy for each monomer (124, 179) and packaging from the concatemer

continues through a maximum of ten viral units, such that the processing site occurs

within 20% (~5 kb) of the analogous *pac* site (180).

Although we have not yet demonstrated terminal redundancy directly at the ends

of the *B. burgdorferi* phage genome, there is evidence for concatemeric phage DNA

formation and possible terminal redundancy, supporting the headful packaging model for

the processing and packaging of φBB-1 DNA. The size of the phage DNA has been

determined as 32.7 kb by electron microscopy (102), 32.3 kb by regression analysis of

phage DNA resolved by conventional field electrophoresis (137), and 31.3 kb by analysis

of phage DNA resolved by FIGE in this work (Figure 13). These sizes are larger than the

actual size for any of the known cp32s [which are 30.3 ± 0.5 kb (42, 176)]. Despite the

smaller size of the φBB-1 DNA determined in this work, the genomic DNA is slightly,

but consistently larger, than the linearized cp32s from the CA-11.2A cp32 population

(Figure 13, lane 2). If φBB-1 DNA is packaged into procapsids by headful packaging,

then the larger size of the phage genome is due to the terminal redundancy of the phage

genome. This redundant DNA may play an important role in the circularizing of the

linear phage genome, as is the case for phage P1 (86, 150).

In addition to the terminal redundancy present in all bacteriophage genomes that

undergo this type of packaging, the headful-packaging model requires the formation of

large concatemers of phage DNA units. When DNA from induced cultures of *B. burgdorferi* CA-11.2A was resolved by two-dimensional electrophoresis, large DNA molecules that could correspond to open circular and linear multimers of phage DNA could be visualized by Southern hybridization with cp32 specific probes (data not shown). The presence of these putative concatemers has not been confirmed by pulse-field electrophoresis, electron microscopy or CsCl-gradient purification.

There are two models (Figure 30) for the processing and packaging of concatemers of phage DNA that can lead to circular permutation, and neither are excluded by the headful packaging model. The two models, sequential packaging from a unique start site (like P1; Figure 30, a) or random packaging of phage units from a large concatemer (like T4; Figure 30, b), are difficult to distinguish by restriction digest mapping in *B. burgdorferi*. The region in which the processing occurs (generating circular permutation) is usually under-represented (sub-stoichiometric) when compared to regions of the phage genome that are not found at the ends (90). However, since *B. burgdorferi* cells contain more than one cp32, and φBB-1 has more than one phage genome, there are always several sub-stoichimetric bands, representing minority cp32 prophages. The results of one experiment, shown in Figure 14, indicate that all fragments of phage DNA are end-labeled equally, suggesting that all fragments contain an end, which would be consistent with random processing from a concatemer. Another possibility, however, is that the concatemers of φBB-1 DNA are large. In this case, the processing might encompass the entire molecule, giving the appearance of random processing. We know of only one bacteriophage (the lytic phage T4) that packages (or even appears to package) the phage genome randomly from a concatemer (2), and the

(a) Sequential encapsidation from a unique starting site

Unique starting site

Alignment of molecules   Distribution of ends

(b) Random encapsidation

Alignment of molecules   Distribution of ends
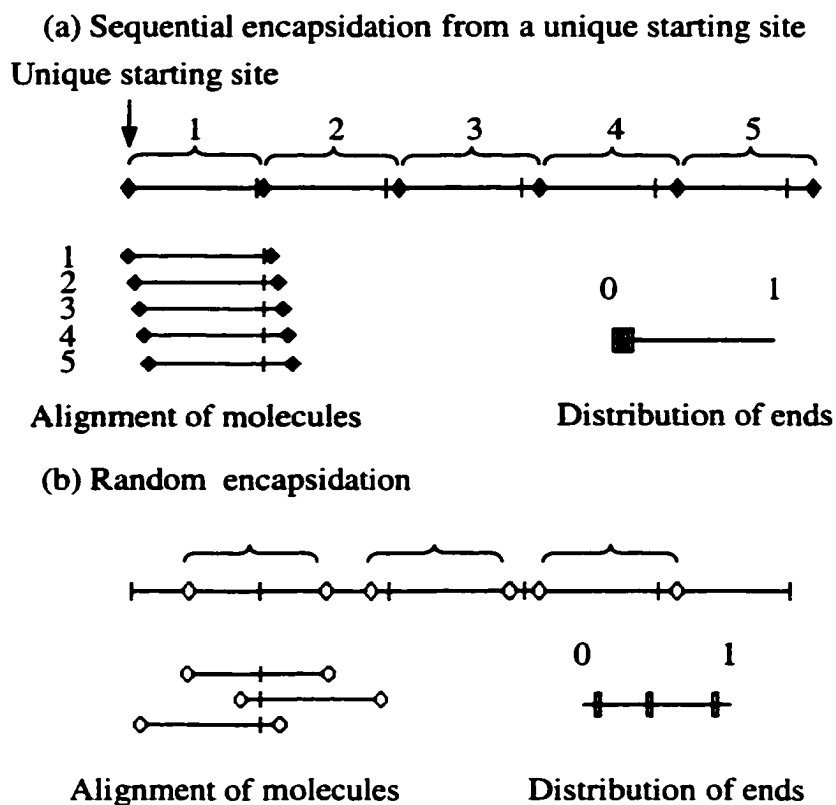
Figure 30. Two models for packaging phage genomes from prophage concatemers. (a) Diagram showing that if the concatemer is long enough for only a small number of headfuls of DNA to be generated and the terminal redundancy is sufficiently small, sequential encapsidation from a unique starting site results in a restricted distribution of ends (restricted permutation). (b) Random encapsidation from a concatemer results in a random distribution of ends (random permutation). Adapted from Tye, *et al.* (180).

labeling of the multiple φBB-1 genomes, as well as the labeling of nicked DNA and incomplete digestion are more likely reasons for the apparent random permutation. We are currently attempting to repeat this experiment under more rigorously controlled conditions.

7.5 Induction of the prophage.

The reversion of a lysogenic prophage from quiescence to a lytic state is often achieved by stressing the host bacterial cell by chemical or physical means (25). Prior to this work, bacteriophage of spirochetes have been produced from cells treated with mitomycin C or ciprofloxacin (33, 87, 117). φBB-1 does not appear to be consistently inducible with either of these chemicals, although we have observed slightly enhanced phage release from one culture of *B. burgdorferi* CA-11.2A treated with mitomycin C (data not shown). MNNG is the most reliable φBB-1 prophage inducer that we have used. Previously, MNNG has been used to generate mutant cyanophage (7, 142) and mutant mycobacteriophage (151), to induce prophage λ from *recA* mutants of *E. coli* (189), and to induce prophages through mutations in *Haemophilus influenzae* (11, 27).

MNNG is a DNA alkylating agent and a potent mutagen. The proposed three-step model for the mechanism of MNNG mutagenesis is (1) the production of miscoding lesions on the DNA, especially O6-methylguanine at specific sites as determined by context (60), and the induction of methyltransferase; (2) the generation of DNA sequences in which O6-methylguanine is paired with thymine; and (3) the conversion of the abnormal base pair to an adenine-thymine pair, generating a transition mutation (145). Presumably, the lesions on the DNA at these locations or at different locations (65) activates the SOS response, initiating the induction of the prophage (see below). Due to the high rate of mutagenesis, and the high toxicity, associated with the use of this chemical, MNNG is not regularly used on those systems where other agents are as reliable for inducing prophage. Future research into the molecular nature of induced

φBB-1 must take into account that mutation frequencies as high as 20% have been observed in the DNA of cells treated with MNNG, affecting the prophage DNA as well as the cellular DNA (101).

Induction of prophage has been best characterized for coliphage λ. Ultraviolet radiation is the inducing agent of choice in this system, but the principles of prophage induction are thought to be the same for other inducing agents. In short, damage to host DNA by a mutagen activates the SOS repair pathway. The activation of the SOS regulon occurs when *recA* mRNA is increased and the RecA protein mediates the cleavage of the LexA repressor. Germane to our understanding of induction is that the RecA protein is also a mediator of the cleavage of the λ *cI* repressor molecule (and the repressor molecules of many other temperate phages) (92, 99, 113, 129). The cleavage of the repressor molecule allows derepression of the genes involved in lytic infection (69). There are also RecA-independent pathways of λ prophage induction, although these are not as well understood (132, 189). As well as playing a role in initiating the SOS response, MNNG must also have a RecA-independent mechanism for induction, as this chemical has been used to induce prophage λ from *recA* mutants of *E. coli* (189).

Not all lysogenic prophages are inducible. Bacteriophage P2, which has a life cycle much like λ, is not artificially inducible, although spontaneous induction does occur at low levels (24, 25). The repressor molecule of this bacteriophage lacks the pair of amino acids that is responsible for the destabilization of the λ repressor molecule and apparently is not susceptible to RecA-mediated cleavage (25, 143). Instead, this bacteriophage requires satellite phage P4 to co-infect the host cell and provide the

derepressor in *trans* (24, 100). Bacteriophage Mu, one of the most efficient

transposons known, is also an uninducible temperate virus. Most of the work done with

phage Mu uses a *cts* mutant, a bacteriophage with a temperature-sensitive repressor

molecule (25, 93, 184). We will return to this in reference to φBB-1 and our system

below.

The natural or induced release of a temperate prophage is often associated with a

decrease in cell density during the 'lytic burst' (25). Barbour and Hayes have suggested

that this phenomenon might account for the periodicity seen during early attempts at

cultivating *Borrelia* (19). We have never witnessed a dramatic decrease in cell density

associated with the release of φBB-1 from *B. burgdorferi* CA-11.2A. Preliminary time

course studies (Figure 7) have shown that during the recovery period following MNNG

treatment there is a modest 16% decrease in cell density between 24 and 36 h, and

another slight 20% decrease between 48 and 60 h (Figure 7B; dashed line). Both of these

apparent decreases are relative to the densities at the previous time point. The drop in

cell density of the treated culture at these time points could be related to cell lysis by the

phage at 36 h and again at 60 h (Figure 7A), but there is no associated decrease in the cell

density of the untreated cells at 36 h when phage is spontaneously released (Figure 7).

Even if the decrease in cell density of the treated culture is due to lysis by φBB-1, this

decrease is still less than the 20 to 50% drop in cell density regularly observed with

mitomycin C-treated *B. hyodysenteriae* that produce VSH-1 (87).

There are two possibilities for the absence of a dramatic lysis event (>50%

decrease in cell density) during phage release: (1) the phage is exiting the cell by some

means other than lysis, or (2) the method of inducing prophage that we have described is inefficient and only a small population of cells are releasing phage at one time. All known double-stranded tailed bacteriophages exit the cell by lysis (2, 191, 192). Additionally, there is a correlation between the increased synthesis of a possible holin-like system encoded by the phage (50) and an increase in phage release (Figure 18). Taken together, this evidence suggests that φBB-1 exits by cell lysis.

There is strong evidence suggesting that the second option, the inefficiency of MNNG-induction, is a viable hypothesis. Of the more than twenty *Borrelia* isolates that have been treated with MNNG, only three have demonstrated the ability to release quantifiable amounts of φBB-1 under the conditions we have described: *B. burgdorferi* B31-UM, *B. burgdorferi* CA-11.2A, and *B. bissettii* DN127 (Figure 8). We have designated our strain as B31-UM to separate this strain from other B31s that are ostensibly the same strain, but appear to have differences (such as in their plasmid complement, including cp32s) that could lead to physiological dissimilarities (43, 68). Among the strains tested were two low passage B31 strains and the uncloned parent of CA-11.2A, CA-11. We have found no low passage isolate that produces φBB-1. We have seen prophage induction in a few uncloned high passage CA-11 cultures, although this does not occur regularly and we have not observed prophage induction from the low passage isolate. The plasmid content of the low-passage CA-11 and CA-11.2A appears to be virtually identical, so the difference in phage release between these two isolates is striking.

CA-11, a California tick isolate, synthesizes outer surface protein C (OspC) constitutively (109, 149). CA-11 was cloned by plating on solid medium and the CA-11.2A clone was selected based on the low synthesis of the outer surface proteins A (OspA) and B (OspB) (109, 130). The synthesis of OspC is inversely correlated with the synthesis of OspA and B, with OspC synthesis upregulated in the mammalian host. The synthesis of these proteins appear to be regulated, at least in part, by temperature-mediated changes in supercoiling (6, 148). The cellular variation that causes the constitutive upregulation of OspC may be related to the general control of protein synthesis or degradation, or to homeostatic regulation of DNA supercoiling. A change in DNA supercoiling would have a global effect, with altered *ospC* expression as the most noticable attribute. Whatever the cause, perhaps this mutation also makes phage production more likely in the clones of strain CA-11. We have tested four other cloned strains of CA-11 and each naturally produces phage at some level (data not shown). The reasons that the uncloned low-passage CA-11 does not produce phage remain unclear.

We return now to the fact that not all tailed-bacteriophages are inducible. We have considered the possibility that the wild-type prophage of ϕBB-1 is not inducible or that the ϕBB-1 prophage in a wild-type host is uninducible, or is naturally inducible at low levels, like P2. Currently, we can detect phage release at only mid to high production ($\geq 10^6$ phage ml^{-1}). This titer requires a fairly large burst size, a size that may not be achieved in low passage isolates that have not yet become adapted (or mutated) to culture conditions.

Additionally, we cannot forget the natural epidemiology of *B. burgdorferi* when considering the conditions under which φBB-1 is released. BSK-complete, while a suitable laboratory medium, is only a poor mimic of the environment that *Borrelia* would encounter within a mammalian host or tick vector. Because of the stress induced by culture conditions on low passage isolates, these cells may not be physiologically capable of generating enough packaged virions for a large lytic burst.

The density of *B. burgdorferi* in a mammalian host is very low; there are often not enough bacteria to culture from infected hosts (146). *B. burgdorferi* has the highest cell density in the tick vector and the greatest opportunity to interact with other cells and even other strains (146). The opportunity for φBB-1 to find a suitable host for infection would increase greatly under these high-density conditions, even at the lower titer achieved by spontaneous induction of the prophage. The study of bacteriophage release, as well as a number of other physiological processes, in the invertebrate vector remains a fertile area of research.

Higher passage isolates are more likely to release φBB-1 than lower passage isolates. Even in the high-passage strains, though, the induction may not be complete due either to the penetrance of the putative mutation or the multi-copy nature of the cp32 plasmids. No work has been done showing what effect the protein products (such as a repressor) of the various cp32s may have on each other in *trans*. In such a complicated system composed of many different plasmids and possible prophages, we can reasonably assume that a whole class of mutants can arise that affect different parts of the phage life cycle. Accordingly, we have documented strains that have almost every phenotype

possible with regard to phage production, transduction and prophage induction (Table

9). We have noted that the transduction of a strain with φBB-1/*kan*[R] (CA-11.2A) does

not confer the typical CA-11.2A/φBB-1 phenotype on that cell (note particularly 1A7 and

the transductant, TR5, which produce no phage under the conditions that we have

described). The cause of prophage derepression may reside in the CA-11.2A host

genome or on another cp32 and not on the φBB-1 (CA-11.2A) prophage.

Table 9. φBB-1-related phenotype of several strains of *B. burgdorferi*

Strain[1]	Natural producer[2]	Inducible	Transducible[3]
B31-1M1T(low passage)	no	no	yes
B31-UM	no	yes	yes
CA-11 (low passage)	no	no[4]	no
CA-11.2A	yes	yes	yes
1A7 (high passage)	no	no	yes
DN127	yes	yes	no

[1] strains include those relevant to our phage work, or different passage equivalents, all other strains are

negative for all three phenotypes; [2] production on a regular basis (>80% of the time) as assessed by EtBr-

stain of DNA; [3] transduction was attempted with CA-11.2A φBB-1/*kan*[R] at a multiplicity of infection of

1000:1; [4] as the passage number increases, the likelihood of prophage induction increases

The temptation to suggest that a comparison of the strains from Table 9 might be

an important step to understanding the life cycle of φBB-1 is moderated by the

knowledge that such a study would be almost prohibitive in its scope. The multicopy

nature of the prophage, the large number of molecules of DNA in the *B. burgdorferi*

genome and the small but perhaps significant sequence variability between each strain

would enhance the difficulties. Additionally, the cp32/prophage correlation may not be

absolute, with only one or more of the complement of *B. burgdorferi* B31 and CA-11.2A

cp32s being the actual prophage, and the others being cryptic prophages incapable of productive infection, although most, if not all, cp32s are packaged. If the mediation of prophage repression is effected in *trans*, then a careful analysis of the entire genome of each strain might be required. However, the ability to study the molecular biology of *B. burgdorferi* is not yet at this level. Identifying a repressor molecule of φBB-1 will be an important key to understanding the φBB-1 life cycle.

7.6 Phage proteins.

Identifying the structural proteins will be critical to further characterizing φBB-1 and to understanding the phage life cycle. One possible explanation for the stability of the phage production phenotype of a strain following transduction is that the introduced cp32 molecule is incapable of making new phage. In this model, the capsid visualized (Figure 4) would actually be a specialized transducing phage that does not encode its own proteins, which would be encoded somewhere else on the *B. burgdorferi* genome. We know of no bacteriophages that carry out specialized transduction by packaging a completely non-phage related genomic element specifically, but we could see the advantages that the subversion of this system would have for the host organism. Such a system could serve as a good mechanism for generating diversity in outer surface proteins. The mechanism by which such a bacteriophage would be repressed would not be on the packaged material (the repression and derepression elements are on another molecule in the genome entirely). This could conceivably prevent super-infection immunity, allowing multiple 'phage' genomes to enter the cell, thus generating even more diversity. Although our data do not support such a model, and Ockham's Razor

would favor the simpler alternative, we also cannot deny that this explanation answers several questions about our observations, as well as raising many new ones. With the knowledge that there are possibly three or four more reported bacteriophage-like particles, associated with *B. burgdorferi* (77, 117, 137), we can envision a scenario that is a hybrid of the 'complete specialized transduction' hypothesis and the more likely 'cp32 as a lysogenic prophage' hypothesis.

In this hybrid model, similar to P2, the repression of φBB-1 is not associated with a cp32 but with another lysogenic prophage or even a cryptic prophage. This prophage would no longer be capable of productive infection (which may also apply to all but a few of the cp32s), but may still synthesize the necessary repressor or derepression elements from its integrated site. This is an attractive model because we could hypothesize that the repressor/derepressor locus on the satellite phages is mutated in CA-11.2A, but, as this mutation would not be transduced with the phage DNA, the φBB-1 (CA-11.2A) prophage would be repressed in another, non-mutated strain, which is consistent with the data. One of the satisfying features of the hybrid model is that the scenario of cp32 as a prophage fits conveniently with the data and is not dismissed, but modified to include a *trans*-acting factor. In the absence of identifying any structural genes or the repressor element on the cp32 molecule, all of these arguments remain speculative.

There are no proteins on the cp32 molecules that are homologous to structural proteins of known tailed phages. However, because of the divergent evolution of bacteriophages with their hosts from other phages and their hosts, phage structural

proteins, while often resembling each other in their tertiary or quaternary conformations, do not share much sequence similarity at the amino acid sequence level (2, 78).

We have proceeded in our investigation with the hypothesis that the most abundant protein in any bacteriophage or virus sample should be the head protein because of the number of subunits (capsomers) required for the formation of the capsid (2, 55). Our search for structural proteins of φBB-1 has been hindered by the serum-based protein-rich medium that is necessary to support cell growth and phage release. We have used multiple CsCl-gradients to remove some of the non-specific proteins and to increase the recovery of clean phage DNA. The only protein that was abundantly present in these purified samples was an apparently ~70-kDa protein (Figure 15). There are bacteriophages that have covalently cross-linked capsid proteins that form large protein multimers (120). Perhaps φBB-1 does not have complete covalent cross-linkage, but covalently dimerizes two or three capsid proteins.

We have also developed a low-protein medium that is capable of supporting modest bacteriophage release. Although we have not successfully identified any proteins that are phage-specific, we have made a preliminary identification of what appears to be a unique protein present in precipitated supernatant samples containing phage (Figure 17). This protein is ~25 kDa, which is slightly smaller than the average head protein (30-35 kDa) of bacteriophages, but is still within a reasonable range. As there is no increase in this protein with the sample that was applied to multiple CsCl-gradients, the significance of this protein is unknown. There are smaller quantities of the 25-kDa protein present in cultures of *B. burgdorferi* B31 and CA-11 (data not shown), neither of which produce

phage in large quantities. The protein is likely associated with the bacterium rather than the bacteriophage. An association with the bacterium would explain the absence of this protein in CsCl-purified phage samples, as a protein of that size would migrate differently through the gradient than the large phage head would. Efforts are currently underway to purify enough of this protein for N-terminal sequencing.

Guina and Oliver had previously cloned two genes, *blyA* and *blyB*, from *B. burgdorferi* (75). The gene products of *blyA* and *blyB* appeared to encode a hemolytic activity (75). These genes were initially identified as two open-reading frames (ORFs) of a four-ORF operon conserved on the cp32 molecules and located in close proximity to the region of cp32 encoding a group of variable lipoproteins (the *mlp* loci) (121). The function of the BlyA and BlyB proteins was initially proposed as a possible virulence factor important for the initial invasion of mammalian cells by *B. burgdorferi* (75). Subsequently, Damman and Oliver have shown that the cryptic *E. coli* hemolysin SheA was responsible for the cell lysis that had been attributed to the *blyA* and *blyB* gene products (50).

Except for the filamentous phage, all known bacteriophage require lysis of the cells for their release (192). Damman and Oliver have found that the predicted structure of BlyA was very similar to bacteriophage-encoded holins. Holins, found in all known tailed-bacteriophages, are small proteins that form stable, non-specific pores in the membrane, allowing an endolysin access to the peptidoglycan (2, 191, 192). BlyA can complement a defect in the *S* gene of phage λ (50). Gene *S* is the holin responsible for the release of the phage-encoded endolysin into the periplasm (191, 192). Although no endolysin has yet been described for φBB-1, the presence of a putative phage-specific

holin encoded on cp32, provides support for the hypothesis of cp32 as a prophage (as

discussed above).

The exact role of BlyB is unknown, although the correlation between the

synthesis of both BlyA and BlyB suggests that BlyB may have some accessory role,

either as a regulatory factor, an assembly factor or possibly an endolysin (50). We have

demonstrated that BlyA and BlyB syntheses are increased as a consequence of MNNG

treatment, and this correlates with phage production (Figure 18). However, in the

experiment shown, the syntheses of these proteins do not correlate with each other, with

the most BlyA being made in CA-11.2A, the reliable phage producer, and more BlyB

being synthesized in B31, which does not produce much phage (Figure 18B). Whether

this was a physiological phenomenon or an experimental artifact was not apparent. BlyB

may have no relationship with BlyA (and φBB-1), other than being encoded on the same

operon. *blyA* and *blyB* are thought to be cotranscribed (75, 121) and Northern analysis

suggests that the transcript is more abundant in B31 than in CA-11.2A. The amount of

RNA recoverable from B31 is much higher than for CA-11.2A, and this may account for

much of the difference, but we cannot exclude the possibility that there is translational

control of the synthesis of the putative holin, allowing the strain with the least transcript

to produce the most BlyA.

7.7 Transduction of the *kan^R*-marker by φBB-1.

The cp32s and homologous sequences are ubiquitous throughout the Lyme

disease spirochetes and many other members of the *Borrelia* genus (42, 43, 68, 164).

Borrelia presents a problem when we define a host range because most of the members

of the genus already contain plasmids that are homologous to the lysogenic prophage of

ϕBB-1. The host range for ϕBB-1 would seem to include all known *B. burgdorferi*

sensu lato species. Our efforts to cure *B. burgdorferi* of cp32s by chemical or electrical

means have been unsuccessful (data not shown). We know of no strain of *B. burgdorferi*

that carries fewer than three cp32s.

Prior to this work, no mechanism for lateral gene transfer, such as conjugation,

had been demonstrated in *Borrelia*. To demonstrate the ability of ϕBB-1 to infect *B.*

burgdorferi cells and transduce DNA, we inserted an antibiotic resistance marker into

one of the lysogenic prophage genomes. Currently, there are only two available

antibiotic-resistance markers for *B. burgdorferi*, one that confers resistance to

coumermycin A_1 (*gyrB^r*) (141), and a recently developed marker that confers resistance

to kanamycin (28). Coumermycin A_1 resistance is generated by a point mutation in the

extant *gyrB* gene (141). A cassette containing the *gyrB* gene with the critical point

mutation was used to demonstrate the first genetic transformation of *B. burgdorferi* (140)

and has been subsequently used for the insertional inactivation of genes on the 26-kb

circular plasmid (29, 131, 177, 178). A single cross-over of a plasmid containing the

gyrB^r gene was used to introduce heterologous DNA into the chromosomal *gyrB* locus

(165). The *gyrB^r*-cassette was also used as a marker for the site-directed disruption of the

B. burgdorferi gac gene (93), which encodes an unusual small DNA-binding protein (94).

A major disadvantage of using the *gyrB^r* to disrupt genes has been the high rate of

homologous recombination into the chromosomal locus of *gyrB*, instead of the targeted

site (131, 139, 140). Our initial plan for ϕBB-1 required inserting the *gyrB^r* gene into the

*Nde*I site of the phage DNA fragment clone 12SK (Table 2). We constructed a plasmid

(analogous to pCE210) that contained both the phage DNA and $gyrB^r$, and electroporated this plasmid into CA-11.2A. Previously, the transformation efficiency of the $gyrB^r$-insertion into the desired location has been reported to be about 0.4% (131, 177); however, we screened over a thousand colonies and were unable to isolate a single clone with the $gyrB^r$ integrated into a cp32 of CA-11.2A.

Bono et al. (28) have recently developed a kanamycin-resistance cassette (kan^R) using the kanamycin-resistance gene from pOK12, a small pUC-derived plasmid (181), expressed from the B. burgdorferi promoter for flgB (72). The kan^R-cassette, because of the divergence from extant B. burgdorferi sequences, decreases the high level of background homologous recombination and increases the efficiency of recombination into the targeted site. With this marker inserted into a fragment of phage DNA and electroporated into CA-11.2A cells, we screened five colonies (out of several hundred) and all five contained the kan^R-insertion into cp32 (Figure 20).

A detailed analysis of the particular cp32 plasmid containing the kanamycin-cassette has not been done. However, by restriction mapping and PCR analysis of VR1, we surmise that the kan^R-cassette is inserted into the cp32 that is the dominant phage genome (Figures 24, 27 and data not shown). φBB-1 is capable of packaging the plasmid containing the kan^R-cassette and appears to do so from the transformant with the same frequency as the phage packages the dominant phage plasmid from parental CA.11-2A (Figure 10 and data not shown).

The ability of φBB-1 to package a cp32 larger than normal may be more evidence that the terminal redundancy at the ends of the phage genome is at least ~1.3 kb, the size

of the inserted kan^R-cassette. We hypothesize that the terminal redundancy of the

φBB-1 genome, which may be as large as 1.5 to 2 kb based on sizing data (102, 137, 138)

(Figure 13), may be smaller on the φBB-1/kan^R genome, but still large enough to allow

the establishment of infection as demonstrated by transduction. For phage P1,

circularization upon injection into the cell, which is a prophage-mediated event, requires

the terminal redundancy at the end of the genomes for recombination (86, 150).

Extending this hypothesis for φBB-1, any amount of DNA that is smaller than the

terminal redundancy can be introduced into the prophage genome without a loss of

packaging efficiency. Any insertion [such as the 2.1-kb $gyrB^R$ (131)] larger than the

terminal redundancy might be packaged. However, with no terminal redundancy the

phage genome might not be able to recircularize in a new host. In this case,

recombination into an existing cellular cp32 locus prior to degradation may be possible,

which would rescue the introduced phenotype.

We have demonstrated transduction into three different strains of *B. burgdorferi*,

including both low (non-inducible) and high (inducible) passage B31, the first direct

evidence that lateral gene transfer can occur in *B. burgdorferi*. The number of strains that

can be transduced by φBB-1 is few considering the large number of strains that we have

tested (see Table 4). The ability of φBB-1 to transduce the antibiotic-resistance marker

into a strain appears to be unrelated to the ability of that strain to produce phage, since

both low passage B31 and high passage 1A7 are transducible, but not inducible. The

efficiency of transduction between different strains appears to be at least 100 times lower

than transduction between cells of the same strain and may play an important role in

limiting transduction to other strains. Further support for this idea is the observation

that ϕBB-1/kan^R (B31) is capable of efficiently transducing the marker into susceptible

high and low passage B31 cells, but not back into CA-11.2A, the original source of the

ϕBB-1/kan^R. If the decrease in efficiency observed when transducing from CA-11.2A

into B31 was constant (that is, 100 times less efficient than transducing back into the

same susceptible strain) whenever the phage moves between strains, such as when ϕBB-

1/kan^R (B31) must transduce the kan^R-marker into CA-11.2A , then the transfer of the

marker between B31 and CA-11.2A would probably require a titer of phage higher than

reasonably achievable for B31. We must also remember that the titer of the phage is

determined only by the presence of DNA, and not by the number of infective particles.

There is currently no assay for determining the titer of infective particles. In addition, we

have no assay for evaluating the efficiency of establishing a new cp32 into a cell that is

already carrying a number of these molecules.

We were surprised to observe even a small amount of DNA transfer between dead

kan^R-cells and live susceptible CA-11.2A cells. BSK-complete has an inherent nuclease

activity (unpublished observations) that would seem to prevent DNA transfer within this

medium, unless by direct cell contact. Additionally, the killed cells were treated

thoroughly with chloroform, which should lyse the cells, although some may have

remained intact. As this transformation was prevented by the addition of proteinase K,

we propose that this phenomenon may be due to bacteriophage remaining either

internally or externally associated with the dead CA-11.2A/kan^R cells. We have not yet

tried this experiment with 1A7 TR5/*kan^R*, which had either no, or substantially

decreased, phage production.

Although the evidence is not conclusive, we believe that the φBB-1/*kan^R* is being

introduced as a discrete plasmid into the cell. Since the host cell loses a VR1 marker as

well as gaining the φBB-1 (CA-11.2A) VR1, this would suggest that displacement of a

host plasmid is occurring (Figure 24), although there are no obvious candidates

discernible from the restriction maps (Figure 27). Perhaps the loss of the host plasmid

associated with the smaller VR1s is required first before the transduction of the φBB-

1/*kan^R*. We are currently generating new clones of these strains to analyze the

relationship between prior plasmid content and the ability to incorporate the φBB-1/*kan^R*

cp32. Alternatively, recombination of the portion of the φBB-1/*kan^R* (CA-11.2A) DNA

into the variable site would result in the loss of the smaller VR1.

We have demonstrated that other strains transduced with φBB-1/*kan^R* (CA-11.2A)

now possess the variable region 1 (Figure 24), restriction fragments containing the

cp32SK*Nde*I DNA (Figure 27), and restriction fragments containing the *blyB* DNA (data

not shown) from φBB-1 (CA-11.2A). Even if this introduction of DNA was occurring

via recombination into an extant locus, the stretch of DNA just described encompasses

over 12 kb, including the entire variable region, which contains all of the lipoproteins

implicated in diversity. Whether the homologous region that includes the putative late

phage genes was also introduced is not clear. Although the restriction maps may be

modestly different, the gene order and content is conserved on all known cp32s, so

whether this region remains intact (resident) or is introduced from φBB-1 has little effect

on the cell. If the introduction of the DNA is occurring through recombination, instead of discrete plasmid displacement, and the conserved region has not been recombined, perhaps this explains the stability of the phage-producing phenotype. That is, the 'phage' genes, at least the late ones, are still derived from the resident cp32s and would maintain the host phenotype for phage production. Because of the conservation of this region within the resolution of restriction digests, determining whether this DNA is resident or transduced ϕBB-1 is a difficult task.

Superinfection immunity, observed with most lysogenic prophages, apparently does not play a role in those *B. burgdorferi* strains that are transducible. Most commonly, as with λ phage, this immunity is due to the presence of a repressor molecule that binds to the operator and prevents replication or integration of any incoming phage DNA that contains the same operator as the lysogen (25, 95). Alternatively, superinfection immunity to related phages can occur by preventing adsorption of phage particles, preventing injection of the DNA, or digesting incoming phage DNA. With ϕBB-1 we were able to introduce the phage DNA back into the lysogen and into other strains that already contain cp32s/putative prophages, suggesting that none of these play a role in preventing the superinfection of CA-11.2A by ϕBB-1/*kan*^{R}.

We have discussed one possible reason why there might be no superinfection immunity conferred by the resident cp32 prophages ('complete specialized transduction model'). A second possibility is that each cp32 has a different repressor molecule. This seems unlikely when considering the number of cp32s not only in an individual strain, but also among other strains. Perhaps there is a population of different repressor

molecules, and each strain has a different complement of these molecules. This could

be the reason that some strains cannot be transduced: they contain cp32s with an

immunity region that prevents infection of φBB-1. With this hypothesis, strains B31 and

1A7 would lack the repressor molecule that prevents φBB-1 (CA.11-2A) infection. This

does not explain, however, why the phenotype of these transduced strains does not

change. Also, consider that CA-11.2A can produce phage, thus contains the φBB-1

prophage, but can also transduce DNA back to susceptible cells of the same strain

containing this plasmid. CA-11.2A may have a mutation that affects the whole immunity

region, which could explain not only the lack of superinfection immunity, but also the

apparent constitutive partial derepression in the strain. A third possibility is that the

kanamycin-resistance cassette recombines into the resident cp32 rather than infecting

with a new cp32. Recombination of infecting temperate phage into the existing lysogenic

prophage is sometimes observed in phage λ (25).

We believe this work to be important not only to the study of *B. burgdorferi*, but

also to the general study of bacteriophage molecular biology. Although our work will

serve as a solid foundation, there remains much to be done with φBB-1. Because of the

nature of the bacterial host, this phage has some very interesting properties that may give

insight into not only the interactions between host and phage, but also how all phages

evolve and interact with their hosts. As an example, we know of no other phages that

have evolved to deal with multiple plasmid genomes and the absence of susceptible

strains. Additionally, we have demonstrated a mechanism for lateral gene transfer that

should be explored further to establish a role in the natural environment, for instance,

during the clinical course of Lyme disease. We believe that further analysis of ϕBB-1,

the first bacteriophage of *B. burgdorferi* described at a molecular level, could have a

critical role in the investigation of plasmid genetics, the development of a genetic system,

and the analysis of metabolic processes in these bacteria as a whole.

Appendix A

Abbreviations

bp	base pairs
BPB	bromophenol blue
BSA	bovine serum albumin
BSK	Barbour-Stoenner-Kelley medium
CBB	Coomassie brilliant blue
CIP	calf intestinal phosphatase
DNA	deoxyribonucleic acid
EtBr	ethidium bromide
F.C.	final concentration
FIGE	field-inversion gel electrophoresis
kb	kilobase pairs
MBN	Mung Bean nuclease
MNNG	1-methyl-3-nitro-nitrosoguanidine
PAGE	polyacrylamide gel electrophoresis
PCR	polymerase chain reaction
PEG	polyethylene glycol
PK	proteinase K
PTA	phosphotungstic acid
RNA	ribonucliec acid
SDS	sodium dodecyl sulfate
SM	suspension medium
TEM	transmission electron microscopy

126

References

1. **Abeles, A. L., S. A. Friedman, and S. J. Austin.** 1985. Partition of unit-copy miniplasmids to daughter cells. III. The DNA sequence and functional organization of the P1 partition region. J. Mol. Biol. **185**:261-272.

2. **Ackerman, H.-W.** 1998. Tailed bacteriophages: the order *Caudovirales*. Adv. Virus Res. **51**:135-201.

3. **Ackerman, H.-W., A. Audurier, L. Berthiaume, L. A. Jones, J. A. Mayo, and A. K. Vidaver.** 1978. Guidelines for bacteriophage characterization. Adv. Virus Res. **23**:1-24.

4. **Ackermann, R., B. Rehse-Kupper, E. Gollmer, and R. Schmitt.** 1988. Chronic neurologic manifestations of erythema migrans borreliosis. Ann. N.Y. Acad. Sci. **539**:16-23.

5. **Akins, D. R., M. J. Caimano, X. Yang, F. Cerna, M. V. Norgard, and J. D. Radolf.** 1999. Molecular and evolutionary analysis of *Borrelia burgdorferi* 297 circular plasmid-encoded lipoproteins with OspE- and OspF-like leader peptides. Infect. Immun. **67**:1526-1532.

6. **Alverson, J., and D. S. Samuels.** 2000. Regulation of the *Borrelia burgdorferi ospC* gene by DNA supercoiling. J. Bacteriol. In revision.

7. **Amla, D. V.** 1979. Mutagenesis of free and intracellular cyanophage AS-1 by ultraviolet, N-methanyl-N'-nitro-N-nitrosoguanidine and acriflavin. Mutat. Res. **59**:147-155.

8. **Anderson, L. M., and K. F. Bott.** 1985. DNA packaging by the *Bacillus subtilis* defective bacteriophage PBSX. J. Virol. **54**:773-780.

9. **Austin, S., and K. Nordstrom.** 1990. Partition-mediated incompatibility of bacterial plasmids. Cell. **60**:351-354.

10. **Ausubel, F. M., R. Brent, R. E. Kingston, D. D. Moore, J. G. Seidman, J. A. Smith, and K. Struhl (ed.).** 1999. Short Protocols in Molecular Biology. John Wiley & Sons, Inc., New York NY.

11. **Balganesh, M., and J. K. Setlow.** 1984. Prophage induction in *Haemophilus influenzae* and its relationship to mutation by chemical and physical agents. Mutat. Res. **125**:15-22.

12. **Baranton, G., and I. G. Old.** 1995. The Spirochaetes: a different way of life. Bull. Inst. Pasteur. **93**:63-95.

13. **Baranton, G., D. Postic, I. Saint Girons, P. Boerlin, J. C. Piffaretti, M. Assous, and P. A. Grimount.** 1992. Delineation of *Borrelia burgdorferi sensu stricto*, *Borrelia garinii* sp. nov., and group VS461 associated with Lyme borreliosis. Int. J. Syst. Bacteriol. **42**:378-383.

14. **Barbour, A. G.** 1984. Isolation and cultivation of Lyme disease spirochetes. Yale J. Biol. Med. **57**:521-525.

15. **Barbour, A. G.** 1988. Plasmid analysis of *Borrelia burgdorferi*, the Lyme disease agent. J. Clin. Microbiol. **26**:475-478.

16. **Barbour, A. G., C. J. Carter, V. Bundoc, and J. Hinnebush.** 1996. The nucleotide sequence of a linear plasmid of *Borrelia burgdorferi* reveals similarities to those of circular plasmids of other prokaryotes. J. Bacteriol. **178**:6625-6639.

127

17. **Barbour, A. G., and D. Fish.** 1993. The biological and social phenomenon of Lyme disease. Science. **260:**1610-1616.

18. **Barbour, A. G., and C. F. Garon.** 1987. Linear plasmids of the bacterium *Borrelia burgdorferi* have covalently closed ends. Science. **237:**409-411.

19. **Barbour, A. G., and S. F. Hayes.** 1986. Biology of *Borrelia* species. Microbiol. Rev. **50:**381-400.

20. **Baril, C., C. Richaud, G. Baranton, and I. Saint Girons.** 1989. Linear chromosome of the bacterium *Borrelia burgdorferi*. Res. Microbiol. **140:**507-516.

21. **Berger, B. W.** 1989. Dermatological manifestations of Lyme disease. Rev. Infect. Dis. **11:**S1475.

22. **Bergquist, P. L.** 1987. Incompatibility, p. 37-78. *In* K. G. Hardy (ed.), Plasmids: a practical approach. IRL Press, Oxford, England.

23. **Berthiaume, L., Y. Elazhary, R. Alain, and H.-W. Ackerman.** 1979. Bacteriophage-like particles associated with a spirochete. Can. J. Microbiol. **25:**114-116.

24. **Bertini, L. E., and E. W. Six.** 1988. The P2-like phages and their parasite, P4, p. 73-143. *In* R. Calendar (ed.), The Bacteriophages. Plenum Press, New York, NY.

25. **Birge, E. A.** 1994. Bacterial and bacteriophage genetics, 3rd ed. Springer-Verlag, New York, N.Y.

26. **Bissett, M. L., and W. Hill.** 1987. Characterization of *Borrelia burgdorferi* strains isolated for *Ixodes pacificus* ticks in California. J. Clin. Microbiol. **25:**2296-2301.

27. **Boling, M. E., and R. F. Kimball.** 1976. Mutation induction by MNNG in a bacteriophage of *Haemophilus influenzae*. Mutat. Res. **37:**1-10.

28. **Bono, J. L., A. F. Elias, J. J. Kupko, B. Stevenson, K. Tilly, and P. Rosa.** 2000. Efficient targeted mutagenesis in *Borrelia burgdorferi*. J. Bacteriol. **182:**2445-2452.

29. **Bono, J. L., K. Tilly, B. Stevenson, D. Hogan, and P. Rosa.** 1998. Oligopeptide permease in *Borrelia burgdorferi*: putative peptide-binding components encoded by both chromosomal and plasmid loci. Microbiology. **144:**1033-1044.

30. **Burgdorfer, W., A. G. Barbour, S. F. Hayes, J. L. Benach, E. Grunwaldt, and J. P. Davis.** 1982. Lyme disease--a tick-borne spirochetosis? Science. **216:**1317-1319.

31. **Burgdorfer, W., R. S. Lane, A. G. Barbour, R. A. Gresbrink, and J. R. Anderson.** 1985. The western black-legged tick, *Ixodes pacificus*: a vector of *Borrelia burgdorferi*. Am. J. Trop. Med. Hyg. **34:**925-930.

32. **Caimano, M. J., X. Yang, T. G. Popova, M. L. Clawson, D. R. Akins, M. V. Norgard, and J. D. Radolf.** 2000. Molecular and evolutionary characterization of the cp32/cp18 family of supercoiled plasmids in *B. burgdorferi* 297. Infect. Immun. **68:**1574-1586.

33. **Calderaro, A., G. Dettori, L. Collini, P. Ragni, R. Grillo, P. Cattani, G. Fadda, and C. Chezzi.** 1998. Bacteriophages induced from weakly beta-haemolytic human intestinal spirochaetes by mitomycin C. J. Basic Microbiol. **38:**323-335.

34. **Calderaro, A., G. Dettori, R. Grillo, P. Plaisant, G. Amalfitano, and C. Chezzi.** 1998. Search for bacteriophages spontaneously occurring in cultures of haemolytic intestinal spirochetes of human and animal origin. J. Basic Microbiol. **38:**313-322.

35. **Carlyon, J. F., D. M. Roberts, and R. T. Marconi.** 2000. Evolutionary and molecular analyses of the *Borrelia bdr* super gene family: delineation of distinct sub-families and demonstration of the genus wide conservation of putative functional domains, structural properties and repeat motifs. Microb. Pathog. **28:**89-105.

36. **Carroll, J.** personal communication.

37. **Casjens, S.** personal communication.

38. **Casjens, S., M. Delange, H. L. Ley, P. Rosa, and W. M. Huang.** 1995. Linear chromosomes of Lyme disease agent spirochetes: genetic diversity and conservation of gene order. J. Bacteriol. **177:**2769-2780.

39. **Casjens, S., G. Hatfull, and R. Hendrix.** 1992. Evolution of dsDNA tailed-bacteriophage genomes. Semin. Virol. **3:**383-397.

40. **Casjens, S., and W. M. Huang.** 1993. Linear chromosomal physical and genetic map of *Borrelia burgdorferi*, the Lyme disease agent. Mol. Microbiol. **8:**967-980.

41. **Casjens, S., M. Murphy, M. DeLange, L. Sampson, R. van Vugt, and W. M. Huang.** 1997. Telomeres of the chromosomes of the Lyme disease spirochetes: nucleotide sequence and possible exchange with linear plasmid telomeres. Mol. Microbiol. **26:**581-596.

42. **Casjens, S., N. Palmer, R. Van Vugt, W. M. Huang, B. Stevenson, P. Rosa, R. Lathigra, G. Sutton, J. Peterson, R. J. Dodson, D. Haft, E. Hickey, M. Gwinn, O. White, and C. M. Fraser.** 2000. A bacterial genome in flux: the twelve linear and nine circular extrachromosomal DNAs in an infectious isolate of the Lyme disease spirochete *Borrelia burgdorferi*. Mol. Microbiol. **35:**490-516.

43. **Casjens, S., R. van Vugt, K. Tilly, P. A. Rosa, and B. Stevenson.** 1997. Homology throughout the multiple 32-kilobase circular plasmids present in Lyme disease spirochetes. J. Bacteriol. **179:**217-227.

44. **Centers for Disease Control and Prevention.** 1997. Lyme disease -- United States, 1996. Morb. Mortal. Wkly. Rep. **45.**

45. **Centers for Disease Control and Prevention.** revision date: 24 June 1999. Lyme Disease: Introduction. [Online.] http://www.cdc.gov/ncidod/dvbid/lymeinfo.htm:Last accessed 11 January 2000.

46. **Centers for Disease Control and Prevention.** 1999. Methods used for creating a national Lyme disease risk map. Morb. Mortal. Wkly. Rep. **48:**21-24.

47. **Chai, S., A. Bravo, G. Luder, A. Nedlin, T. A. Trautner, and J. C. Alonso.** 1992. Molecular analysis of the *Bacillus subtilis* bacteriophage SPP1 region encompassing genes 1 to 6. The products of gene 1 and gene 2 are required for *pac* cleavage. J. Mol. Biol. **224:**87-102.

48. **Champion, C. I., R. D. Blanco, J. T. Skare, D. A. Haake, M. Giladi, D. Foley, J. N. Miller, and M. A. Lovett.** 1994. A 9.0-kilobase-pair circular plasmid of *Borrelia burgdorferi* encodes an exported protein: evidence for expression only during infection. Infect. Immun. **62:**2653-2661.

49. **Cheetham, B., and M. Katz.** 1995. A role for bacteriophages in the evolution and transfer of bacterial virulence determinants. Mol. Microbiol. **18:**201-208.

50. **Damman, C. J., C. H. Eggers, D. S. Samuels, and D. B. Oliver.** Characterization of *Borrelia burgdorferi* BlyA and BlyB proteins: a plasmid-encoded holin-like system. In preparation.

51. **Davidson, B., J. MacDougall, and I. Saint Girons.** 1992. Physical map of the linear chromosome of the bacterium *Borrelia burgdorferi* 212, a causative agent of Lyme disease and localization of rRNA genes. J. Bacteriol. **174:**3766-3774.

52. **Davies, M. E., and R. W. Bingham.** 1985. Spirochaetes in the equine caecum. Res. Vet. Sci. **39:**95-98.

53. **Dennis, D. T.** 1998. Epidemiology, ecology, and prevention of Lyme disease, p. 7-34, Lyme Disease. American College of Physicians, Philadelphia, PA.

54. **Dhote, R., A. L. Basse-Guerineau, C. Bachmeyer, B. Christoforov, and M. V. Assous.** 1998. [Lyme borreliosis: therapeutic aspects]. Presse Med. **27:**2043-2047.

55. **Dong, J., P. Fan, and R. Frizzell.** 1996. Quantitative analysis of the packaging capacity of recombinant adeno-associated virus. Hum Gen Ther. **7:**2101-2112.

56. **Dorward, D. W., and C. F. Garon.** 1990. DNA is packaged within membrane-derived vesicles of Gram-negative but not Gram-positive bacteria. Appl. Environ. Microbiol. **56:**1960-1962.

57. **Dorward, D. W., C. F. Garon, and R. J. Judd.** 1989. Export and intracellular transfer of DNA via membrane blebs of *Neisseria gonorrhoeae*. J. Bacteriol. **171:**2499-2505.

58. **Droge, A., and P. Tavares.** 2000. *In vitro* packaging of DNA of the *Bacillus subtilis* bacteriophage SPP1. J. Mol. Biol. **296:**103-115.

59. **Dunn, J. J., S. R. Buchstein, L.-L. Butler, S. Fisenne, D. S. Polin, B. N. Lade, and B. J. Luft.** 1994. Complete nucleotide sequence of a circular plasmid from the Lyme disease spirochete, *Borrelia burgdorferi*. J. Bacteriol. **176:**2706-2717.

60. **Durante, M., C. Geri, S. Bonatti, and R. Parenti.** 1989. Non-random alkylation of DNA sequences induced *in vivo* by chemical mutagens. Carcinogenesis. **10:**1357-1361.

61. **Dykstra, M. J.** 1993. A Manual of Applied Techniques for Biological Electron Microscopy. Plenum Press, New York NY.

62. **Dyson, N. J.** 1991. Immobilization of nucleic acids and hybridization analysis, p. 111-156. *In* T. A. Brown (ed.), Essential Molecular Biology: A Practical Approach, vol. 2. IRL Press, Oxford.

63. **Eggers, C. H., and D. S. Samuels.** 1999. Molecular evidence for a new bacteriophage of *Borrelia burgdorferi*. J. Bacteriol. **181:**7308-7313.

64. **El Hage, N., L. D. Lieto, and B. Stevenson.** 1999. Stability of *erp* loci during *Borrelia burgdorferi* infection: recombination is not required for chronic infection of immunocompetent mice. Infect. Immun. **67:**3146-3150.

65. **Elesparu, R. K., S. K. Gonda, and S. G. Moore.** 1984. Genetic and biochemical factors affecting the induction of bacteriophage lambda by N-nitroso compounds. IARC Sci. Publ. **57:**731-739.

66. **Felsenfield, O.** 1971. *Borrelia.* Strains, vectors, human and animal borreliosis. Warren H. Green, St. Louis, MO.

67. **Ferdows, M. S., and A. G. Barbour.** 1989. Megabase-sized linear DNA in the bacterium *Borrelia burgdorferi,* the Lyme disease agent. Proc. Natl. Acad. Sci. USA. **86:**5969-5973.

68. **Fraser, C. M., S. Casjens, W. M. Huang, G. G. Sutton, R. Clayton, R. Lathigra, O. White, K. A. Ketchum, R. Dodson, E. K. Hickey, M. Gwinn, B. Dougherty, J.-F. Tomb, R. D. Fleischmann, D. Richardson, J. Peterson, A. R. Kerlavage, J. Quackenbush, S. Salzberg, M. Hanson, R. van Vugt, N. Palmer, M. D. Adams, J. Gocayne, J. Weidman, T. Utterback, L. Watthey, L. McDonald, P. Artiach, C. Bowman, S. Garland, C. Fujii, M. D. Cotton, K. Horst, K. Roberts, B. Hatch, H. O. Smith, and J. C. Venter.** 1997. Genomic sequence of a Lyme disease spirochaete, *Borrelia burgdorferi.* Nature. **390:**580-586.

69. **Freifelder, D.** 1987. Molecular Biology, 2nd ed. Jones and Bartlett Publishers, Inc, Boston, MA.

70. **Fuchs, R., S. Jauris, F. Lottspeich, V. Preac-Mursic, B. Wilske, and E. Soutschek.** 1992. Molecular analysis and expression of a *Borrelia burgdorferi* gene encoding a 22-kDa protein (pC) in *Escherichia coli.* Mol. Microbiol. **6:**503-509.

71. **Garon, C. F., D. W. Dorward, and M. D. Corwin.** 1989. Structural features of *Borrelia burgdorferi*--the Lyme disease spirochete: silver staining for nucleic acids. Scanning Microsc. **3:**109-115.

72. **Ge, Y., I. G. Old, I. Saint Girons, and N. W. Charon.** 1997. Molecular characterization of a large *Borrelia burgdorferi* motility operon which is initiated by a consensus sigma70 promoter. J. Bacteriol. **179:**2289-2299.

73. **Gilmore, R. D. J., and M. L. Mbow.** 1998. A monoclonal antibody generated by antigen inoculation via tick bite is reactive to the *Borrelia burgdorferi* Rev protein, a member of the 2.9 gene family locus. Infect. Immun. **66:**980-986.

74. **Gual, A., and J. C. Alonso.** 1998. Characterization of the small subunit of the terminase enzyme of the *Bacillus subtilis* bacteriophage SPP1. Virology. **242:**279-287.

75. **Guina, T., and D. B. Oliver.** 1997. Cloning and analysis of a *Borrelia burgdorferi* membrane-interactive protein exhibiting haemolytic activity. Mol. Microbiol. **24:**1201-1213.

76. **Hanahan, D.** 1983. Studies on transformation of *Escherichia coli* with plasmids. J. Mol. Biol. **166:**557-580.

77. **Hayes, S. F., W. Burgdorfer, and A. G. Barbour.** 1983. Bacteriophage in the *Ixodes dammini* spirochete, etiological agent of Lyme disease. J. Bacteriol. **154:**1436-1439.

78. **Hendrix, R. W.** 1999. Evolution: the long evolutionary reach of viruses. Curr. Biol. **9:**914-917.

79. **Hershey, A., E. Burgi, and L. Ingraham.** 1963. Cohesion of DNA molecules isolated from phage lambda. Proc. Natl. Acad. Sci. USA. **49:**748-755.

80. **Hightower, R. C., D. W. Metge, and D. V. Santi.** 1987. Plasmid migration using orthagonal-field-alternation gel electrophoresis. Nucleic Acis Res. **15:**8387-8398.

81. **Hinnebusch, B. J.** 1991. Structure and replication of *Borrelia burgdorferi* linear plasmids. PhD Dissertation. University of Texas Health Science Center, San Antonio.

82. **Hinnebusch, J., and A. G. Barbour.** 1992. Linear- and circular-plasmid copy numbers in *Borrelia burgdorferi*. J. Bacteriol. **174:**5251-5257.

83. **Hinnebusch, J., and A. G. Barbour.** 1991. Linear plasmids of *Borrelia burgdorferi* have a telomeric structure and sequence similar to those of a eukaryotic virus. J. Bacteriol. **173:**7233-7239.

84. **Hinnebusch, J., S. Bergström, and A. G. Barbour.** 1990. Cloning and sequence analysis of linear plasmid telomeres of the bacterium *Borrelia burgdorferi*. Mol. Microbiol. **4:**811-820.

85. **Hinnebusch, J., and K. Tilly.** 1993. Linear plasmids and chromosomes in bacteria. Mol. Microbiol. **10:**917-922.

86. **Hochmanm, L., N. Segev, N. Sternberg, and G. Cohen.** 1983. Site-specific recombinational circularization of bacteriophage P1 DNA. Virology. **131:**11-17.

87. **Humphrey, S. B., T. B. Stanton, and N. S. Jensen.** 1995. Mitomycin C induction of bacteriophages from *Serpulina hyodysenteriae* and *Serpulina innocens*. FEMS Microbiol. Lett. **134:**189-194.

88. **Humphrey, S. B., T. B. Stanton, N. S. Jenson, and R. L. Zuerner.** 1997. Purification and characterization of VSH-1, a generalized transducing bacteriophage of *Serpulina hyodysenteriae*. J. Bacteriol. **179:**323-329.

89. **Ikeda, H., and J. I. Tomizawa.** 1969. Prophage P1, an extrachromosomal replication unit. Cold Spring Harbor Symp. Quant. Biol. **30:**791-798.

90. **Jordan, M., L. Meile, and T. Leisinger.** 1989. Organization of *Methanobacterium thermoautoprophicum* bacteriophage ψM1 DNA. Mol. Gen. Genet. **220:**161-164.

91. **Judson, H. F.** 1996. The Eigth Day of Creation: Makers of the Revolution in Biology, Expanded ed. Cold Spring Harbor Laboratory Press, Cold Spring Harbor NY.

92. **Kim, B., and J. W. Little.** 1993. LexA and lambda cI repressor as enzymes: specific cleavage in an intermolecular reaction. Cell. **73:**1165-1173.

93. **Knight, S. W., B. J. Kimmel, C. H. Eggers, and D. S. Samuels.** 2000. Disruption of the *Borrelia burgdorferi gac* gene, encoding the naturally synthesized GyrA C-terminal domain. J. Bacteriol. **182:**2048-2051.

94. **Knight, S. W., and D. S. Samuels.** 1999. Natural synthesis of a DNA-binding protein from the C-terminal domain of DNA gyrase A in *Borrelia burgdorferi*. EMBO J. **18:**4875-4881.

95. **Kornberg, A., and T. A. Baker.** 1992. DNA replication, 2nd ed. W.H. Freeman and Company, New York, N.Y.

96. **Kurashige, S., M. Bissett, and L. Oshiro.** 1990. Characterization of a tick isolate of *Borrelia burgdorferi* that possesses a major low-molecular-weight surface protein. J. Clin. Microbiol. **28:**1362-1366.

97. **Lam, T. T., T.-P. K. Nguyen, R. R. Montgomery, F. S. Kantor, E. Fikrig, and R. A. Flavell.** 1994. Outer surface proteins E and F of *Borrelia burgdorferi*, the agent of Lyme disease. Infect. Immun. **62:290-298**.

98. **Lane, T., P. Serwer, S. J. Hayes, and F. Eiserling.** 1990. Quantized viral DNA packaging revealed by rotating gel electrophoresis. Virology. **174:472-478**.

99. **Little, J. W.** 1984. Autodigestion of *lexA* and phage lamda repressors. Proc. Natl. Acad. Sci. USA. **81:1375-1379**.

100. **Liu, T., S. K. Renberg, and E. Haggard-Ljungquist.** 1997. Derepression of prophage P2 by satellite phage P4: cloning of the P4 epsilon gene and identification of its product. J. Virol. **71:4502-4508**.

101. **Loechler, E. L., C. L. Green, and J. M. Essigmann.** 1984. *In vivo* mutagenesis by O6-methylguanine built into a unique viral genome. Proc Natl Acad Sci USA. **81:6271-6275**.

102. **Lubke, L. L., C. F. Garon, and D. S. Samuels.** Unpublished data.

103. **MacHattie, L. A., M. Rhoades, C. A. J. Thomas, and C. C. Richardson.** 1972. Large repetition in the non-permuted nucleotide sequence of bacteriophage TI DNA. J. Mol. Biol. **72:645-656**.

104. **Marconi, R. T., L. Lubke, W. Hauglum, and C. F. Garon.** 1992. Species-specific identification of and distinction between *Borrelia burgdorferi* genomic groups by using 16S rRNA-directed oligonucleotides. J. Clin. Microbiol. **30:628-632**.

105. **Marconi, R. T., D. S. Samuels, and C. F. Garon.** 1993. Transcriptional analyses and mapping of the *ospC* gene in Lyme disease spirochetes. J. Bacteriol. **175:926-932**.

106. **Marconi, R. T., D. S. Samuels, T. G. Schwan, and C. F. Garon.** 1993. Identification of a protein in several *Borrelia* species which is related to OspC of the Lyme disease spirochetes. J. Clin. Microbiol. **31:2577-2583**.

107. **Marconi, R. T., S. Y. Sung, C. A. Norton-Hughes, and J. A. Carlyon.** 1996. Molecular and evolutionary analyses of a variable series of genes in *Borrelia burgdorferi* that are related to *ospE* and *ospF*, constitute a gene family, and share a common upstream homology box. J. Bacteriol. **178:5615-5626**.

108. **Margolis, N., D. Hogan, K. Tilly, and P. A. Rosa.** 1994. Plasmid location of *Borrelia* purine biosynthesis gene homologs. J. Bacteriol. **176:6427-6432**.

109. **Margolis, N., and P. Rosa.** 1993. Regulation of expression of major outer surface proteins in *Borrelia burgdorferi*. Infect. Immun. **61:2207-2210**.

110. **Masuda, K., and T. Kawata.** 1979. Bacteriophage-like particles induced from the Reiter treponeme by mitomycin C. FEMS Microbiol. Lett. **6:29-31**.

111. **Miller, J. C., N. El Hage, and B. Stevenson.** 2000. *Borrelia burgdorferi* B31 Erp proteins that are dominant immunoblot antigens of animals infected with isolate B31 are recognized by only a subset of human Lyme disease patient sera. J. Clin. Microbiol. **38:1569-1574**.

112. **Moody, M.** 1999. Geometry of phage head construction. J. Mol. Biol. **293:401-433**.

113. **Mustard, J. A., and J. W. Little.** 2000. Analysis of *Escherichia coli* RecA interactions with LexA, lambda cI, and UmuD by site-directed mutagenesis of *recA*. J. Bacteriol. **182**:1659-1670.

114. **National Center for Biotechnology Information.** last revised: 2 March 2000. Genbank. [Online.] http://www.ncbi.nlm.nih.gov:last accessed: 5 April 2000.

115. **Neely, M. N., and D. I. Friedman.** 1998. Arrangement and functional identification of genes in the regulatory region of lambdoid phage H-19B, a carrier of a Shiga-like toxin. Gene. **26**:105-113.

116. **Neely, M. N., and D. I. Friedman.** 1998. Functional and genetic analysis of regulatory regions of coliphage H-19B: location of shiga-like toxin and lysis genes suggest a role for phage functions in toxin release. Mol. Microbiol. **28**:1255-1267.

117. **Neubert, U., M. Schaller, E. Januschke, W. Stolz, and H. Schmieger.** 1993. Bacteriophages induced by ciprofloxacin in a *Borrelia burgdorferi* skin isolate. Zentralbl. Bakteriol. **279**:307-315.

118. **Nocton, J. J., and A. C. Steere.** 1995. Lyme disease. Adv. Intern. Med. **40**:69-117.

119. **Norris, S. J., J. K. Howell, S. A. Garza, M. S. Ferdows, and A. G. Barbour.** 1995. High- and low-infectivity of phenotypes of clonal populations of *in vitro*-cultured *Borrelia burgdorferi*. Infect. Immun. **63**:2206-2212.

120. **Popa, M. P., T. A. McKelvey, J. Hempel, and R. W. Hendrix.** 1991. Bacteriophage HK97 structure: wholesale covalent cross-linking between the major head shell subunits. J. Bacteriol. **65**:3227-3237.

121. **Porcella, S. F., T. G. Popova, T. G. Akins, M. Li, J. D. Radolf, and M. V. Norgard.** 1996. *Borrelia burgdorferi* supercoiled plasmids encode multicopy tandem open reading frames and a lipoprotein gene family. J. Bacteriol. **178**:3293-3307.

122. **Postic, D., N. Marti Ras, R. S. Lane, M. Hendson, and G. Baranton.** 1998. Expanded diversity among Californian *Borrelia* isolates and description of *Borrelia bissettii* sp. nov. (formerly *Borrelia* group DN127). J. Clin. Microbiol. **36**:3497-3504.

123. **Ravin, N., and D. Lane.** 1999. Partition of the linear plasmid N15: interactions of N15 partition functions with the *sop* locus of the F plasmid. J. Bacteriol. **181**:6898-6906.

124. **Rhoades, M., L. A. MacHattie, and C. A. J. Thomas.** 1968. The P22 bacteriophage DNA molecule. I. The mature form. J. Mol. Biol. **37**:21-40.

125. **Ritchie, A. E., and L. N. Brown.** 1971. An agent possibly associated with swine dysentary. Vet. Rec. **89**:608-609.

126. **Ritchie, A. E., and H. C. Ellinghausen.** 1969. Presented at the Proc. 27th Annu. EMSA Meeting, St. Paul, Minn.

127. **Ritchie, A. E., I. M. Robinson, L. A. Joens, and J. M. Kinyon.** 1978. A bacteriophage for *Treponema hyodysenteriae*. Vet. Rec. **103**:34-35.

128. **Roberts, D. M., J. A. Carlyon, M. Thiesen, and R. T. Marconi.** 2000. The *bdr* gene families of the Lyme disease and relapsing fever spirochetes: potential influence on biology, pathogenesis, and evolution. Emerg. Infect. Dis. **6**:110-122.

129. **Roberts, J. W., and R. Devoret.** 1983. Lysogenic induction, p. 123-144. *In* R. W. Hendrix, J. W. Roberts, F. W. Stahl, and R. A. Weisberg (ed.), Lambda II. Cold Spring Harbor Laboratory, Cold Spring Harbor NY.

130. **Rosa, P., and D. Hogan.** 1992. Presented at the First International Conference on Tick Borne Pathogens at the Host-Vector Interface: An Agenda for Research, University of Minnesota, St. Paul.

131. **Rosa, P., D. S. Samuels, D. Hogan, B. Stevenson, S. Casjens, and K. Tilly.** 1996. Directed insertion of a selectable marker into a circular plasmid of *Borrelia burgdorferi*. J. Bacteriol. **178:**5946-5953.

132. **Rozanov, D. V., R. D'Ari, and S. P. Sineoky.** 1998. RecA-independent pathways of lambdoid prophage in *Eshericia coli*. J. Bacteriol. **180:**6306-6315.

133. **Saheb, S. A.** 1974. Spirochetal organisms from pigs.--III. Preliminary observations on bacteriophage particles associated with spirochetes of the genus *Treponema*. Rev. Can. Biol. **33:**67-70.

134. **Saint Girons, I., D. Margarita, P. Amouriaux, and G. Baranton.** 1990. First isolation of bacteriophages for a spirochete: potential genetic tools for *Leptospira*. Res. Microbiol. **143:**615-621.

135. **Sambrook, J., E. F. Fritsch, and T. Maniatis.** 1989. Molecular cloning: a laboratory manual, 2nd ed. Cold Spring Harbor Laboratory Press, Cold Spring Harbor, N.Y.

136. **Samuels, D. S.** 1995. Electrotransformation of the spirochete *Borrelia burgdorferi*, p. 253-259. *In* J. A. Nickoloff (ed.), Electroporation Protocols for Microorganisms, vol. 47. Humana Press, Totowa, New Jersey.

137. **Samuels, D. S.** Unpublished data.

138. **Samuels, D. S., and C. F. Garon.** 1993. Coumermycin A_1 inhibits growth and induces relaxation of supercoiled plasmids in *Borrelia burgdorferi*, the Lyme disease agent. Antimicrob. Agents Chemother. **37:**46-50.

139. **Samuels, D. S., and C. F. Garon.** 1997. Oligonucleotide-mediated genetic transformation of *Borrelia burgdorferi*. Microbiol. **143:**519-522.

140. **Samuels, D. S., K. E. Mach, and C. F. Garon.** 1994. Genetic transformation of the Lyme disease agent *Borrelia burgdorferi* with coumarin-resistant *gyrB*. J. Bacteriol. **176:**6045-6049.

141. **Samuels, D. S., R. T. Marconi, W. M. Huang, and C. F. Garon.** 1994. *gyrB* mutations in coumermycin A_1-resistant *Borrelia burgdorferi*. J. Bacteriol. **176:**3072-3075.

142. **Sarma, T. A., and R. Singh.** 1994. Isolation and characterization of temperature-sensitive mutants of cyanophage N-1. Acta Virol. **38:**11-16.

143. **Sauer, R. T., J. Pan, P. Hopper, K. Hehir, J. Brown, and A. R. Poteete.** 1981. Primary structure of the phage P22 repressor and its gene c2. Biochemistry. **20:**3591-3598.

144. **Schaller, M., and U. Neubert.** 1994. Bacteriophages and ultrastructural alteration of *Borrelia burgdorferi* induced by ciprofloxacin. J. Spirochet. Tickborne Dis. **1:**37-40.

145. **Schendel, P., and I. Michaeli.** 1984. A model for the mechanism of alkylation mutagenesis. Mutat. Res. **125**:1-14.

146. **Schwan, T. G.** 1996. Ticks and *Borrelia*: model systems for investigating pathogen-arthropod interactions. Infect. Ag. Dis. **5**:167-181.

147. **Schwan, T. G., W. Burgdorfer, and C. F. Garon.** 1988. Changes in infectivity and plasmid profile of the Lyme disease spirochete, *Borrelia burgdorferi*, as a result of *in vitro* cultivation. Infect. Immun. **56**:1831-1836.

148. **Schwan, T. G., J. Piesman, W. T. Golde, M. C. Dolan, and P. A. Rosa.** 1995. Induction of an outer surface protein on *Borrelia burgdorferi* during tick feeding. Proc. Natl. Acad. Sci. USA. **92**: 2909-2913.

149. **Schwan, T. G., M. E. Schrumpf, R. H. Karstens, J. R. Clover, J. Wong, M. Daugherty, M. Struthers, and P. A. Rosa.** 1993. Distribution and molecular analysis of Lyme disease spirochetes, *Borrelia burgdorferi*, isolated from ticks throughout California. J. Clin. Microbiol. **31**:3096-3108.

150. **Segev, N., and G. Cohen.** 1981. Control of circularization of bacteriophage P1 DNA in *Esherichia coli*. Virology. **114**:333-342.

151. **Seres, S., R. Lazraq, and H. Ohayon.** 1991. Isolation and characterization of temperature sensitive mutants of the F5 deletion mutant of mycobacteriophage D29. Int. J. Med. Microbiol. Virol. Parasitol. Dis. **275**:54-62.

152. **Simpson, W. J., C. F. Garon, and T. G. Schwan.** 1990. Analysis of supercoiled circular plasmids in infectious and non-infectious *Borrelia burgdorferi*. Microb. Pathog. **8**:109-118.

153. **Simpson, W. J., C. F. Garon, and T. G. Schwan.** 1990. *Borrelia burgdorferi* contains repeated DNA sequences that are species specific and plasmid associated. Infect. Immun. **58**:847-853.

154. **Skare, J. T., D. M. Foley, S. R. Hernandez, D. C. Moore, D. R. Blanco, J. N. Miller, and M. A. Lovett.** 1999. Cloning and molecular characterization of plasmid-encoded antigens of *Borrelia burgdorferi*. Infect. Immun. **67**:4407-4417.

155. **Sobral, B. W. S., and A. G. Atherly.** 1989. Pulse time and agarose concentration affect the electrophoretic mobility of cccDNA during electrophoresis in CHEF and FIGE. Nucleic Acids Res. **17**:7359-7369.

156. **Stanley, E., G. F. Fitzgerald, C. Le Marrec, B. Fayard, and D. van Sinderen.** 1997. Sequence analysis and characterization of ϕO1205, a temperate bacteriophage infecting *Streptococcus thermophilus* CNRZ1205. Microbiology. **143**:3417-3429.

157. **Steere, A. C.** 1994. Lyme disease: a growing threat to urban populations. Proc. Natl. Acad. Sci. USA. **91**:2378-2383.

158. **Steere, A. C.** 1989. Medical progress: Lyme disease. N. Engl. J. Med. **321**:586-596.

159. **Steere, A. C., N. H. Bartenhagen, J. E. Craft, G. J. Hutchinson, J. H. Newman, D. W. Rahn, L. H. Sigal, P. H. Spieler, K. S. Stenn, and S. E. Malawista.** 1983. The early clinical manifestations of Lyme disease. Ann. Intern. Med. **99**:76-82.

160. **Steere, A. C., R. L. Grodzicki, J. E. Craft, M. Shrestha, A. N. Kornblatt, and S. A. Malawista.** 1984. Recovery of Lyme disease spirochetes from patients. Yale J. Biol. Med. **57**:557-560.

161. **Steere, A. C., R. L. Grodzicki, A. N. Kornblatt, J. E. Craft, A. G. Barbour, W. Burgdorfer, G. P. Schmid, E. Johnson, and S. E. Malawista.** 1983. The spirochetal etiology of Lyme disease. N. Engl. J. Med. **308**:733-740.

162. **Steere, A. C., R. T. Shoen, and E. Taylor.** 1987. The clinical evolution of Lyme arthritis. Ann. Intern. Med. **107**:725-731.

163. **Sternberg, N.** 1987. Recognition and cleavage of the bacteriophage P1 packaging site (*pac*). I. Differential processing of the cleaved ends *in vivo*. J. Mol. Biol. **194**:453-468.

164. **Stevenson, B., S. F. Porcella, K. L. Oie, C. A. Fitzpatrick, S. J. Raffel, L. Lubke, M. E. Schrumpf, and T. G. Schwan.** 2000. The relapsing fever spirochete *Borrelia hermsii* contains multiple, antigen-encoding plasmids that are homologous to the cp32 plasmids of Lyme disease spirochetes. Infect. Immun. **68**:in press.

165. **Stevenson, B., J. L. Bono, A. Elias, K. Tilly, and R. P.** 1998. Transformation of the Lyme disease spirochete *Borrelia burgdorferi* with heterologous DNA. J. Bacteriol. **180**:4850-4855.

166. **Stevenson, B., J. L. Bono, T. G. Schwan, and P. Rosa.** 1998. *Borrelia burgdorferi erp* proteins are immunogenic in mammals infected by tick bite, and their synthesis is inducible in cultured bacteria. Infect. Immun. **66**:2648-2654.

167. **Stevenson, B., S. Casjens, and P. Rosa.** 1998. Evidence of past recombination events among the genes encoding the Erp antigens of *Borrelia burgdorferi*. Microbiol. **144**:1869-1879.

168. **Stevenson, B., S. Casjens, R. van Vugt, S. F. Porcella, K. Tilly, J. L. Bono, and P. Rosa.** 1997. Characterization of cp18, a naturally truncated member of the cp32 family of *Borrelia burgdorferi* plasmids. J. Bacteriol. **179**:4285-4291.

169. **Stevenson, B., K. Tilly, and P. A. Rosa.** 1996. A family of genes located on four separate 32-kilobase circular plasmids in *Borrelia burgdorferi* B31. J. Bacteriol. **178**:3508-3516.

170. **Streisinger, G., J. Emrich, and M. M. Stahl.** 1967. Chromosome structure in phage T4, III. Terminal redundancy and length determination. Proc. Natl. Acad. Sci. USA. **57**:292-295.

171. **Su, M.-T., T. V. Venkatesh, and R. Bodmer.** 1998. Large- and small-scale preparation of bacteriophage λ lysate and DNA. BioTechniques. **25**:44-46.

172. **Sung, S. Y., J. V. McDowell, J. A. Carlyon, and R. T. Marconi.** 2000. Mutation and recombination in the upstream homology box-flanked *ospE*-related genes of the Lyme disease spirochetes result in the development of new antigenic variants during infection. Infect. Immun. **68**:1319-1327.

173. **Svarchevsky, A. N., and V. N. Rybchin.** 1984. Characterization of plasmid properties of bacteriophage N15. Mol. Genet. Mikrobiol. Virusol. **5**:34-39.

174. **Svarchevsky, A. N., and V. N. Rybchin.** 1984. Physical mapping of plasmid N15 DNA. Mol. Genet. Mikrobiol. Virusol. **10**:16-22.

175. **Tavares, P., M. A. Santos, R. Lurz, G. Morelli, H. de Lencastre, and T. A. Trautner.** 1992. Identification of a gene in *Bacillus subtilis* bacteriophage SPP1 determining the amount of packaged DNA. J. Mol. Biol. **225**:81-92.

176. **The Institute for Genomic Research.** Last revised: 2 December 1999. *Borrelia burgdorferi* genomic sequence. [Online.] http://www.tigr.org/tdb/CMR/gbb/htmls/SplashPage.html:Last accessed: 8 March 2000.

177. **Tilly, K., S. Casjens, B. Stevenson, M. Bono, D. S. Samuels, D. Hogan, and P. Rosa.** 1997. The *Borrelia burgdorferi* circular plasmid cp26: conservation of plasmid structure and targeted inactivation of the *ospC* gene. Mol. Microbiol. **23**:361-373.

178. **Tilly, K., L. Lubke, and P. Rosa.** 1998. Characterization of circular plasmid dimers in *Borrelia burgdorferi.* J. Bacteriol. **180**:5676-5681.

179. **Tye, B. K., R. K. Chan, and D. Botstein.** 1974. Packaging of an oversize transducing genome by *Salmonella* phage P22. J. Mol. Biol. **85**:485-500.

180. **Tye, B. K., J. A. Huberman, and D. Botstein.** 1974. Non-random circular permutation of phage P22 DNA. J. Mol. Biol. **85**:501-528.

181. **Vieira, J., and J. Messing.** 1991. New pUC-derived cloning vectors with different selectable markers and DNA replication origins. Gene. **100**:189-194.

182. **Wang, G., A. van Dam, I. Schwartz, and J. Dankert.** 1999. Molecular typing of *Borrelia burgdorferi sensu lato:* taxonomic, epidemiological, and clinical implications. Clin. Microbiol. Rev. **12**:633-653.

183. **Weber, K., G. Schierz, B. Wilske, and V. Preac-Mursic.** 1984. European erythema migrans disease and related disorders. Yale J. Biol. Med. **57**:13-21.

184. **Westmaas, G. C., W. L. van der Maas, and P. van de Putte.** 1976. Defective prophages of bactriophage Mu. Mol. Gen. Genet. **145**:81-87.

185. **Wilske, B., V. Preac-Mursic, S. Jauris, A. Hofmann, I. Pradel, E. Soutschek, E. Schwab, G. Will, and G. Wanner.** 1993. Immunological and molecular polymorphisms of OspC, an immunodominant major outer surface protein of *Borrelia burgdorferi.* Infect. Immun. **61**:2182-2191.

186. **Wilske, B., V. Preac-Mursic, G. Schierz, and K. V. Busch.** 1986. Immunochemical and immunological analysis of European *Borrelia burgdorferi* strains. Zentralbl. Bakteriol. Hyg. A. **263**:92-102.

187. **Wilske, B., V. Preac-Mursic, V. Schierz, R. Kuhbeck, B. A. G, and M. Kramer.** 1988. Antigenic variability of *Borrelia burgdorferi*, p. 126-143. *In* J. L. Benach and E. M. Bosler (ed.), Lyme Disease and Related Disorders. New York Academy of Sciences, New York NY.

188. **Xu, Y., and R. C. Johnson.** 1995. Analysis and comparison of plasmid profiles of *Borrelia burgdorferi* sensu lato strains. J. Clin. Microbiol. **33**:2679-2685.

189. **Yamamoto, K., H. Shinagawa, and S. Kondo.** 1983. Induction of prophage λ in *Escherichia coli recA* strain by N-methyl-N'-nitro-N-nitrosoguanidine. Mutat. Res. **107**:33-40.

190. **Yang, X., T. G. Popova, K. E. Hagman, S. K. Wikel, G. B. Shoeler, M. J. Caimano, J. D. Radolf, and M. V. Norgard.** 1999. Identification, characterization, and expression of three new members of the *Borrelia burgdorferi* Mlp (2.9) lipoprotein gene family. Infect. Immun. **67:**6008-6018.

191. **Young, R.** 1992. Bacteriophage lysis: mechanism and regulation. Microbiol. Rev. **56:**430-481.

192. **Young, R., and U. Bläsi.** 1995. Holins: form and function in bacteriophage lysis. FEMS Microbiol. Rev. **17:**191-205.

193. **Yun, T., and D. Vapnek.** 1977. Electron microscopic analysis of bacteriophage P1, P1Cm, and P7. Determination of genome sizes, sequence homology, and location of antibiotic resistance determinants. Virol. **77:**376-385.

194. **Zückert, W. R., and A. G. Barbour.** 1999. Comparative analysis and immunological characterization of the *Borrelia* Bdr protein family. Infect. Immun. **67:**3257-3266.

195. **Zückert, W. R., and A. G. Barbour.** 2000. Stability of *Borrelia burgdorferi bdr* loci *in vitro* and *in vivo*. Infect. Immun. **68:**1727-1730.

196. **Zückert, W. R., and J. Meyer.** 1996. Circular and linear plasmids of Lyme disease spirochetes have extensive homology: characterization of a repeated DNA element. J. Bacteriol. **178:**2287-2298.